RAPID EVALUATION OF CORROSION-RESISTANT CONCRETE REINFORCING STEEL IN THE PRESENCE OF DEICERS

By

Shawn M. Schwensen

David Darwin

Carl E. Locke, Jr.

A Report on Research Sponsored by

THE NATIONAL COOPERATIVE HIGHWAY RESEARCH PROGRAM
Innovations Deserving Exploratory Analysis Program
Contract No. NCHRP-93-ID009

FLORIDA STEEL CORPORATION

STRUCTURAL ENGINEERING AND ENGINEERING MATERIALS
SL REPORT 95-6

UNIVERSITY OF KANSAS CENTER FOR RESEARCH, INC.
LAWRENCE, KANSAS
JULY 1995

RAPID EVALUATION OF CORROSION-RESISTANT CONCRETE REINFORCING STEEL IN THE PRESENCE OF DEICERS

ABSTRACT

Research to evaluate the properties of a corrosion resistant concrete reinforcing steel is reported. The steel is microalloyed (using copper, chromium, and phosphorous), and subjected to a special heat treatment, to provide corrosion resistance superior to conventional reinforcing steel. Rapid tests, developed at the University of Kansas, are modified and used to evaluate the corrosion properties of four types of steel representing combinations of alloying elements and heat treatment. The steels include two conventional steels, one hot-rolled and one subjected to a quenching and tempering heat treatment, and two corrosion-resistant steels, one hot-rolled and one heat-treated. The steels are evaluated in the presence of three deicing chemicals: sodium chloride, calcium chloride, and calcium magnesium acetate.

The results indicate that the corrosion resistant steels exhibit a corrosion rate equal to about one half that of the conventional steels. At low concentrations, calcium chloride and calcium magnesium acetate appear to have a corrosive effect similar to sodium chloride. Calcium magnesium acetate appears to be less corrosive than calcium chloride and sodium chloride at intermediate concentrations. High concentrations of $CaCl_2$ and CMA appear to cause instability in the macrocell test, causing alternating patterns of active corrosion and passivation of the anode specimens.

Key words: chlorides; concrete; corrosion; deicers; heat treatment; microalloys; reinforcing bars

INTRODUCTION

Corrosion of reinforcing steel in concrete structures costs taxpayers billions of dollars for preventive maintenance, repair, and shortened structure life. Due to a "bare roads year-round policy," deicing salts are used in many parts of the country to melt snow and ice off the roads. Deicing salts contain chloride ions, which penetrate the concrete and reach the steel reinforcement in bridge decks and parking garage floors.

Many methods have been developed to prevent the corrosion of reinforcing steel in concrete, with varying degrees of success. These methods often require special procedures in application or handling. Epoxy-coated reinforcing steel, for example, must be handled delicately in the field. If the epoxy coating is damaged, it must be repaired to prevent localized corrosion from occurring. A robust product, which can be handled without "kid gloves" during construction, is needed.

Tata Iron and Steel Company, Ltd., a company from India, has developed a new concrete reinforcing steel that uses microalloying and heat treatment (quenching and tempering) to achieve superior corrosion resistance (Tata 1991a, Jha, Singh, and Chattergee 1992). This steel is designed to corrode significantly less than conventional reinforcing bars in the presence of deicers, while retaining all the mechanical properties of normal bars.

It is desirable to evaluate the corrosion-resistant properties of the microalloyed steel in cementious materials, since there are many materials that resist corrosion in the atmosphere but perform poorly in concrete. Rapid corrosion tests, developed at the University of Kansas (Martinez, Darwin, McCabe, and Locke 1990), allow the evaluation to be carried out in three months, rather than one to two years. Florida Steel Corporation, a company in the United States, is able to produce the new steel alloy, in both hot-rolled and quenched and tempered forms. The Florida Steel product will be evaluated for its corrosion properties in the presence of several commonly used deicers and corrosion inhibitors.

Corrosion process

Corrosion is the destructive result of a chemical reaction between a metal or metal alloy and its environment (Jones 1992). An understanding of how corrosion occurs is essential to develop methods to prevent its progress.

Corrosion is an electrochemical reaction, usually occurring in an aqueous solution. Two reactions, oxidation and reduction, occur simultaneously. For steel (an iron alloy), possible reactions are:

$$Fe \longrightarrow Fe^{+2} + 2e^{-} \qquad \text{oxidation}$$

$$O_2 + 2H_2O + 4e^- \text{ ---> } 4OH^- \quad \text{reduction}$$

Oxidation occurs when iron releases electrons and Fe^{+2} goes into solution. Reduction occurs as free oxygen, O_2 , and water, H_2O, react with the electrons released from the steel to form hydroxyl ions, OH^-. When these two reactions are combined, the hydroxyl ions and the Fe^{+2} react to form ferrous hydroxide.

$$2Fe + O_2 + 2H_2O \text{ ---> } 2FeO(OH)_2$$

Ferrous hydroxide, $FeO(OH)_2$, spontaneously oxidizes to form hydrated ferric oxide, $Fe_2O_3 \cdot nH_2O$, which is commonly called rust (Mindess and Young 1981). It is formed at the anode, where the oxidation reaction occurs. Water and oxygen are supplied at the cathode, where the reduction reaction occurs.

Three conditions must be present for corrosion to occur. First, an electrical connection must exist to allow electrons to flow from the anode to the cathode. Second, oxygen must be present to react with the Fe^{+2}. Third, the anode and cathode must be in contact with an electrolyte (often water) to complete the circuit and allow Fe^{+2} and OH^- to go into solution.

Potential is a thermodynamic property that indicates whether a metal in a given environment will resist corrosion. The potential of a metal can be measured electrically using a reference electrode and a digital voltmeter. A highly negative potential usually means that the metal is active, or prone to corrosion, while a slightly negative (or positive) potential indicates that the metal is noble, or resistant to corrosion (ASTM G 3). An active metal which, when exposed to certain environmental conditions, has a less negative potential and greatly reduced corrosion rate is defined as being passivated. If steel reinforcement in concrete has a potential of -0.150 to -0.200 V or higher, with respect to a $Cu/CuSO_4$ reference electrode, it can be considered passive, while potentials of -0.350 V or lower indicate that corrosion is possible (Locke 1986). This corresponds to a passive potential range of -0.076 to -0.126 V or higher with respect to a standard calomel electrode (SCE), the reference electrode used in this study, while the possibility of corrosion is indicated by potentials of -0.276 V or lower.

Corrosion cells are either microcells or macrocells. In microcell corrosion, the anodes and cathodes are adjacent to each other. An example is a single steel reinforcing bar in concrete exposed to chloride ions. Potential differences exist at various places along the length of the bar due to localized changes in the environment and bar surface. These potential differences drive microcell corrosion. In macrocell corrosion, two distinct regions in a structure become the anode and cathode. An example is a bridge deck, where two mats of steel are used as

reinforcement. If chloride ions from deicing salts have penetrated into the concrete to the level of the top mat of steel, but have not reached the bottom mat, a potential difference exists due to the different environments surrounding the mats of steel. When connected electrically, a macrocell corrosion potential develops, distinct from the separate corrosion potentials of each element of the macrocell.

Concrete provides reinforcing steel with a passive oxide layer that protects the steel from further corrosion by providing a barrier to water and oxygen. Chloride ions from deicing salts penetrate the concrete over time. As chloride ions reach the bar, they cause the passive oxide layer to break down, exposing steel to additional chloride ions, moisture, and oxygen. This may shift the potential downward by several hundred millivolts. Once active corrosion is initiated, a porous oxide layer forms that does not adhere well to the steel surface, exposing the steel to further corrosion. This cycle of corrosion builds up an oxide layer that occupies a greater volume than the original volume of the steel from which it came, causing the concrete to crack. Once the crack propagates to the surface of the concrete, deicing salts have a direct route to the steel, accelerating the corrosion process. After time, the concrete spalls off entirely, and the bridge deck must be replaced.

Existing methods of preventing corrosion of reinforcing steel in concrete include the use of epoxy-coated reinforcing steel, silica fume concrete, corrosion inhibitors, and cathodic protection. Epoxy coating effectively seals the steel surface, preventing the access of oxygen, water, and chloride ions. Epoxy coatings are relatively smooth and reduce the bond strength between the steel and the concrete. Epoxy is also prone to damage in the field, and must be repaired, if damaged, to prevent localized corrosion from occurring. Silica fume concrete is extremely dense, greatly impeding the transport of chloride ions, oxygen, and moisture, but tends to prevent water from bleeding during concrete placement, resulting in cracks due to plastic shrinkage. Corrosion inhibitors are chemical admixtures that are added to the concrete during the mixing process. Organic inhibitors generally act as sealants, decreasing the permeability of concrete and impeding the transport of chloride ions. Inorganic inhibitors react chemically with chloride ions, making them unavailable to initiate corrosion at the steel surface. Cathodic protection involves imposing an electric current through a structure in such a way that forces corrosion to occur at "sacrificial anodes", in effect making the structure act as the cathode.

Previous work

Tata Iron and Steel Company, Ltd. has attempted to prevent corrosion in a different way. By using additional alloying elements, a superior oxide layer is produced that will halt or significantly slow subsequent corrosion by adhering to the steel, cutting off water and oxygen, and providing high electrical resistance (Tata 1991a).

The new reinforcing steel differs from steel used in standard U.S. practice in several ways. Additional alloying elements consisting of copper, chromium, and phosphorous are used, along with a special heat treatment, to provide the corrosion resistant properties of the steel (Tata 1991b, Jha et al. 1992). The bars possess lower carbon content than is usual in U.S. practice, and exceed the ASTM limit on phosphorous content (ASTM A 615/A 615M-94, ASTM A 706/A 706M-93a). The bars are quenched and tempered immediately following the rolling operation, a step that places the exterior of the bars in compression. The apparent corrosion-resisting mechanisms include the formation of a corrosion retarding layer of copper chloride-copper hydroxide at the steel surface in the presence of chlorides, the formation of phosphorous oxides, which serve as corrosion inhibitors, the formation of iron-chromium oxide at the steel surface, which is a poor electrical conductor, and the reduction of microfractures in the surface from the rolling operation due to the quenching and tempering process (Tata 1991a, Jha et al. 1992). The corrosion products that form are much denser than for normal reinforcing steel, which further reduces the availability of oxygen and water at the steel surface. The reduced microfracturing due to the quenching and tempering heat treatment further reduces the surface area available for corrosion.

The procedures used to evaluate the steel prior to the current study have focused primarily on the corrosion resistance of bars not in contact with concrete. Only one series of accelerated corrosion tests were used to study bars in contact with concrete. In these tests, concrete blocks containing reinforcing bars were subjected to total immersion in salt water. Macrocell corrosion did not occur due to the uniform exposure to chloride ions. The tests, therefore, do not present a complete picture of the corrosion process of steel in concrete and are not accepted in U.S. practice (Pfeifer, Sandgren, and Zoob, 1987).

Scope

The specific technical issue addressed in this study involves the demonstration of the corrosion resistance of the steel embedded in mortar. Earlier studies have established that the steel is more resistant to corrosion in the

atmosphere. Atmospheric tests alone, however, cannot guarantee superior corrosion resistance, since there are many materials that resist corrosion in the atmosphere but perform poorly in concrete.

Four steels are evaluated for their corrosion properties [two conventional steels and two microalloyed steels based on the recommendations of Tata Iron and Steel Company, Ltd. (Tata 1991a, Tata 1991b)]: regular hot rolled steel (H), regular quenched and tempered steel (T), corrosion resistant hot rolled steel (CRSH), and corrosion resistant quenched and tempered steel (CRST). All four steels are subjected to three deicing chemicals: sodium chloride (NaCl), calcium chloride ($CaCl_2$), and calcium magnesium acetate (CMA).

Sodium Chloride- Four molal ion concentrations of NaCl, 0.4, 1.0, 1.6, and 6.04 (15%) are used. Two macrocell tests and two corrosion potential tests are performed for each steel, per concentration.

Calcium Chloride, Calcium Magnesium Acetate- For $CaCl_2$ and CMA, three molal ion concentrations, 0.4, 1.6, and 6.04 are used. One potential test and two macrocell tests are performed for each steel, per concentration. In addition, the corrosion potentials of the anodes and cathodes in the macrocells using $CaCl_2$ and CMA are measured.

Inhibitors- All four steels are tested with both inorganic and organic corrosion inhibitors cast in the mortar surrounding the steel specimens. Two macrocell tests are performed for each combination of steel and inhibitor using 1.6m NaCl.

EXPERIMENTAL WORK

The procedure for constructing the specimens and setting up the tests is based in large part upon earlier rapid corrosion test research performed at the University of Kansas (Martinez et al. 1990).

Test Specimen

The test specimen, shown in Fig. 1, consists of a 5 in. (127 mm) long No. 5 (16 mm) reinforcing bar, symmetrically embedded 3 in. (76 mm) in a 1.18 in. (30 mm) diameter mortar cylinder. The mortar cylinder is 4 in. (102 mm) long, and the overall specimen length is 6 in. (153 mm).

The mold for the specimen is made from standard PVC pipe and fittings (ASTM D 2241 and D 2466). Fig. 2 shows the dimensions of the mold. Instructions for machining the PVC pipe and fittings can be found in the Appendix A of Martinez et al. (1990). The reinforcing steel is positioned with laboratory grade rubber stoppers to accurately maintain proper cover. A cradle holds eight molds (two rows with four specimens per row) in place while

the specimens are cast. Each cradle consists of two 2 in. (50 mm) thick by 7 in. (180 mm) wide by 15 in. (380 mm) long pieces of wood connected with threaded rods. The wood is counterbored to accept the molds, which are sandwiched between the wooden pieces by tightening the threaded rods.

To prepare a specimen, a 5 in. (127 mm) long reinforcing bar is cut and tapped at one end to receive a steel screw to provide an electrical connection. The bar is then cleaned with acetone (ASTM G 1), and a 0.6 in. (15 mm) wide band of epoxy is applied around the bar, 2.75 in. (70 mm) from the untapped end of the bar. The purpose of the epoxy band is to prevent crevice corrosion of the steel at the interface between the steel and the surrounding mortar. To prevent voids in the epoxy coating, two coats are applied. After each coat, the bars are heated in an oven at 100° F (38° C) to harden the epoxy. The epoxy coating applied around the bar is mixed and applied following the manufacturer's instructions.

To cast the specimen, the small rubber stopper, A (Fig. 2), is inserted into a machined PVC connector, B, so that the wide end of the stopper is in contact with the internal surface of the connector. The bar is assembled in the mold by inserting the untapped end of the reinforcing bar into a hole centered in the small rubber stopper, A, narrow end of the stopper first. The bar is pulled through the stopper until the epoxy band emerges from the hole on the wide end of the stopper

The end of small connector, B, is inserted into connector, D. The reinforcing bar is then pulled downward until the tapped end is flush with the top edge of connector, D. The large rubber stopper, C, is then inserted in the large connector, D, and positioned as shown in Fig. 2. The 1.18 in. (30 mm) inside diameter PVC pipe, E, is inserted into connector, B, until it is flush with rubber stopper, A, and the assembled mold is inserted into lower wooden member, F. Once eight specimens are assembled and inserted into the lower wood member, the top wood member, F, is placed over the specimens, and the assembly is tightened using threaded rods, G. The openings in the rubber stoppers are enlarged to match the size of the reinforcing bar. The 1.18 in. (30mm) pipe, E, is split longitudinally (for ease of disassembly) and taped (with masking tape) before the mold is assembled.

Materials

Reinforcing Steel- Four steels (produced by Florida Steel Corporation) are evaluated: Conventional hot-rolled Grade 40 steel (H) and quenched and tempered (by the Thermex/Tempcore process) Grade 60 steel (T) fully conform to ASTM A 615. The new corrosion resistant steels, hot rolled Grade 40 (CRSH) and quenched and

tempered Grade 60 (CRST) meet the mechanical requirements of ASTM A 615, but exceed the allowable amount of phosphorous. The chemical analyses of the steels, as well as the chemical requirements recommended in the original study (Tata 1991a, Tata 1991b) are presented in Table 1. The CRSH/CRST steel meets most of the recommended requirements (Tata 1991a, Tata 1991b), with the exception of carbon content (0.20 percent versus a maximum of 0.18 percent) and carbon equivalent (0.53 percent versus a range of 0.30 to 0.45 percent). The phosphorous content, 0.080 percent, is below the recommended maximum of 0.120 percent. All bars have a nominal diameter of 16 mm (ASTM designation: No. 5).

Mortar- The mortar mixture is made with Type I portland cement (ASTM C 150), ASTM C 778 graded Ottawa sand, and deionized water. The mixture proportions of the mortar represent the mortar constituent of concrete with a design strength of 4000 psi. The mortar has a water/cement ratio of 0.5 and a sand/cement ratio of 2.0 by weight. Mix designs are included in Table 2.

Inhibitors- The organic inhibitor used is Rheocrete 222 manufactured by Master Builders, Inc. The inorganic inhibitor used is DCI-S, a calcium nitrite compound manufactured by W.R. Grace & Co.

Epoxy- Morton Powder Coatings Corvel® Epoxy Patch Compound 10-6071 PC

Deicers- Chloride-based deicers were made using laboratory grade NaCl and $CaCl_2$. CMA (calcium magnesium acetate: 3 moles of calcium acetate per 7 moles of magnesium acetate) was manufactured by Cryotech Deicing Technology.

Specimen Fabrication

Sixteen specimens, two cradles containing eight specimens each, are cast at one time. The mix proportions are shown in Table 2. The specimens are cast in three layers. Each layer is rodded 25 times with a straightened coat hanger, and vibrated on a vibrating table at an amplitude of 0.006 in. (0.15 mm) and a frequency of 60 cycles/sec for 15 sec. Specimens are covered with a moist towel and wrapped in a plastic bag for one day. After one day, the specimens are removed from the cradle and taken out of their molds.

To remove a specimen from the mold, the large connector, D (Fig. 2), is removed by hand. The end of the exposed bar is then placed against the outer jaw of a bench vise. The edge opposite the exposed end of the bar of the small connector, B, is placed against the other jaw. As the vise is tightened, the lollipop specimen, still encased in pipe, E, slides out of the small connector, until it can be removed by hand. The masking tape is next removed from

the longitudinal seam in pipe, E. Using a dull, flat instrument (e.g. old butterknife), the longitudinal seam in pipe, E, is pried apart, breaking any bond between the PVC and the mortar. The specimen is removed from the pipe by pulling on the exposed bar with one hand while restraining the pipe with the other hand, leaving the butterknife in the seam. The specimens are placed in a curing tank (ASTM C 511). The limewater curing solution should be saturated with $Ca(OH)_2$ and have a pH of 12.5.

Test Procedure

Corrosion Potential Test- The corrosion potential test is used to evaluate the tendency of the four steels to corrode in the presence of deicing chemicals. The potential of each specimen is measured once a day for 40 to 60 days. The test setup is shown schematically in Fig. 3.

The test requires two plastic containers. The test specimen is placed in one 5-liter container along with crushed mortar fill and either simulated pore solution or pore solution containing a deicing chemical. A standard calomel reference electrode is placed in the second container, along with saturated potassium chloride (KCl) solution. The two containers are connected ionically by a salt bridge. The potential difference between the specimen and the calomel electrode is measured once a day for 40 to 60 days using a digital voltmeter.

The mortar fill consists of the same mixture as used in the test specimen. The fill is used primarily to serve as a buffer and to help simulate the relative amount of cementious material that exists in an actual structure. The fill is cast in a 1 in. (25 mm) thick layer using a metal cookie sheet as the form. The form is vibrated for 15 seconds on the vibration table. The fill is cast at the same time as the test specimen. After one day, the mortar is broken into pieces, and stored in large buckets. When corrosion inhibitors are used, care must be taken not to mix mortar with the different inhibitors together.

The containers used to hold the specimens are made of a high density polyethylene that is insensitive to both the caustic pore solution and the deicing chemicals.

The constituents in the simulated pore solution were selected, in part, based on the analyses of expressed pore solution performed by Farzammehr (1985). Each liter of pore solution contains 18.81g of KOH and 17.84 g of NaOH. The small component of NaCl (0.14 g) used per liter of pore solution by Martinez et al. (1990) was eliminated in the current study.

To complete the corrosion cell, the two containers are connected ionically by a salt bridge. The salt bridge is prepared following procedures described by Steinbach and King (1950): A gel is prepared by stirring 4.5 g of agar and 30 g of KCl in 100 ml of deionized water over a hot plate. The gel is then poured into 3 ft (914 mm) lengths of 0.25 in (6.4 mm) inside diameter laboratory grade plastic tubing and boiled for 30 minutes, taking care to keep the ends of the tubes out of the water. After boiling, the lengths of gel-filled tubing are allowed to cool (until firm), and cut to appropriate length to serve as salt bridges. To have a good ionic path, the gel in the tubing must be continuous, without interruption by air bubbles or cracks.

A standard calomel electrode (SCE) is used to measure corrosion potential. The electrode is submerged in a saturated KCl solution consisting of 15 g of KCl per 100 ml of water.

Laboratory grade sodium chloride (NaCl) and calcium chloride ($CaCl_2$) and commercially produced calcium magnesium acetate (CMA: 3 moles of calcium acetate per 7 moles of magnesium acetate) are used to evaluate the effects of various concentrations of deicing chemicals on the four steels. The effects of the chemicals are compared on an isomolal ion basis (equal number of ions), since ion concentration in moles per unit volume of water controls ice melting capacity. Molal ion concentrations of 0.4, 1.0, 1.6, and 6.04 (15%) are used for NaCl deicing solutions. For $CaCl_2$ and CMA deicing solutions, molal ion concentrations of 0.4, 1.6, and 6.04 are used. The weights of materials in grams per liter of pore solution for each molal ion concentration and deicing chemical are presented in Table 3.

Fourteen days after casting, the specimens are taken from the curing tank. The tapped end of the reinforcing bar is thoroughly dried using compressed air, and a cable is connected to the bar with a steel screw. The cable is then passed through a hole in the lid of the container. The specimen is placed on the bottom of the container, bar up, and the fill material is added to the container to a level even with the top edge of the mortar on the specimen. The salt bridge is placed in the container through a second hole in the lid. The other end of the salt bridge is placed in the second container. The respective solutions are then placed in the containers, to within 0.5 in. (13 mm) of the top edge of the mortar. As the final step, the screw connection between the wire and the bar is covered with epoxy.

Macrocell Test- The macrocell test is used to evaluate the relative corrosion properties of the regular and corrosion resistant steels in the presence of deicing chemicals by setting up an active macrocell. A schematic of the test set up is shown in Fig. 4.

In this test, specimens, located in separate containers, are electrically connected across a 10 ohm resistor. The use of a 10 ohm resistor represents a change from the procedure used in Martinez et al. (1990), where a 100,000 ohm resistor was used. Electrical conductivity between the solutions in the two containers is provided by a salt bridge. Standard fill material is placed in both containers. For macrocells evaluating steel in NaCl, four specimens are exposed to a simulated pore solution, while two specimens are exposed to simulated pore solution containing NaCl. In macrocells evaluating steel in $CaCl_2$ and CMA, the number of specimens is reduced from four to two at the cathode and from two to one at the anode. This is a departure from the procedure used in Martinez et al (1990), where the anode and cathode each consisted of a single specimen. For future applications of the macrocell test, a 2:1 ratio of cathode to anode specimens is recommended.

To prevent oxygen depletion at the cathode from limiting the corrosion rate, scrubbed air must be supplied to the solution containing the cathode specimens. The use of an air scrubber represents a change from the procedure used in Martinez et al (1990), where air was not provided to the cathode specimens. An air scrubber is used to remove carbon dioxide from compressed air before being piped to the specimens. To build the air scrubber, a 5 gallon (18.9 liter) plastic container is filled with a 1 Molar sodium hydroxide solution containing 40g NaOH per 1000g of water. The air is bubbled through the scrubber using tubing that has been perforated with a sharp knife. After inserting the tubing through the lid, basalt coarse aggregate is used to hold down the tubing at the bottom of the container. The scrubbing solution is then poured into the container until it is approximately three-quarters full. The remaining space in the container is pressurized by scrubbed air to be delivered to the cathodes. A polycarbonate T-joint is inserted into the top of the container to accept the scrubbed air and deliver it to the air piping system. Air is delivered to the cathode buckets by running tubes from the T-joint at the top of the air scrubber directly to the pore solution through a small hole in the cathode bucket lid. The air pressure is controlled at the source by a regulator, while air flow at each bucket is controlled by a screw-adjustable hose clamp.

The 10 ohm resistor allows corrosion to occur while providing a measurable potential drop. The specimens are connected electrically by wiring the cathode specimens in series to a nylon binding post in a control box. The anode specimen is wired directly to a second binding post directly across from the cathode post. The posts are connected across a 10 ohm resistor. The voltage drop across the 10 ohm resistor is measured once a day for 100 days using a

digital voltmeter. The macrocell tests using 1.6 and 6.04 m concentrations of $CaCl_2$ and CMA were extended to 130 days.

The potentials of both the anode and the cathode specimens in macrocells using $CaCl_2$ and CMA are taken once a week to help explain the magnitude of the corrosion rate, check the integrity of the salt bridge, and provide additional corrosion potential data. The measurement of the anode and cathode potentials within the macrocell test represents another addition to the procedure in Martinez et al. (1990), where no macrocell potentials were taken. The potentials of the anode and cathode are measured by first disconnecting the anode wire from its binding post to break the electrical circuit. This is done so that the anode and cathode may return to their equilibrium potentials from the macrocell corrosion potential. After two hours, readings are taken. To do this, a standard calomel electrode is inserted into the bucket containing only pore solution and connected to the digital voltmeter. Care must be taken to wash the SCE before inserting it into the cathode solution to prevent the pore solution from being contaminated with chloride ions from other solutions, such as the saturated KCl solution in the potential reference bucket. The other lead from the voltmeter is connected to the previously detached anode wire to measure the anode potential and connected to the cathode binding post to measure the cathode potential. The salt bridge provides the ionic connection so that the anode potential may be taken while the SCE is in the pore solution. If the salt bridge is defective, the anode potential reading cannot be taken, providing a check on the integrity of the salt bridge.

RESULTS

An analysis of the corrosion potential tests shows little difference between the four steels. The principal results of this study are based upon the data from the macrocells and presented in terms of corrosion rates versus time. Time is expressed in days for both the corrosion potential and the rapid macrocell tests.

Corrosion Potential Tests

An analysis of the corrosion potential tests shows little difference between H, T, CRSH, and CRST steels. Results from corrosion potential tests evaluating the steel in deicers and pore solution are shown in Figs. 5-14 and Fig. 15, respectively.

Sodium Chloride- Corrosion potential tests evaluating NaCl exhibited potentials that averaged between -0.300 and -0.500 V at all concentrations (Figs. 5-8). As the concentration of NaCl increased, the potentials tended to be

more negative. This is consistent with the results of the tests conducted by Martinez et al. (1990), which used only H steel. Many of the potential tests in the current study, however, contain specimens that remained passive (-0.150 to -0.250 V) for the entire test (Figs. 6c; 7a,b,c; and 8a); of these, only the passive H steel specimen in 6.04 m NaCl later depassivated to resemble its twin specimen. This extended passive behavior may be due to chloride ions taking longer to penetrate the mortar and reach the steel in some specimens than in others.

Calcium Chloride, Calcium Magnesium Acetate- Potential tests in the current study using $CaCl_2$ and CMA deicing chemicals in 0.4 and 1.6 m ion concentrations exhibited potentials of -0.500 V. This is consistent with results obtained by Martinez et al. (1990), with the exception of the earlier tests using 0.4 m CMA (Fig. 16e, Martinez et al. 1990), which approached a passive state (-0.250 to -0.300 V). All 6.04 m $CaCl_2$ corrosion potential tests in the current study exhibited potentials of -0.600 V, as do H and CRSH steels evaluated in 6.04 m CMA. The T specimen in 6.04 m CMA, Fig. 14b, passivated (-0.175 V), while the CRST specimen, Fig. 14d, had an potential of -0.350 V. Using 6.4 m (not 6.04 m) $CaCl_2$ and CMA solutions, Martinez et al. (1990), observed potentials between -0.500 and -0.600 V. Martinez et al. also experienced some fluctuation in the 6.4 m CMA potential tests (Fig. 16a, Martinez et al. 1990), which, together with the passive behavior exhibited by the T and CRST specimens in the current study, may indicate some instability at high concentrations of CMA.

Simulated Pore Solution- In pore solution (Fig. 15), only CRSH approached a passive condition (-0.225 V), while the other steels were clearly not passive (-0.400 V). This differs from the results observed by Martinez et al. (1990), in which the H steel exhibited potentials in the range of -0.150 to -0.300 V. It is possible that crevice corrosion occurred under the epoxy band of the H, T, and CRST specimens, preventing them from passivating.

Macrocell Potentials- The potentials of the anodes and cathodes of the $CaCl_2$ and CMA macrocells were taken once a week throughout the duration of the test. The potentials are shown in Figs. 16b-39b, directly below graphs showing the corrosion rates for the individual macrocells (Figs. 16a-39a); an "A" denotes an anode specimen, while a "C" denotes a cathode specimen. The potential readings of the anode specimens were similar to those measured in the corrosion potential tests. The corrosion potential of the cathode specimens, however, were somewhat less negative than the values obtained in the corrosion potential tests in pore solution, with values between -0.250 and -0.400 V.

The potential difference (absolute value of the arithmetic difference of the anode and cathode potentials) can affect the magnitude of the corrosion rate (as the potential difference increases, the macrocell corrosion rate tends to increase). In $CaCl_2$ macrocells, the potential difference increased as the concentration of the deicer increased. In contrast, the potential difference in CMA macrocells decreased as the concentration increased from 0.4 m to 1.6 m. CMA macrocells using a 6.04 m solution (Figs. 36-39) were unstable; the potentials of the anodes started highly negative (-0.400 to -0.600 V), temporarily approached passivation (-0.200 to -0.300 V), and returned to a lower potential (-0.450 to -0.550 V).

No cathode bars truly passivated in any macrocell [passivation is defined according to Locke (1986): -0.150 to -0.200 V with respect to a $Cu/CuSO_4$ reference electrode or -0.076 to -0.126 V with respect to the SCE], although several reached -0.250 V. In fact, the specimen which passivated to the greatest degree was the H-2 anode in 6.04 m CMA, Fig. 36 b, with a potential of -0.125 V.

Macrocell Tests

There are significant differences in the performance of the steels in the macrocell tests. The corrosion rates, calculated using Faraday's Law based on the measured corrosion currents (Jones 1992), are expressed in micrometers per year (25.4 μm = 0.001 in.). Sample calculations are shown in Appendix A. The figures show the average corrosion rates for the number of specimens indicated (1, 2, or 3). Specimens that did not exhibit a corrosion rate of at least 1 μm/yr at some time during the 100 days during which the tests were carried out are not used to develop the average results shown.

Sodium Chloride- The results are illustrated in Figs. 40a, b, c, and d for specimens subjected to 0.4, 1.0, 1.6, and 6.04 (15%) molal ion solutions of sodium chloride, respectively. Overall, the CRSH and CRST steels exhibit measurably lower corrosion rates than do the H and T steels, with the CRST steel, on average, exhibiting a lower corrosion rate than the CRSH steel. For the 0.4 and 1.0 m ion NaCl solutions (Figs. 40a and 40b), the new steels exhibit corrosion rates on the order of one-half of the corrosion rates exhibited by the two conventional steels. For the 1.6 m ion concentration (Fig. 40c), the CRST steel exhibits very low corrosion (less than 1 μm/yr for most of the test), which is significantly less than that exhibited by the CRSH steel (about 3 μm/yr at the end of the test) and the H and T steels (in excess of 4 μm/yr for most of the test). For the 6.04 m ion solution (Fig. 40d), the CRSH and T steels exhibit the lowest corrosion rate (about 2 μm/yr), followed by the CRST steel (about 4 μm/yr) and H steel

(about 6 μm/yr). The relatively high corrosion rate exhibited by the CRST steel is the result of a high corrosion rate exhibited by one of the three specimens included in the average, which is possibly the result of crevice corrosion.

Calcium Chloride, Calcium Magnesium Acetate- Calcium chloride and calcium magnesium acetate are also used to evaluate the relative corrosion performance of the four steels. As explained before, the comparisons are made on a molal ion basis, since it is the ion concentration that controls the ice melting capability of a compound. At any molal ion concentration, calcium chloride will provide a higher chloride ion content than NaCl.

The results of this analysis are illustrated in Figs. 41 and 42 for the 0.4 and 1.6 molal ion concentrations, respectively. At the 6.04 m ion concentration, the addition of calcium chloride to the simulated pore solution resulted in the formation of a large amount of precipitate (calcium hydroxide), and the addition of calcium magnesium acetate resulted in the formation of a gel-like substance (calcium hydroxide and magnesium hydroxide). Saturated $Ca(OH)_2$ has a pH of 12.5, and may have lowered the pH of the simulated pore solution, which normally has a pH of 13.8. The test results at these high concentrations were highly unstable and are not used to draw any conclusions about the corrosion performance of the steels.

Figs. 41a and 41b illustrate the corrosion performance of the four steels at a 0.4 m ion concentration for $CaCl_2$ and CMA. For calcium chloride, the CRST specimens exhibit a slightly lower corrosion rate than do the H specimens (both at about 2 μm/yr), followed by the CRSH specimens (about 3 μm/yr) and finally the T specimens (4 μm/yr). For the 0.4 m ion CMA macrocells, at the end of 100 days, the CRSH and CRST specimens exhibit the lowest corrosion rates (2.5 and 3.5 μm/yr, respectively), followed by the T and the H specimens (4 and 5 μm/yr, respectively). The corrosion rates are generally similar to those exhibited by the four steels in the 0.4 m ion NaCl macrocells (Fig. 40a).

The results for the 1.6 molal ion concentrations of $CaCl_2$ and CMA are shown in Figs. 42a and 42b, respectively. For $CaCl_2$, CRST appears to provide the lowest corrosion rate (2 μm/yr), while CRSH provides the highest corrosion rate (6 μm/yr), with the T and H steels in between (both at 4 μm/yr). For the 1.6 m ion concentration of CMA, the CRSH, CRST, and H steels exhibit very low corrosion rates (less than 1 μm/yr at 120 days); even the T steel exhibits a corrosion rate no higher than 3 μm/yr.

Comparison of Deicers- A comparison of the relative corrosion effects of NaCl, $CaCl_2$, and CMA on each type of steel can be made using data from macrocells using 0.4 and 1.6 m solutions (6.04 m concentrations of the three deicers are not made due to the instability of the test results).

For H steel, the corrosion rate increased slightly (4 to 5 μm/yr) as the concentration of NaCl increased from 0.4 to 1.6 m, while doubling, from 2 to 4 μm/yr, when exposed to increasing concentrations of $CaCl_2$. The increase in concentration of CMA led to a marked decrease in corrosion rate (5 to 1 μm/yr).

When T steel was exposed to NaCl and $CaCl_2$, there was no change in the corrosion rate (6 and 4 μm/yr , respectively) as the concentration increased from 0.4 to 1.6 m. The corrosion rate was reduced by half, from 4 to 2 μm/yr, as the concentration of CMA increased.

For CRSH steel, the corrosion rate doubled when the concentration of NaCl and $CaCl_2$ increased from 0.4 to 1.6 m (1.75 to 3 and 3 to 6 μm/yr, respectively). The rate decreased five-fold, from 2.5 to 0.5 μm/yr, as the concentration of CMA was increased.

The corrosion rate for CRST steel dropped to almost zero when the concentration of NaCl and CMA was increased from 0.4 to 1.6 m, while remaining constant (2 μm/yr) when exposed to increasing concentrations of $CaCl_2$.

In general, at concentrations of 0.4 m, there is very little difference in the corrosion effects of the deicers. At 1.6 m concentrations, however, the CMA is by far the least corrosive of the three deicers, exhibiting a marked decrease in the corrosion rates for all four steels, while NaCl and $CaCl_2$ are only slightly more corrosive compared to 0.4 m concentrations. Calcium magnesium acetate is marketed as a deicing chemical that results in lower corrosion rates than chlorides, which appears to be supported by the results illustrated in Fig. 42b.

Inhibitors- All macrocells evaluating the corrosion resistance of the four steels in conjunction with corrosion inhibitors in 1.6 m NaCl exhibited corrosion rates higher than earlier macrocell tests performed at the same concentration of NaCl (1.6 m) but without corrosion inhibitors. The reason for this behavior may be that during curing, the pH of the limewater bath in the curing tank dipped to between 10 and 11, indicating that the bath was not fully saturated with $Ca(OH)_2$. Calcium hydroxide may have leached out of the specimens, making the mortar more permeable and decreasing the effectiveness of the inhibitors. These tests should be repeated to evaluate the effectiveness of inhibitors with corrosion resistant steel.

SUMMARY AND CONCLUSIONS

The results of research to evaluate the properties of a corrosion resistant concrete reinforcing steel are reported. The steel is microalloyed (using copper, chromium, and phosphorous), and subjected to a special heat treatment, to provide corrosion resistance that is superior to conventional reinforcing steel. Rapid tests, developed at the University of Kansas, are modified and used to evaluate the corrosion properties of four types of steel representing combinations of alloying elements and heat treatment. The steels include two conventional steels, one hot-rolled and one subjected to a quenching and tempering heat treatment, and two forms of corrosion-resistant steel, one hot-rolled and one heat-treated. The steels are evaluated in the presence of three deicing chemicals: sodium chloride, calcium chloride, and calcium magnesium acetate.

The following conclusions are based on the experimental results and analyses presented in this report.

1. The microalloying procedure, using increased phosphorous, chromium, and copper, improves the corrosion resistance of steel reinforcing bars cast in mortar and subjected to deicing chemicals. The corrosion rate of the corrosion resistant steels is approximately one-half of the corrosion rate of conventional reinforcing steels.
2. The use of a quenching and tempering heat treatment process that follows hot rolling of reinforcing steel appears to provide some additional corrosion resistance, when used in conjunction with the microalloying procedure.
3. Calcium chloride and calcium magnesium acetate appear to have a corrosive effect similar to sodium chloride at low concentrations.
4. Calcium magnesium acetate appears to be less corrosive than calcium chloride and sodium chloride at intermediate concentrations.
5. High concentrations of $CaCl_2$ and CMA appear to cause instability in the macrocell test, causing alternating patterns of active corrosion and passivation of the anode specimens.

FUTURE WORK

As pointed out earlier, the macrocells used to evaluate the effect of the corrosion inhibitors were faulty and must be repeated to evaluate the performance of these admixtures with the corrosion resistant steel. New heats of corrosion resistant steel, with a phosphorus content closer to the recommended maximum of 0.120 % and a

chromium content approaching 0.80 % should be tested to see if the corrosion performance observed in the current study can be improved (the steel used in the current study had phosphorus and chromium contents of 0.080 % and 0.53 %, respectively).

The use of the corrosion potential tests should be discontinued. Taking the potentials of the macrocell specimens gives the same information as the corrosion potential tests, but from within an active macrocell. The resources saved by eliminating the corrosion potential tests can be put to better use by conducting supplementary tests, such as linear polarization. Linear polarization (ASTM G 59) can predict the microcell corrosion rate, a phenomenon not accounted for in the macrocell studies. If both the macrocell and microcell corrosion rates of a specimen can be calculated, the total corrosion rate can be found.

ACKNOWLEDGEMENTS

This report is based on research by Shawn M. Schwensen and Matthew R. Senecal in partial fulfillment of the requirements for the M.S.C.E. degree. The research was sponsored by the NCHRP IDEA Program and Florida Steel Corporation. The inorganic corrosion inhibitor, DCI-S, was provided by W.R. Grace & Co., and the organic inhibitor, Rheocrete 222, was provided by Master Builders, Inc. Calcium magnesium acetate was donated by Cryotech Deicing Technology.

REFERENCES

ASTM (1995). "Standard Specification for Deformed and Plain Billet-Steel Bars for Concrete Reinforcement," (ASTM A 615/A 615M-94) *1995 Annual Book of ASTM Standards*, Vol. 1.04, American Society for Testing and Materials, Philadelphia, PA, pp. 300-304.

ASTM (1995). "Standard Specification for Low-Alloy Steel Deformed Bars for Concrete Reinforcement," (ASTM A 706/A 706M-93a) *1995 Annual Book of ASTM Standards*, Vol. 1.04, American Society for Testing and Materials, Philadelphia, PA, pp. 342-346.

ASTM (1994). "Standard Specification for Portland Cement", (ASTM C 150-94) *1994 Annual Book of ASTM Standards*, Vol. 4.02, American Society for Testing and Materials, Philadelphia, PA, pp. 88-92.

ASTM (1994). "Standard Specification for Moist Cabinets, Moist Rooms and Water Storage Tanks Used in the Testing of Hydraulic Cements and Concretes," (ASTM C 511-93) *1994 Annual Book of ASTM Standards*, Vol. 4.02, American Society for Testing and Materials, Philadelphia, PA, pp. 267-268.

ASTM (1994). "Standard Specification for Standard Sand," (ASTM C 778-92a) *1994 Annual Book of ASTM Standards*, Vol. 4.01, American Society for Testing and Materials, Philadelphia, PA, pp. 323-325.

ASTM (1995). "Standard Specification for Poly (Vinyl Chloride) (PVC) Pressure-Rated Pipe (SDR Series)," (ASTM D 2241-93) *1995 Annual Book of ASTM Standards*, Vol. 8.04, American Society for Testing and Materials, Philadelphia, PA, pp. 95-102.

ASTM (1995). "Standard Specification Poly (Vinyl Chloride) (PVC) Plastic Pipe, Fittings, Schedule 40," (ASTM D 2466-94a) *1995 Annual Book of ASTM Standards*, Vol. 8.04, American Society for Testing and Materials, Philadelphia, PA, pp. 152-157.

ASTM (1994). "Standard Practice for Preparing, Cleaning, and Evaluating Corrosion Test Specimens," (ASTM G 1-90) *1994 Annual Book of ASTM Standards*, Vol. 3.02, American Society for Testing and Materials, Philadelphia, PA, pp. 25-31.

ASTM (1994). "Standard Practice for Conventions Applicable to Electrochemical Measurements in Corrosion Testing," (ASTM G 3-89) *1994 Annual Book of ASTM Standards*, Vol. 3.02, American Society for Testing and Materials, Philadelphia, PA, pp. 46-54.

ASTM (1994). "Standard Practice for Conducting Potentiodynamic Polarization Resistance Measurements," (ASTM G 59-91) *1994 Annual Book of ASTM Standards*, Vol. 3.02, American Society for Testing and Materials, Philadelphia, PA, pp. 230-233.

Farzammehr, H. (1985). "Pore Solution Analysis of Sodium Chloride and Calcium Chloride Containing Cement Pastes," Master of Science Thesis, University of Oklahoma, Norman, Oklahoma, 101 pp.

Jha, R.; Singh, S.K.; and Chattergee, A. (1992). "Development of New Corrosion-Resistant Steel Reinforcing Bars," *Materials Performance*, NACE, Vol. 31, No. 4 April, pp. 68-72.

Jones, Denny A. (1992). *Principles and Prevention of Corrosion.* MacMillan Publishing Company, New York, 568 pp.

Locke, C.E. (1986). "Corrosion of Steel in Portland Cement Concrete: Fundamental Studies," *Corrosion Effects of Stray Currents and the Techniques for Evaluating Corrosion of Rebars in Concrete*, ASTM STP 906, V. Chaker, Ed. American Society for Testing and Materials, Philadelphia, PA, pp. 5-14.

Martinez, S.L.; Darwin, D.; McCabe, S.L.; and Locke, C.E. (1990). "Development of a Rapid Test to Measure the Corrosion Effects of Deicing Chemicals in Reinforced Concrete," *SL Report No. 90.4*, University of Kansas, Lawrence, Kansas, August, 61 pp.

Mindess, Sidney, and Young, Francis J. (1981) *Concrete,* Prentice Hall, Inc., Englewood Cliffs, NJ, 671 pp.

Pfeifer, D. W.; Sandgren, R. J.; and Zoob, A. (1987). "Protective Systems for New Prestressed and Substructure Concrete," *Report No. FHWA/RD-86/193.* Federal Highway Administration, McLean, VA, April.

Steinbach, O.F., and King, C.V. (1950). *Experiments in Physical Chemistry*, American Book Company, New York, 250 pp.

Tata (1991a). "Development of New Corrosion-Resistant Steel (CRS) at Tata Steel." Tata Iron and Steel Co., Ltd., Jamshedpur, India. 24 pp.

Tata (1991b). "Proposed Specification for Corrosion-Resistant Deformed Steel Bars for Concrete Reinforcement." Tata Iron and Steel Co., Ltd., Jamshedpur, India. 30 pp.

Table 1

Chemical Composition of 16 mm (No. 5) Steel Reinforcing Bars, in percent

Steel Type	Heat ID No.	C	Mn	S	V	Si	Ni	Sn	Mo	P	Cr	Cu	P+Cr+Cu	C.E.*
H, T	K5-5546	0.32	0.72	0.044	0.000	0.22	0.14	0.011	0.018	0.026	0.14	0.34	0.51	0.50
CRSH, CRST	K3-1725	0.20	0.76	0.032	0.003	0.23	0.11	0.011	0.011	0.080	0.53	0.44	1.05	0.53
CRS	Recommended (1-3)	0.18 max.	0.85 max.	0.035 max.		0.45 max.				0.120 max.	0.80 max.	0.50 max.	0.90 min.	0.30/0.45

*Carbon Equivalent = C + Mn/6 + (Cu + Ni)/15 + (Cr + Mo)/5 + V/0.5

Table 2

Mortar Mix Proportions

Types of Mortar	Water (g)	Cement (g)	Sand (g)	Rheocrete 222 (ml)	DCI-S (ml)
Regular	2640	5280	10560	---	---
Organic Inhibitor added	2607	5280	10560	33	---
Inorganic Inhibitor added	2510	5280	10560	---	130

Table 3

Quantities of deicing chemicals in grams per liter of simulated pore solution*

Molal Ion Concentration	0.4	1.0	1.6	6.04
NaCl	11.4	28.5	45.6	172.1
$CaCl_2$	14.4	----	57.7	217.4
CMA**	20.8	----	83.4	314.1

* Simulated pore solution: 18.81 g of KOH and 17.84 g of NaOH per liter of solution. Solvent = deionized water.

** 3 moles of calcium acetate per 7 moles of magnesium acetate

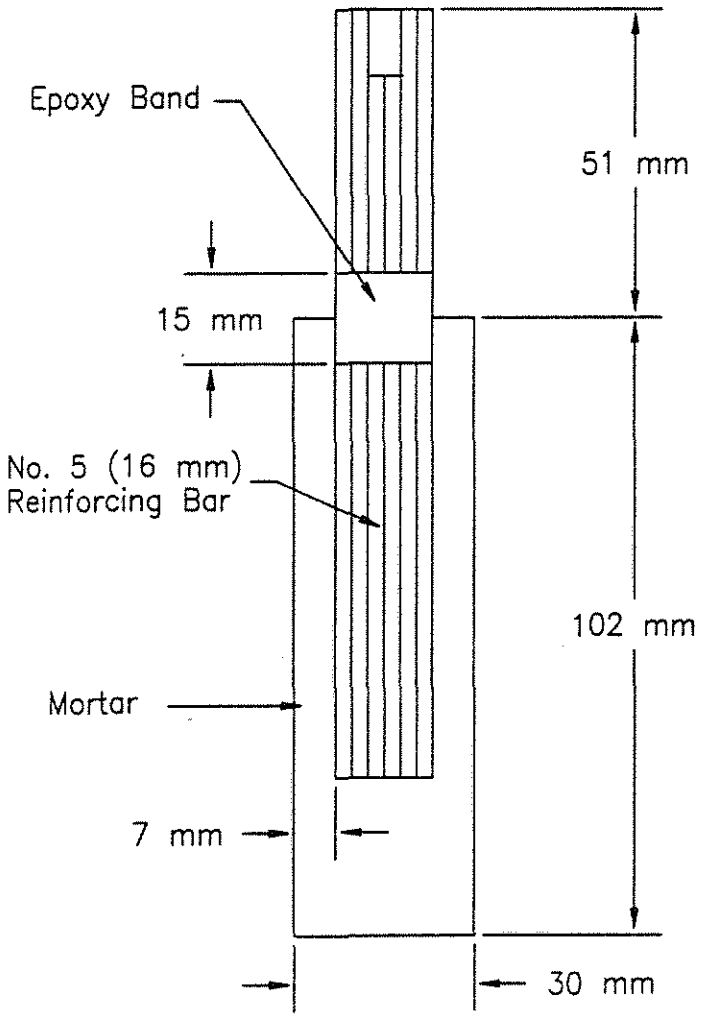

Fig. 1 Cross Section of Test Specimen

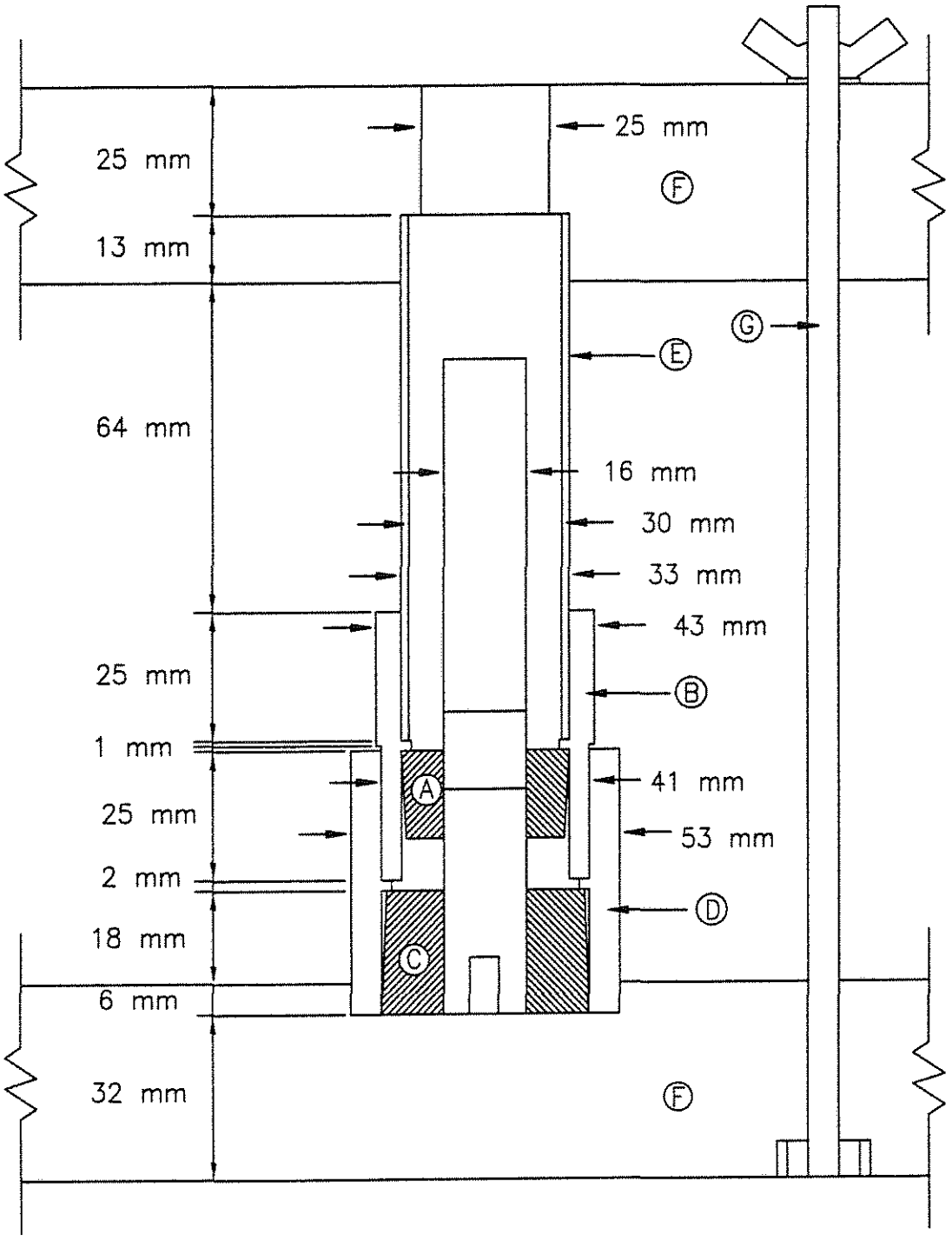

Fig. 2 Cross Section of Mold for the Test Specimen

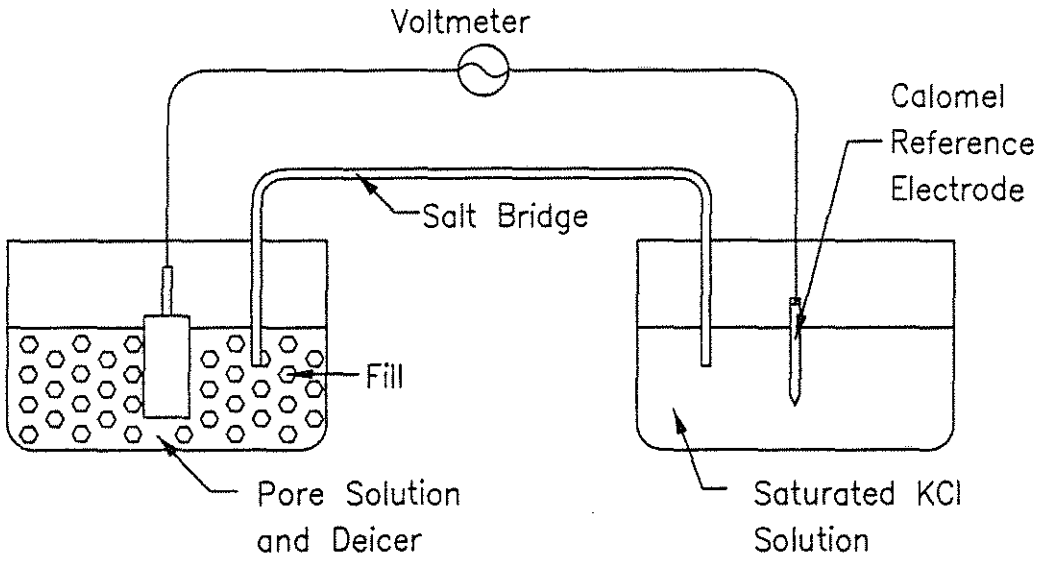

Fig. 3 Schematic of Corrosion Potential Test

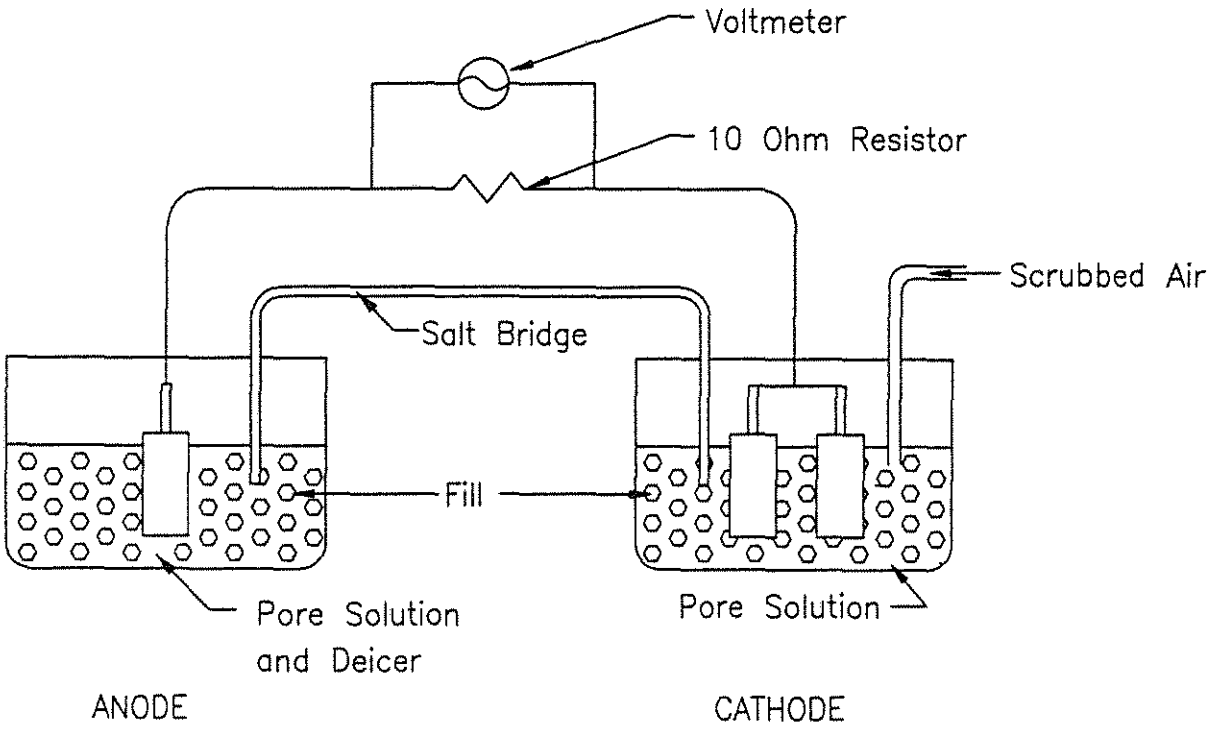

Fig. 4 Schematic of Macrocell Corrosion Test

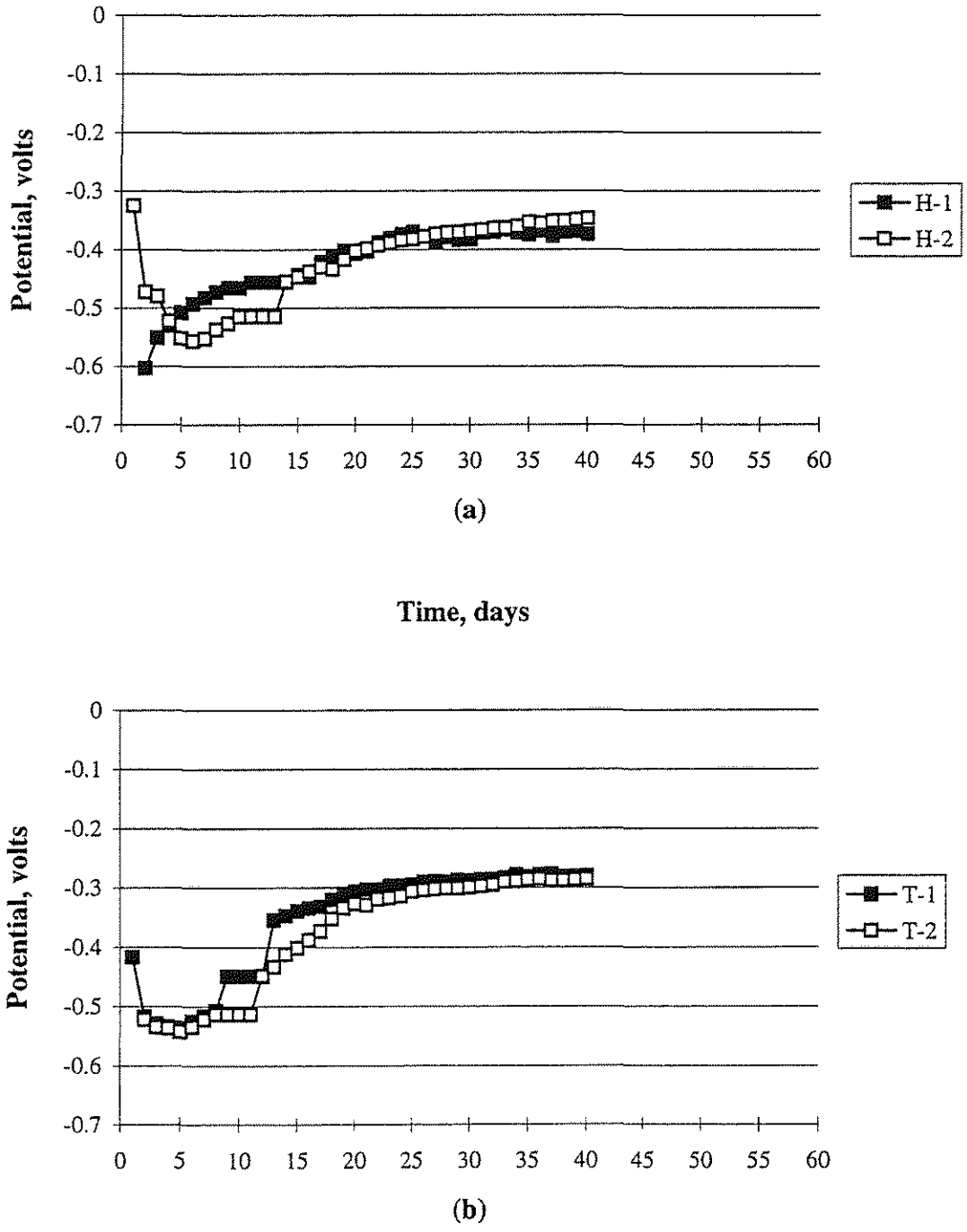

Fig. 5 Corrosion potential versus time for specimens exposed to 0.4 m NaCl in simulated pore solution. (a) H steel, (b) T steel, (c) CRSH steel, and (d) CRST steel.

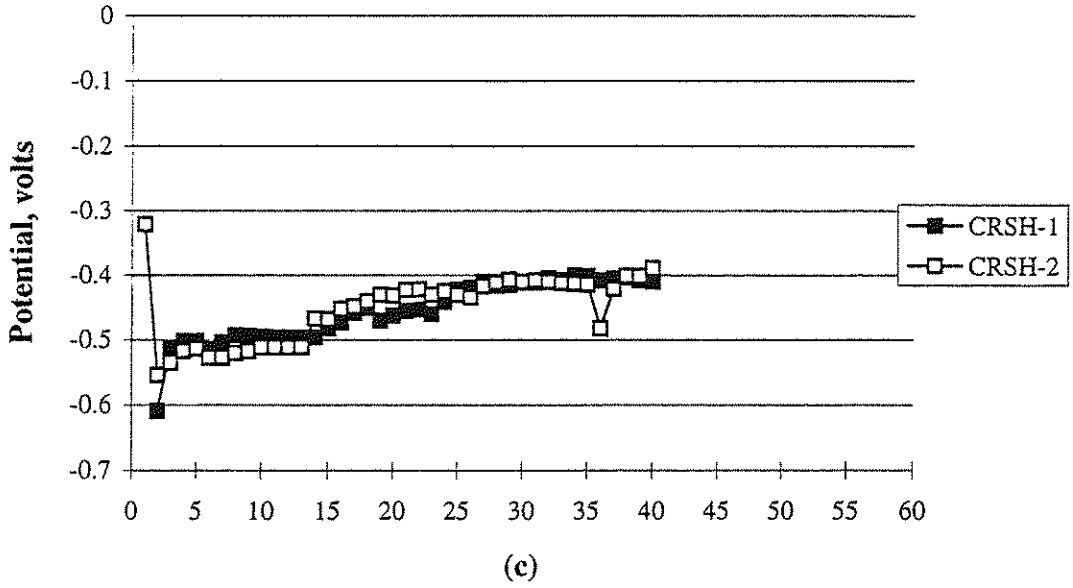

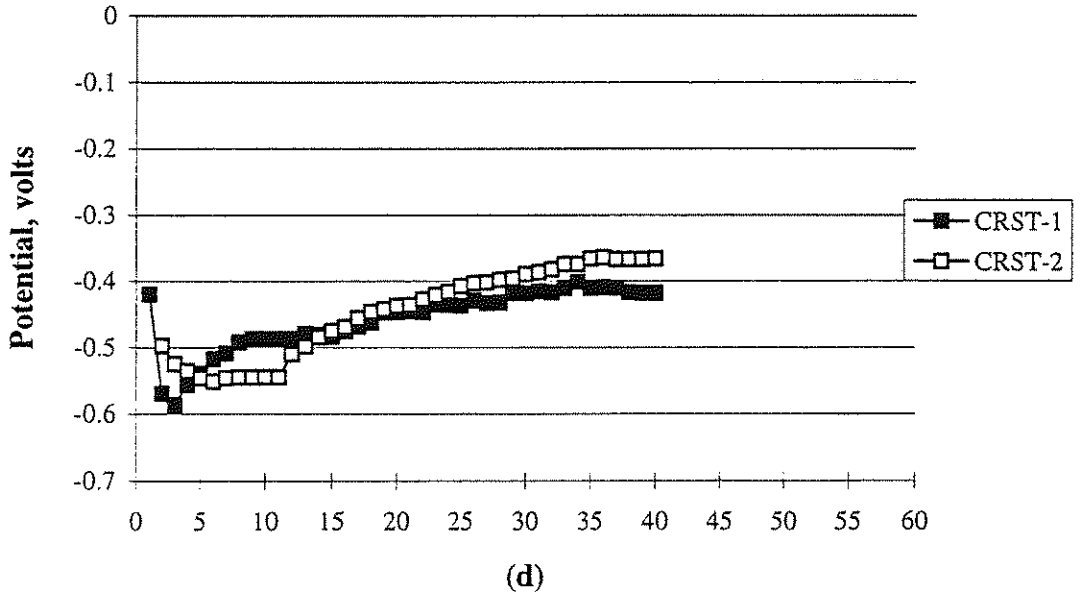

Fig. 5 Corrosion potential versus time for specimens exposed to 0.4 m NaCl in simulated pore solution. (a) H steel, (b) T steel, (c) CRSH steel, and (d) CRST steel.

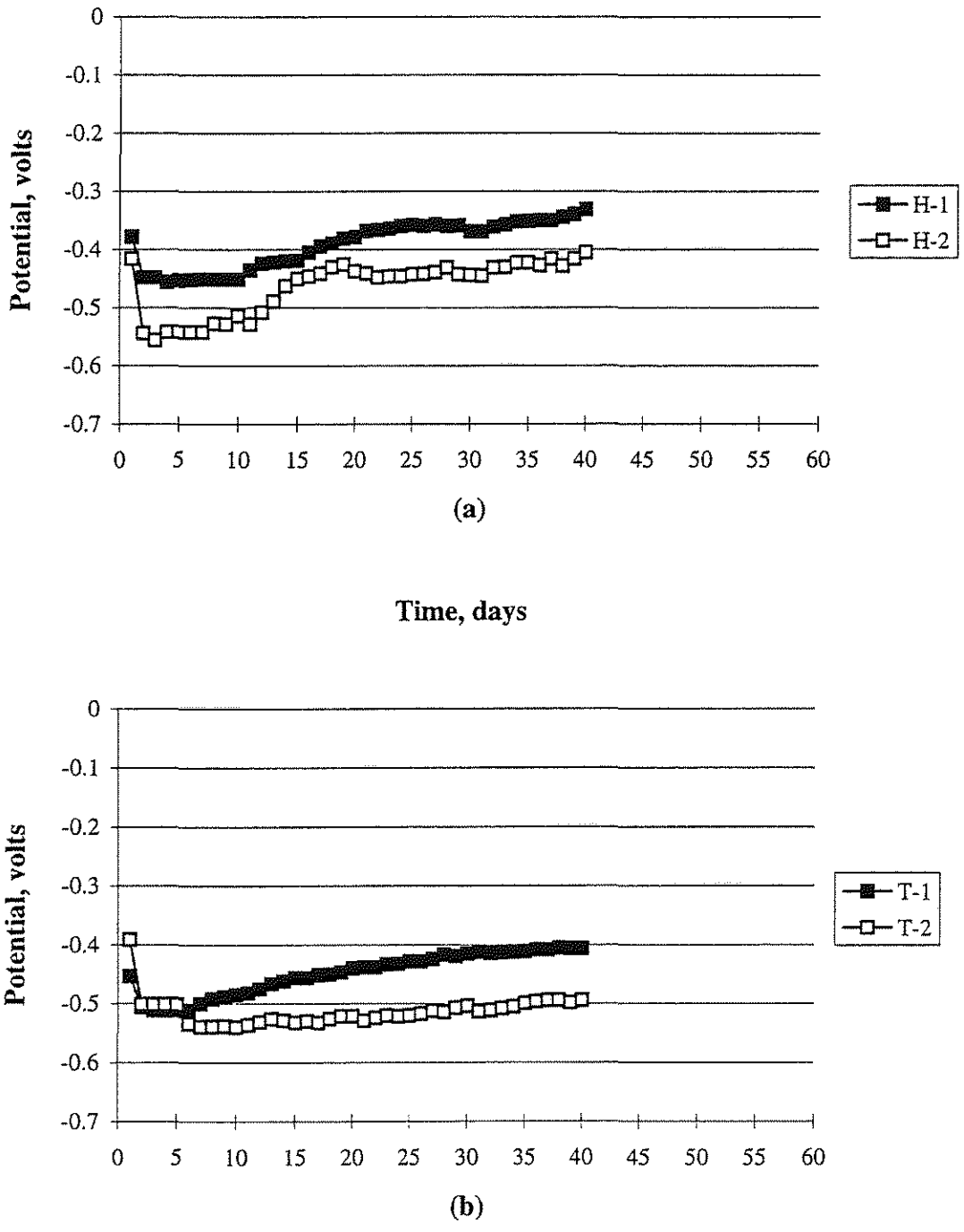

Fig. 6 Corrosion potential versus time for specimens exposed to 1.0 m NaCl in simulated pore solution. (a) H steel, (b) T steel, (c) CRSH steel, and (d) CRST steel.

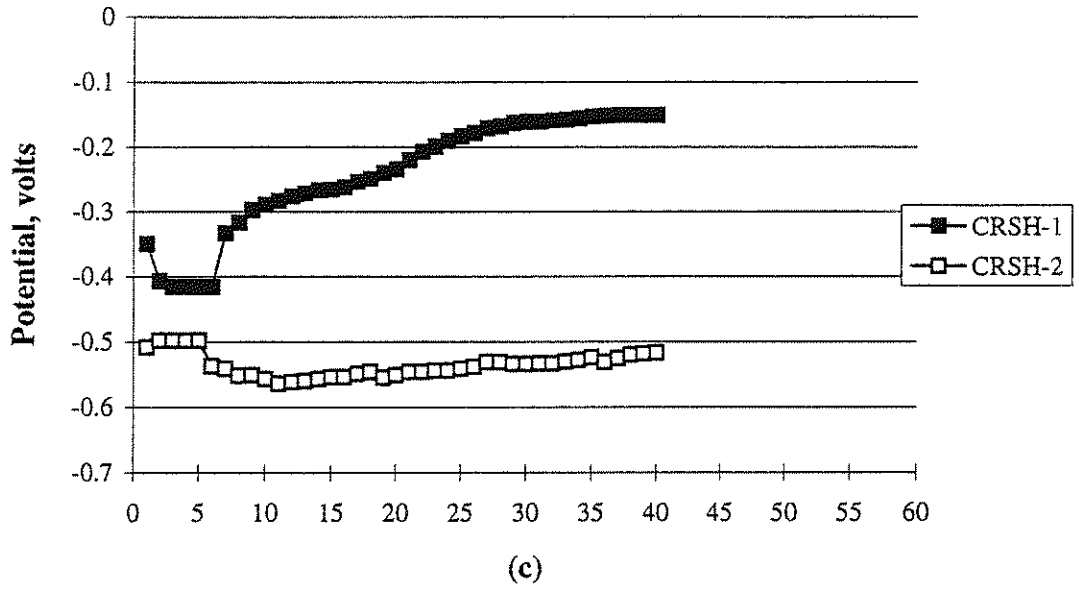

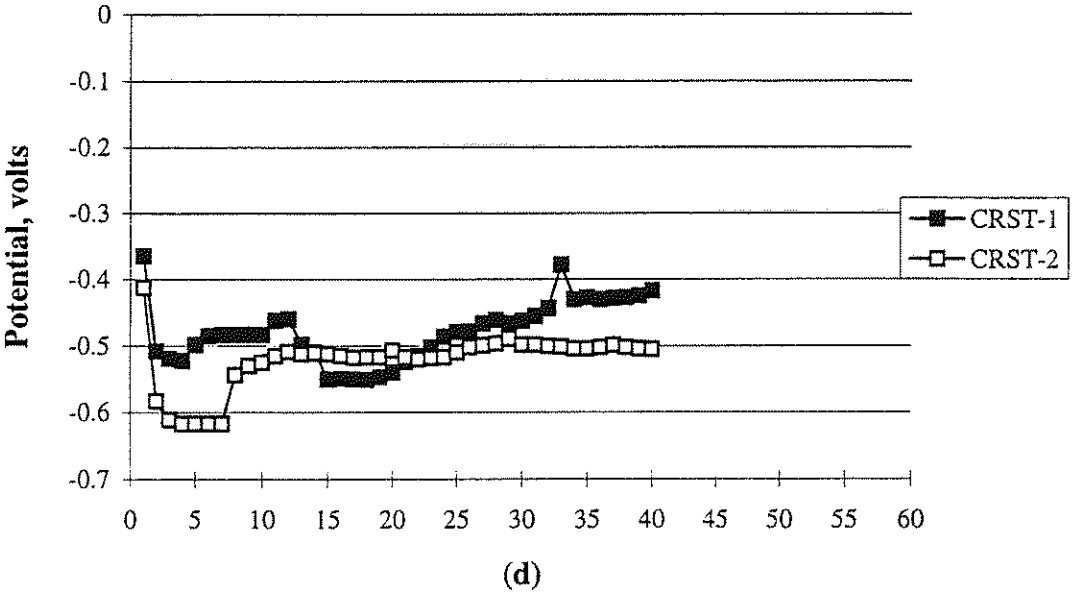

Fig. 6 Corrosion potential versus time for specimens exposed to 1.0 m NaCl in simulated pore solution. (a) H steel, (b) T steel, (c) CRSH steel, and (d) CRST steel.

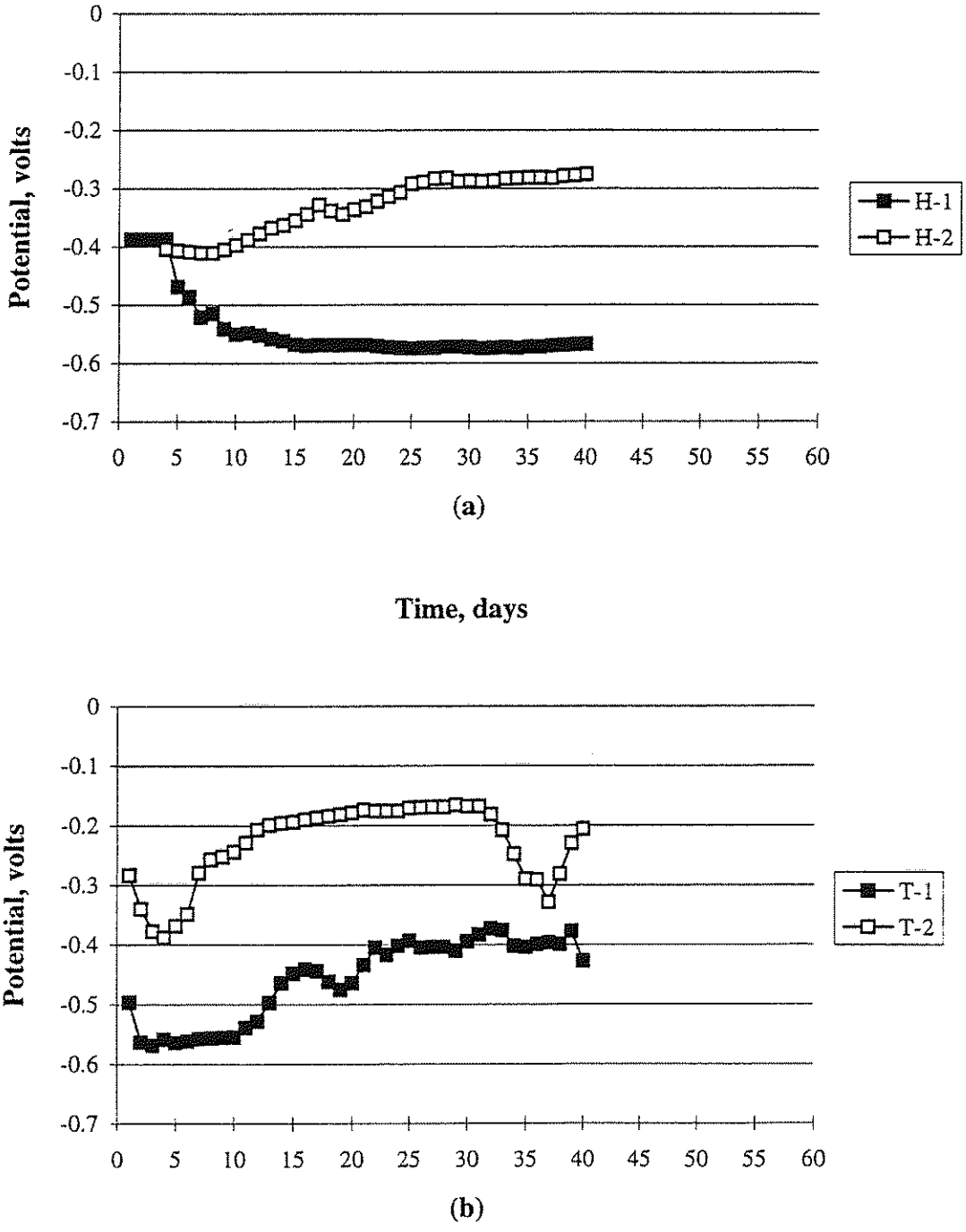

Fig. 7 Corrosion potential versus time for specimens exposed to 1.6 m NaCl in simulated pore solution. (a) H steel, (b) T steel, (c) CRSH steel, and (d) CRST steel.

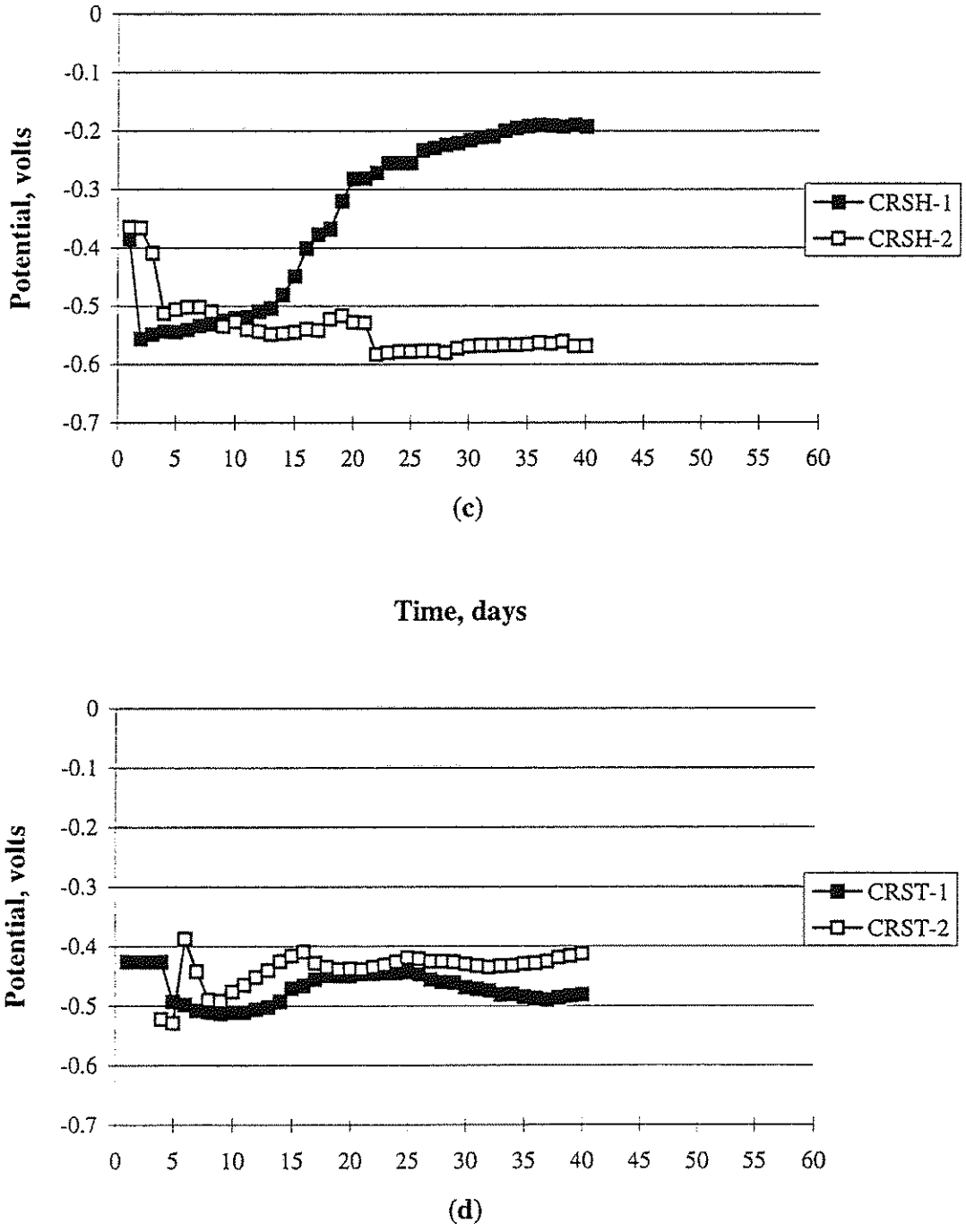

Fig. 7 Corrosion potential versus time for specimens exposed to 1.6 m NaCl in simulated pore solution. (a) H steel, (b) T steel, (c) CRSH steel, and (d) CRST steel.

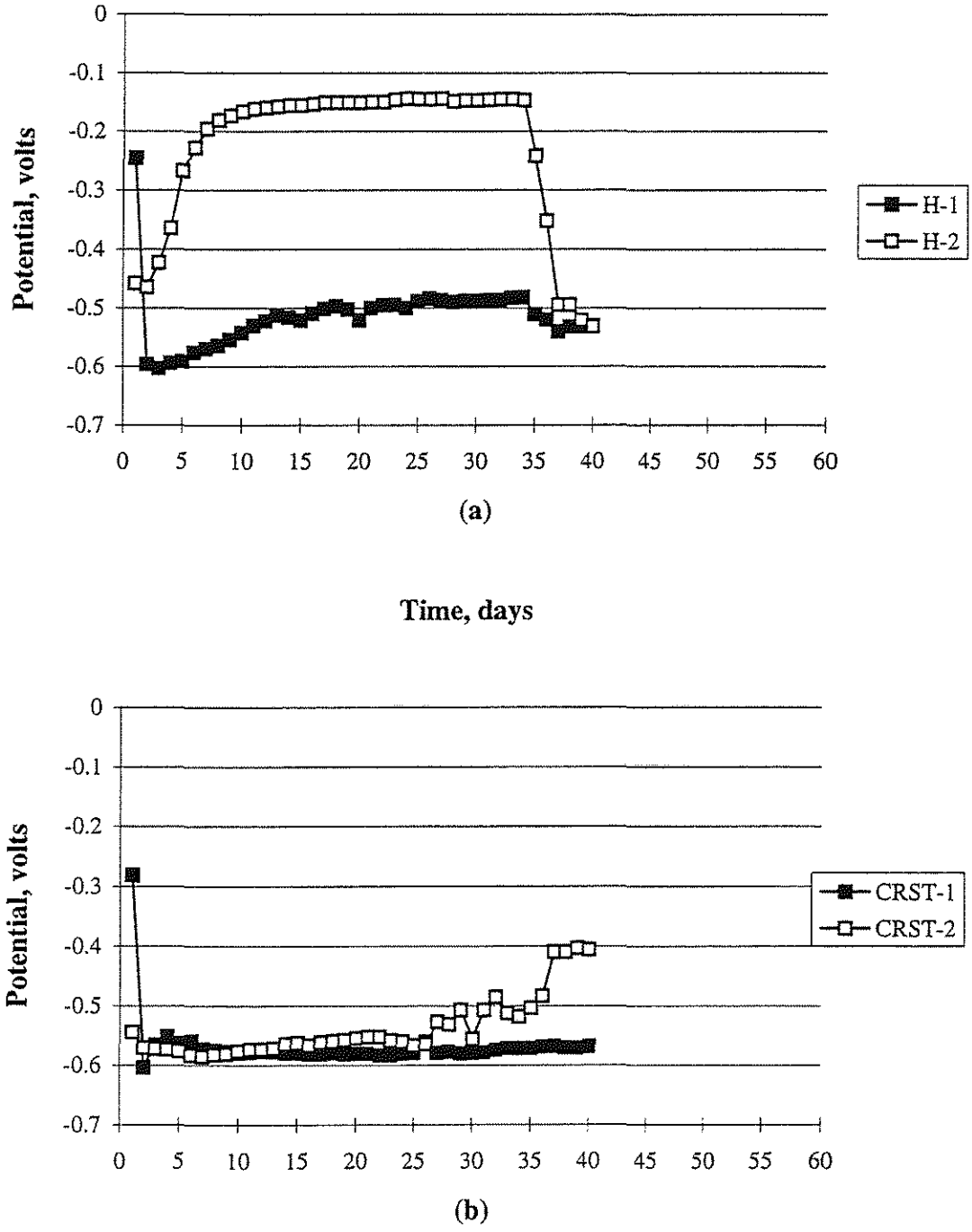

Fig. 8 Corrosion potential versus time for specimens exposed to 6.04 m NaCl in simulated pore solution. (a) H steel, (b) CRST steel.

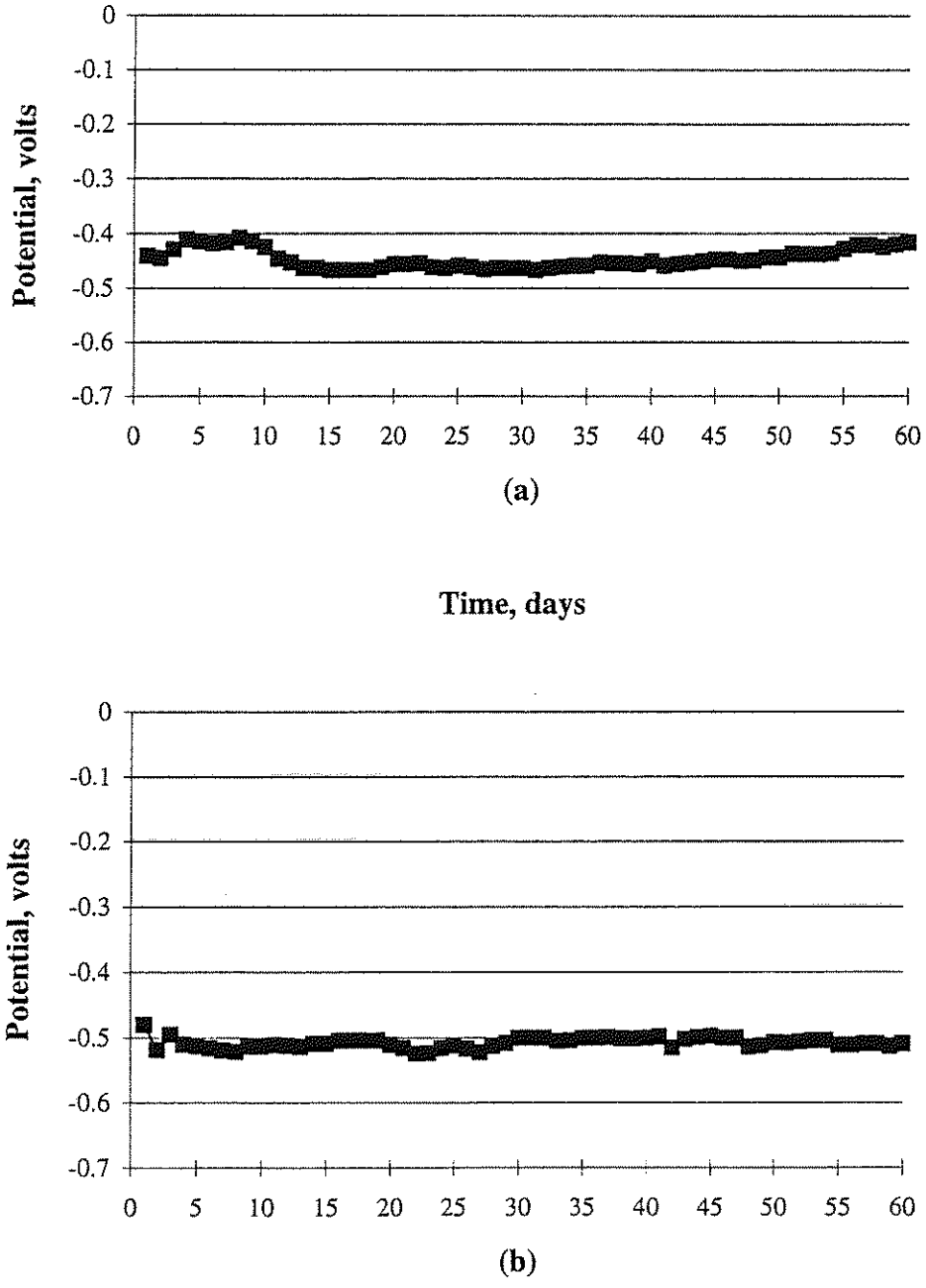

Fig. 9 Corrosion potential versus time for specimens exposed to 0.4 m $CaCl_2$ in simulated pore solution. (a) H steel, (b) T steel, (c) CRSH steel, and (d) CRST steel.

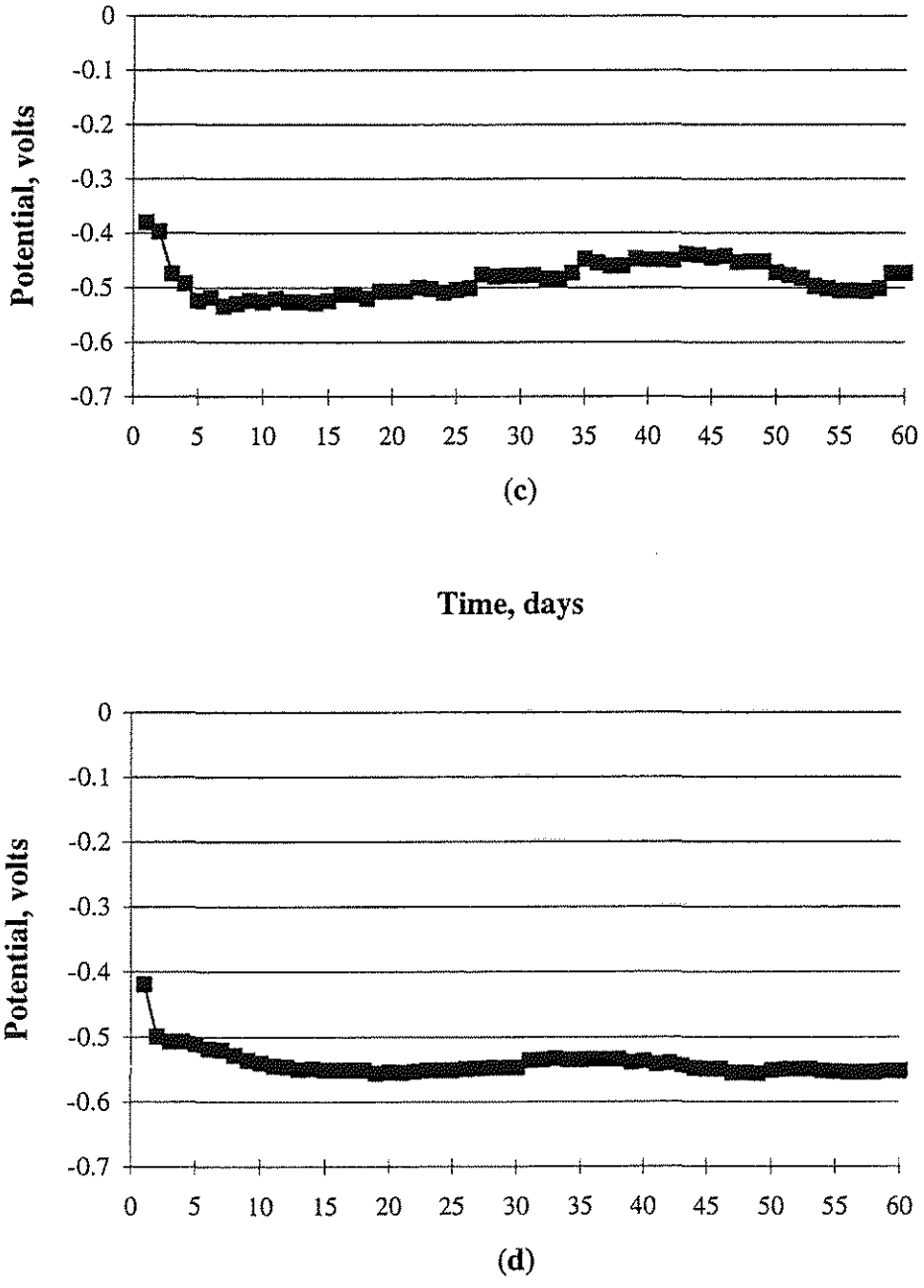

Fig. 9 Corrosion potential versus time for specimens exposed to 0.4 m $CaCl_2$ in simulated pore solution. (a) H steel, (b) T steel, (c) CRSH steel, and (d) CRST steel.

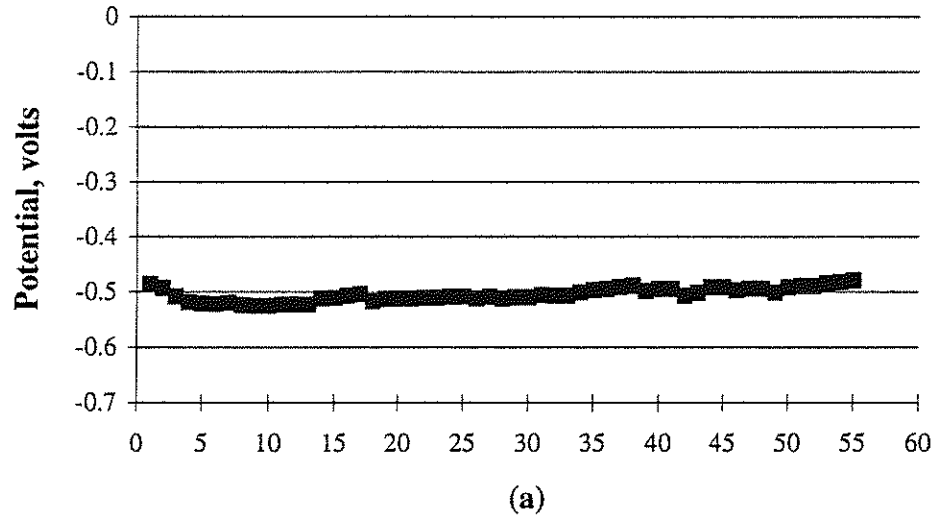

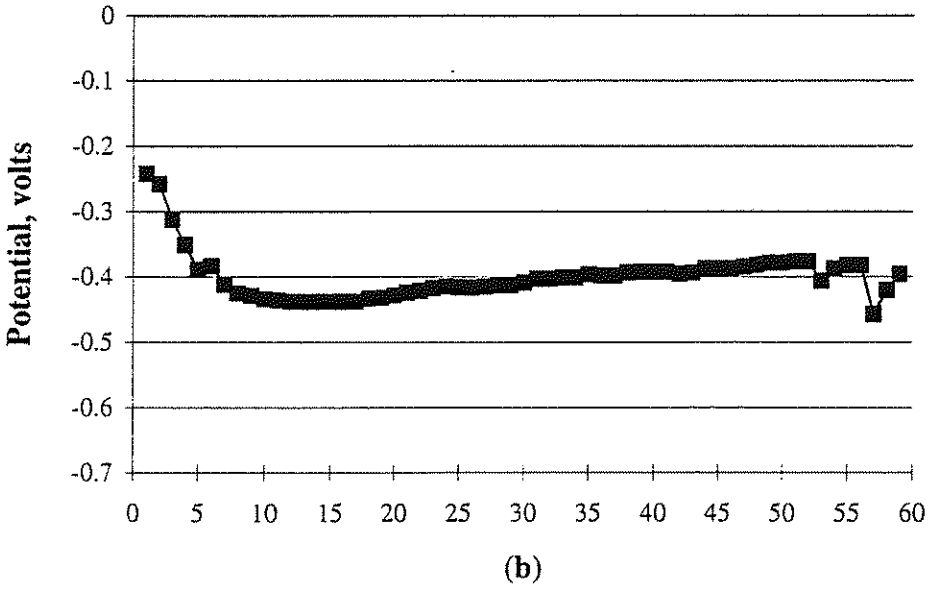

Fig. 10 Corrosion potential versus time for specimens exposed to 1.6 m $CaCl_2$ in simulated pore solution. (a) H steel, (b) T steel, (c) CRSH steel, and (d) CRST steel.

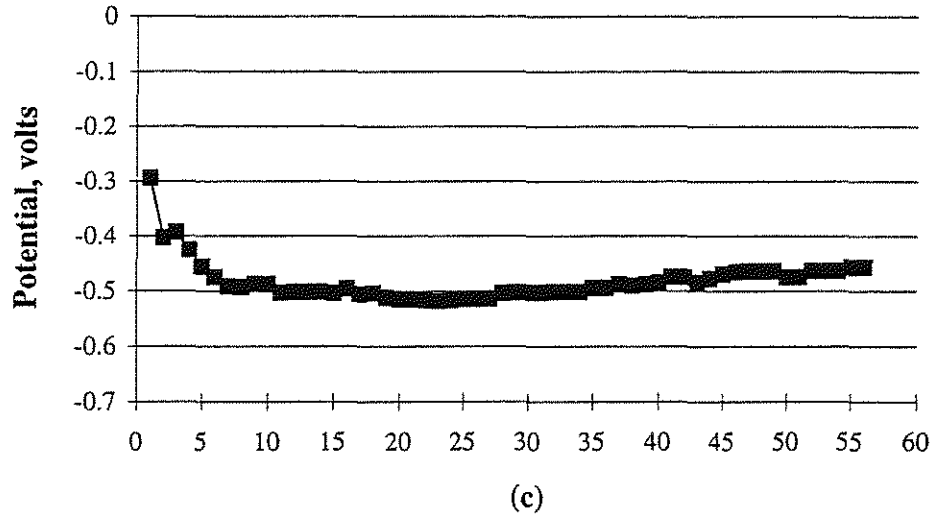

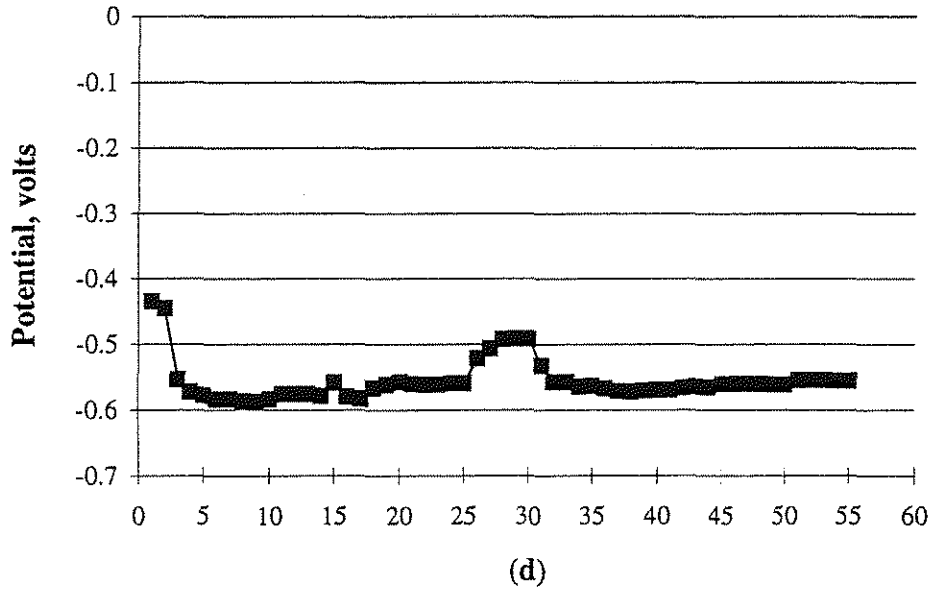

Fig. 10 Corrosion potential versus time for specimens exposed to 1.6 m $CaCl_2$ in simulated pore solution. (a) H steel, (b) T steel, (c) CRSH steel, and (d) CRST steel.

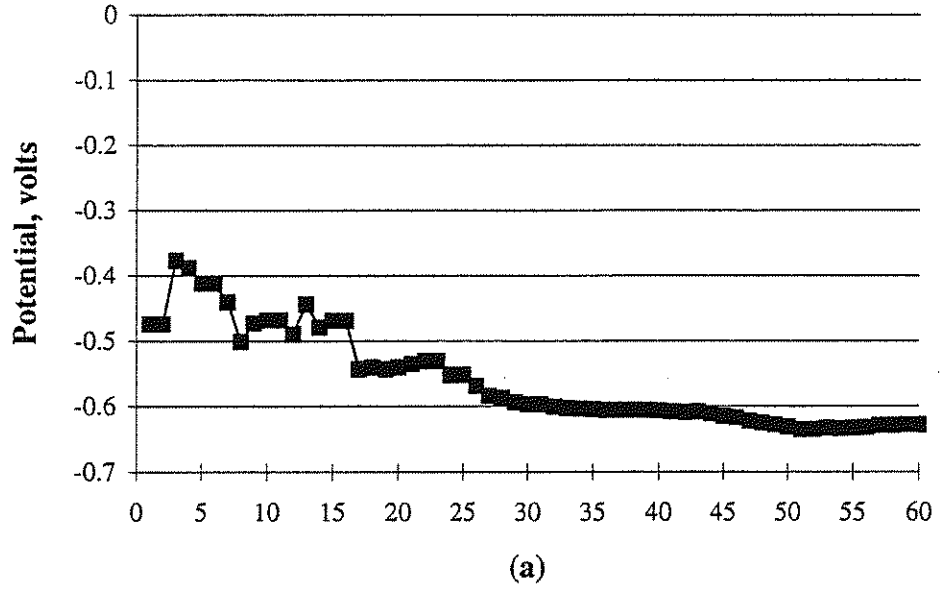

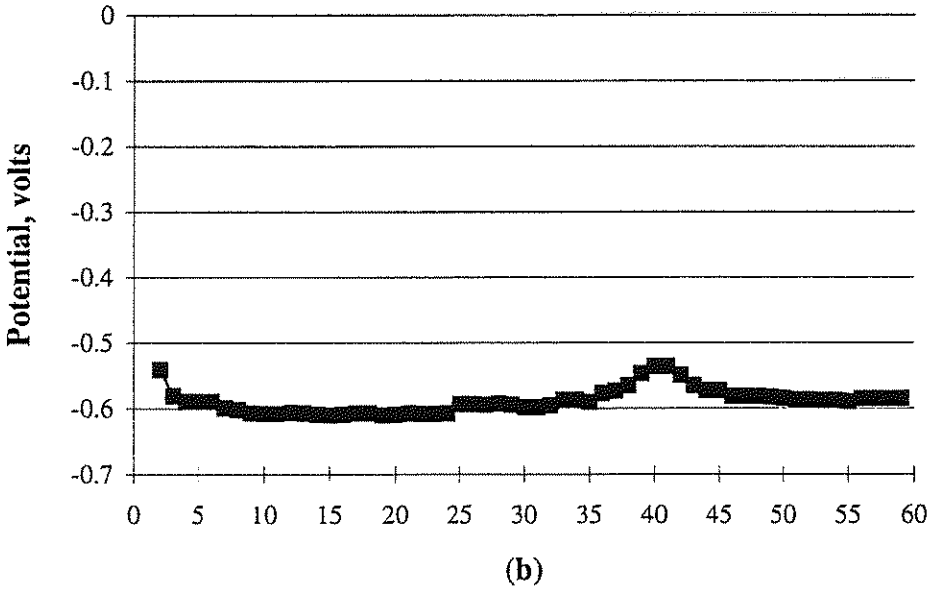

Fig. 11 Corrosion potential versus time for specimens exposed to 6.04 m $CaCl_2$ in simulated pore solution. (a) H steel, (b) T steel, (c) CRSH steel, and (d) CRST steel.

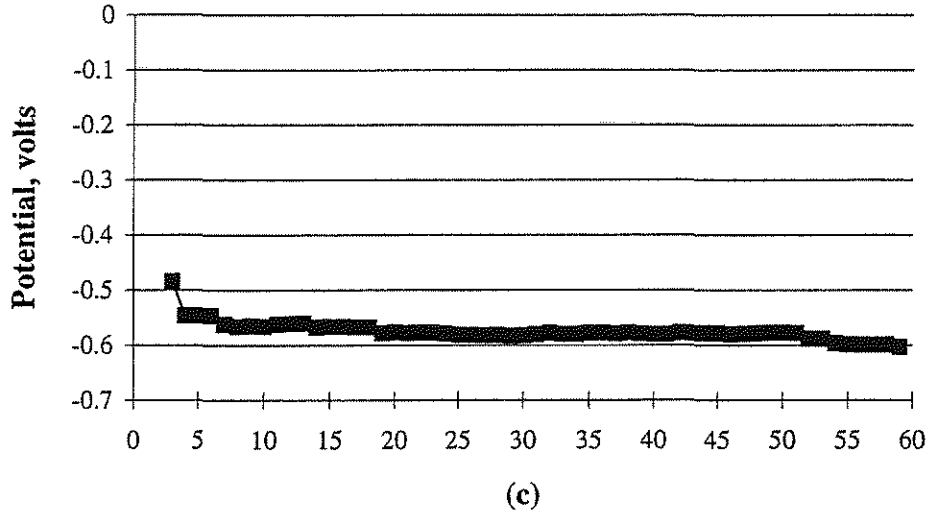

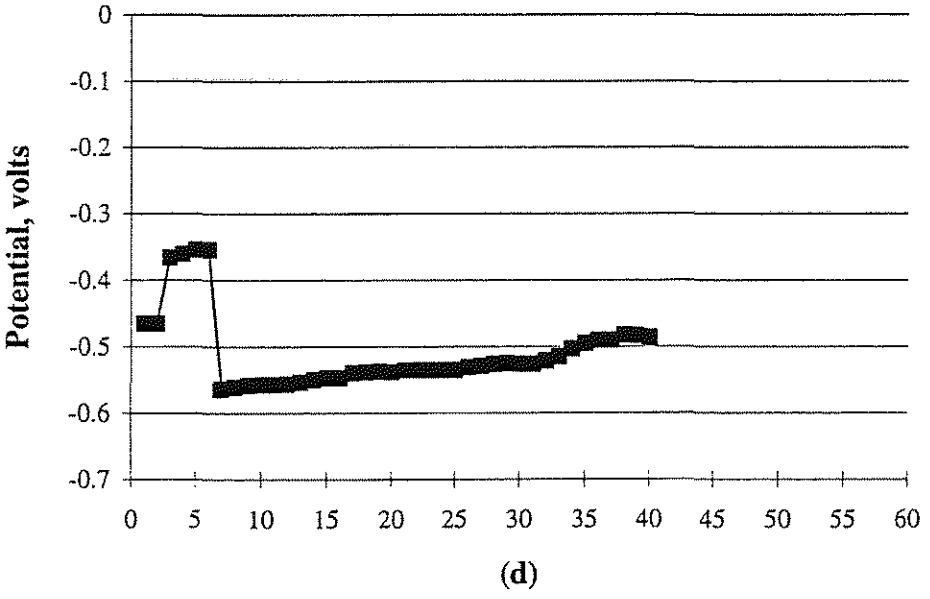

Fig. 11 Corrosion potential versus time for specimens exposed to 6.04 m $CaCl_2$ in simulated pore solution. (a) H steel, (b) T steel, (c) CRSH steel, and (d) CRST steel.

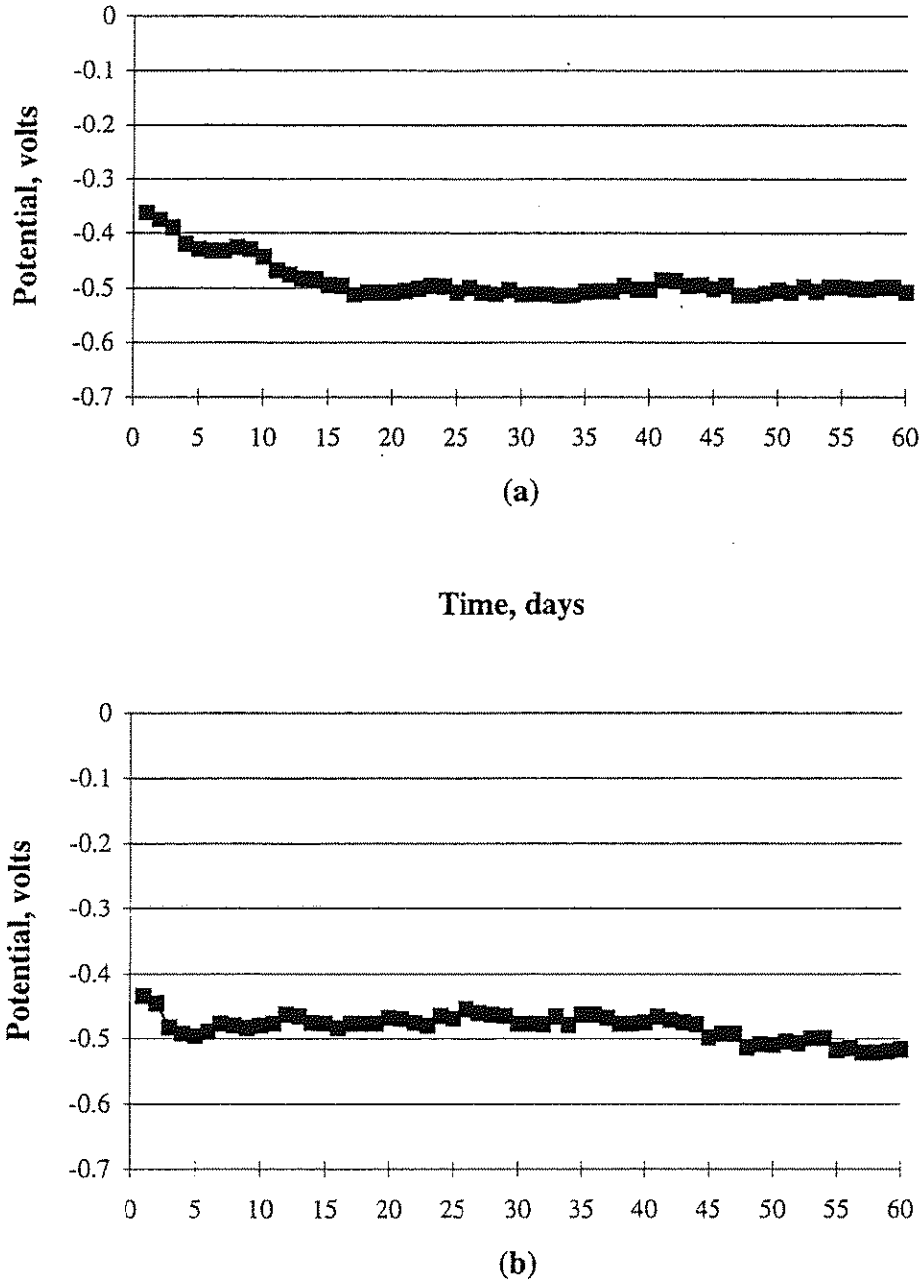

Fig. 12 Corrosion potential versus time for specimens exposed to 0.4 m CMA in simulated pore solution. (a) H steel, (b) T steel, (c) CRSH steel, and (d) CRST steel.

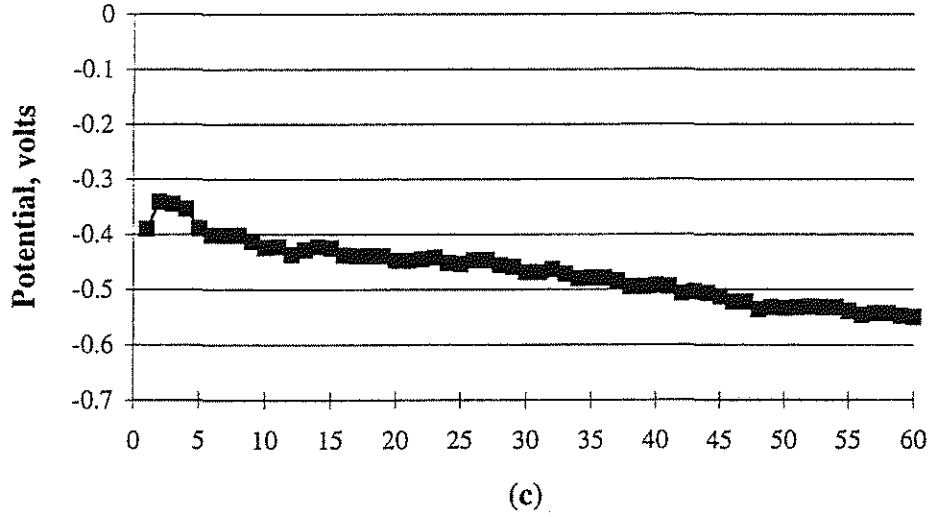

Time, days

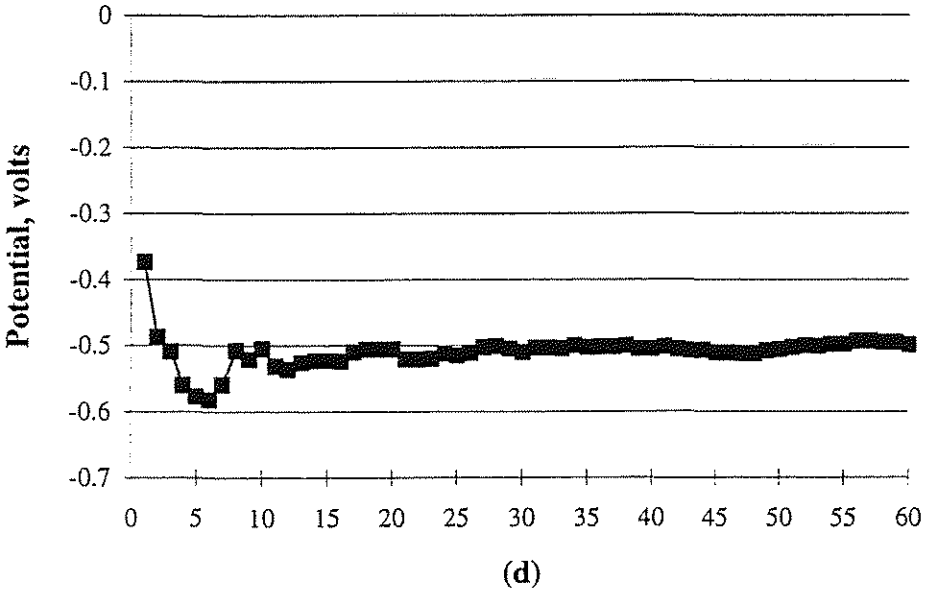

Fig. 12 Corrosion potential versus time for specimens exposed to 0.4 m CMA in simulated pore solution. (a) H steel, (b) T steel, (c) CRSH steel, and (d) CRST steel.

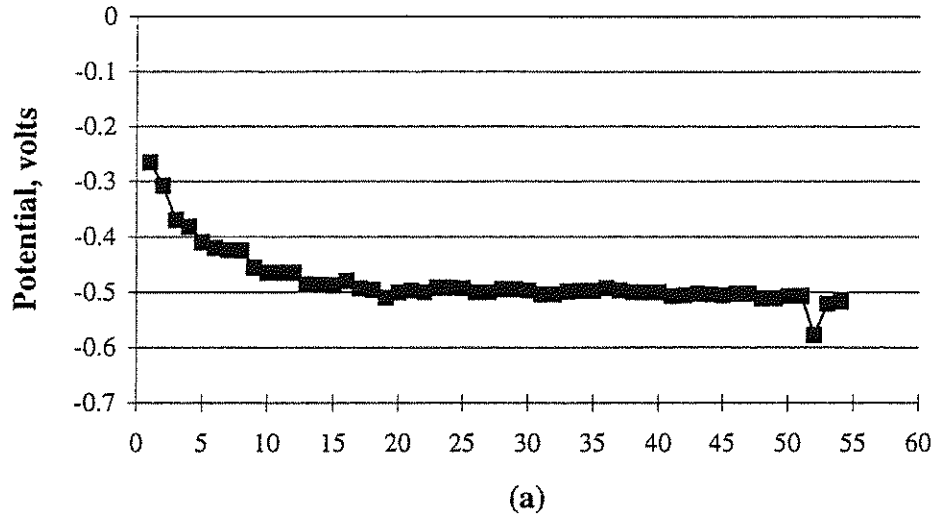

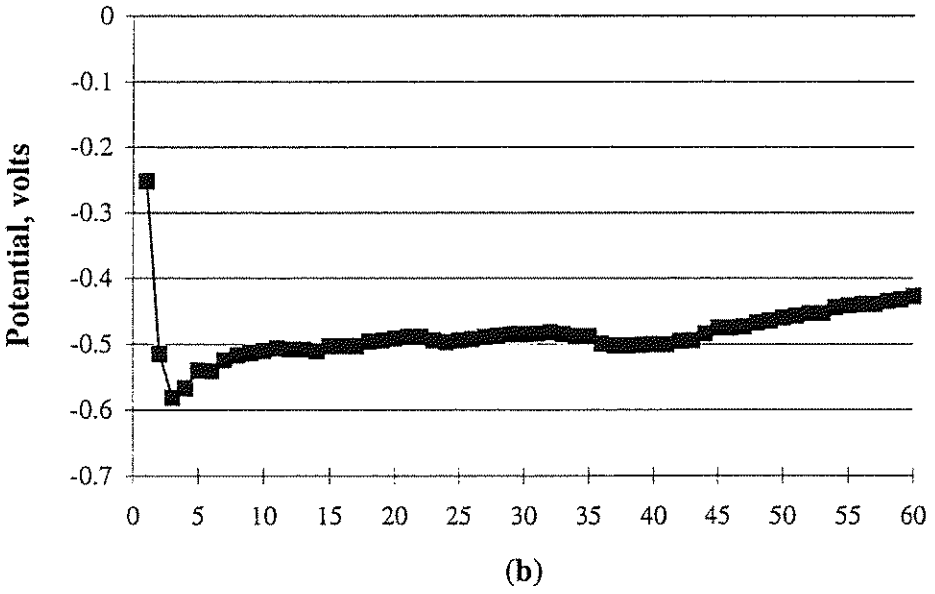

Fig. 13 Corrosion potential versus time for specimens exposed to 1.6 m CMA in simulated pore solution. (a) H steel, (b) T steel, (c) CRSH steel, and (d) CRST steel.

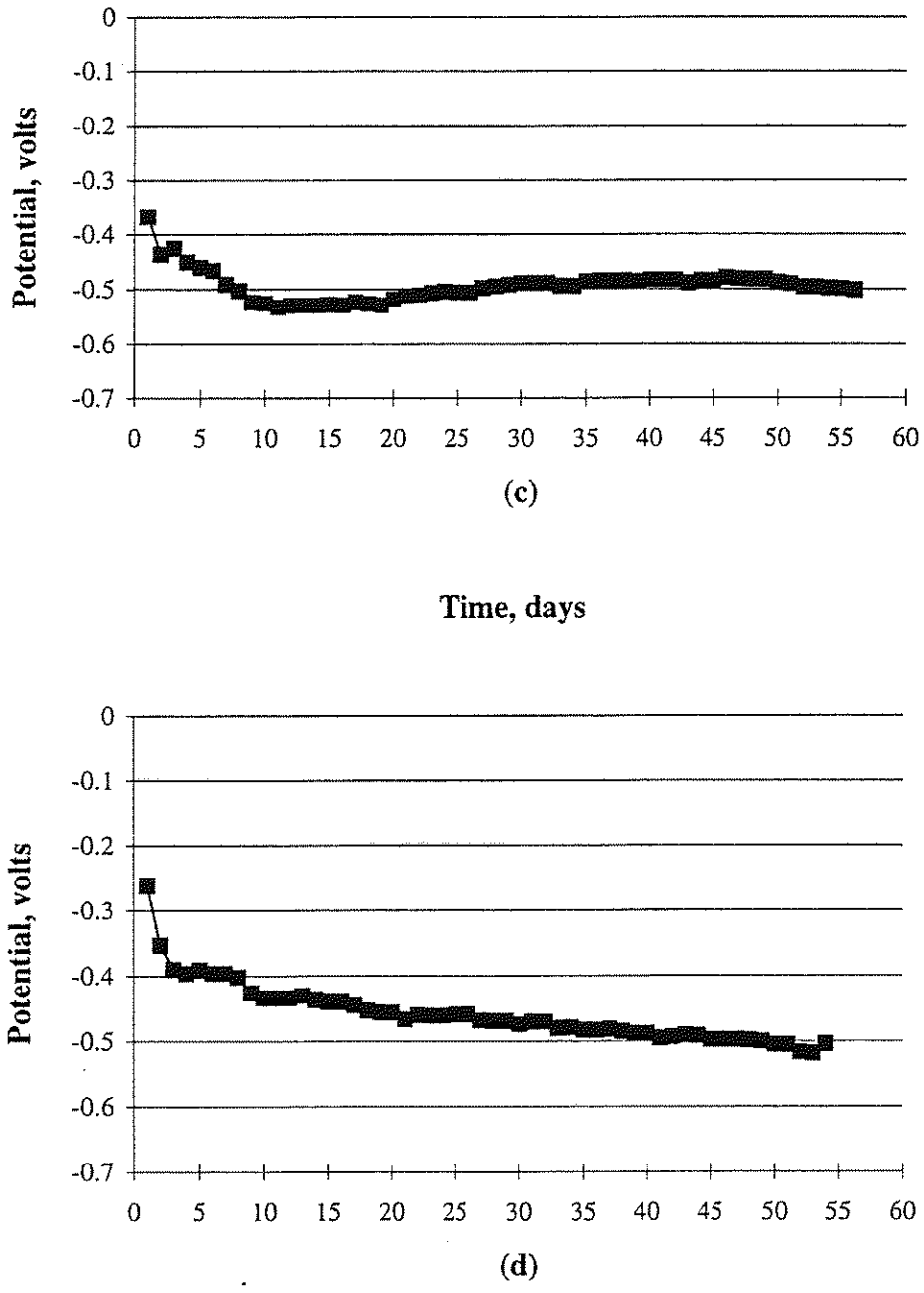

Fig. 13 Corrosion potential versus time for specimens exposed to 1.6 m CMA in simulated pore solution. (a) H steel, (b) T steel, (c) CRSH steel, and (d) CRST steel.

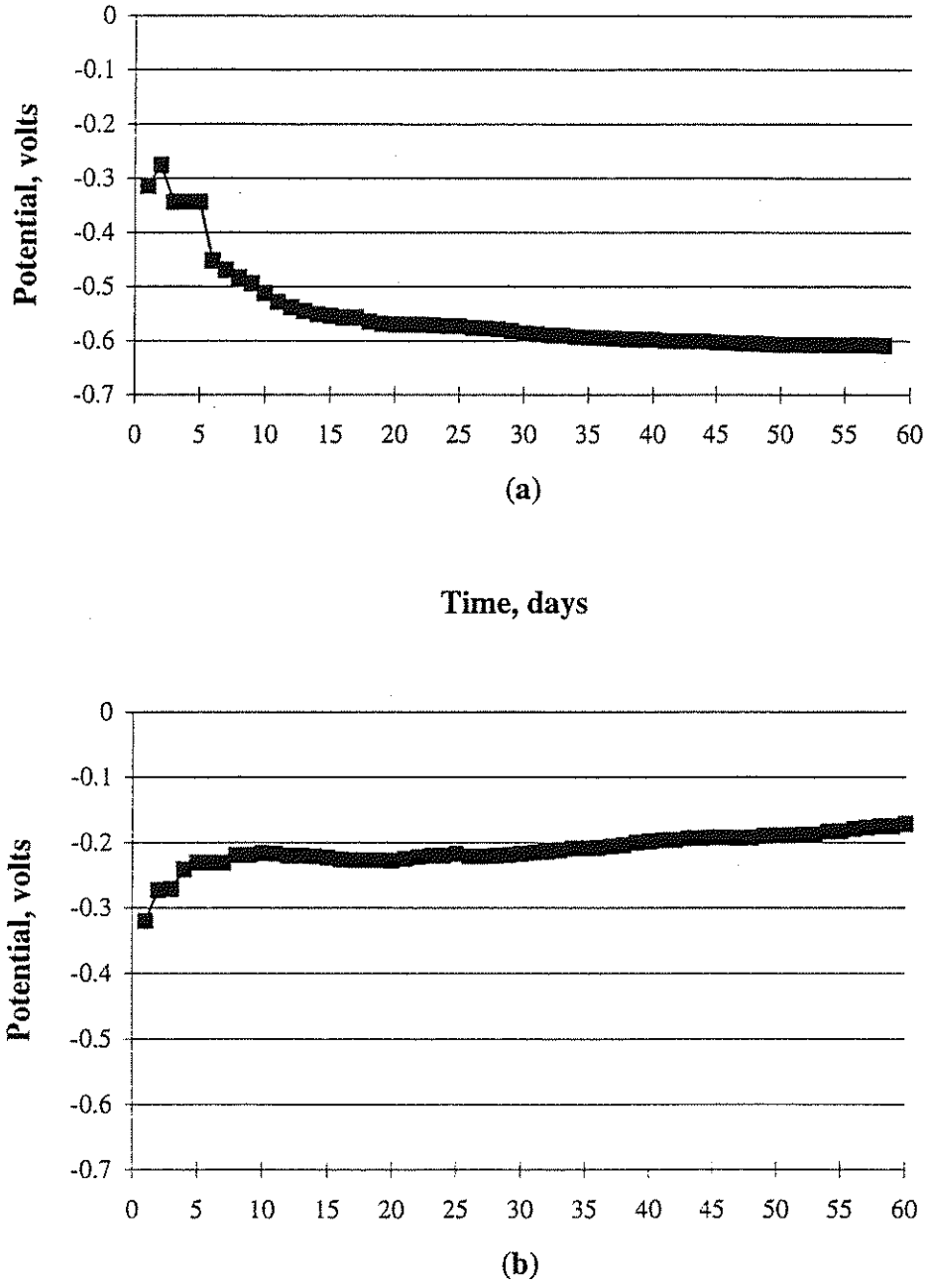

Fig. 14 Corrosion potential versus time for specimens exposed to 6.04 m CMA in simulated pore solution. (a) H steel, (b) T steel, (c) CRSH steel, and (d) CRST steel.

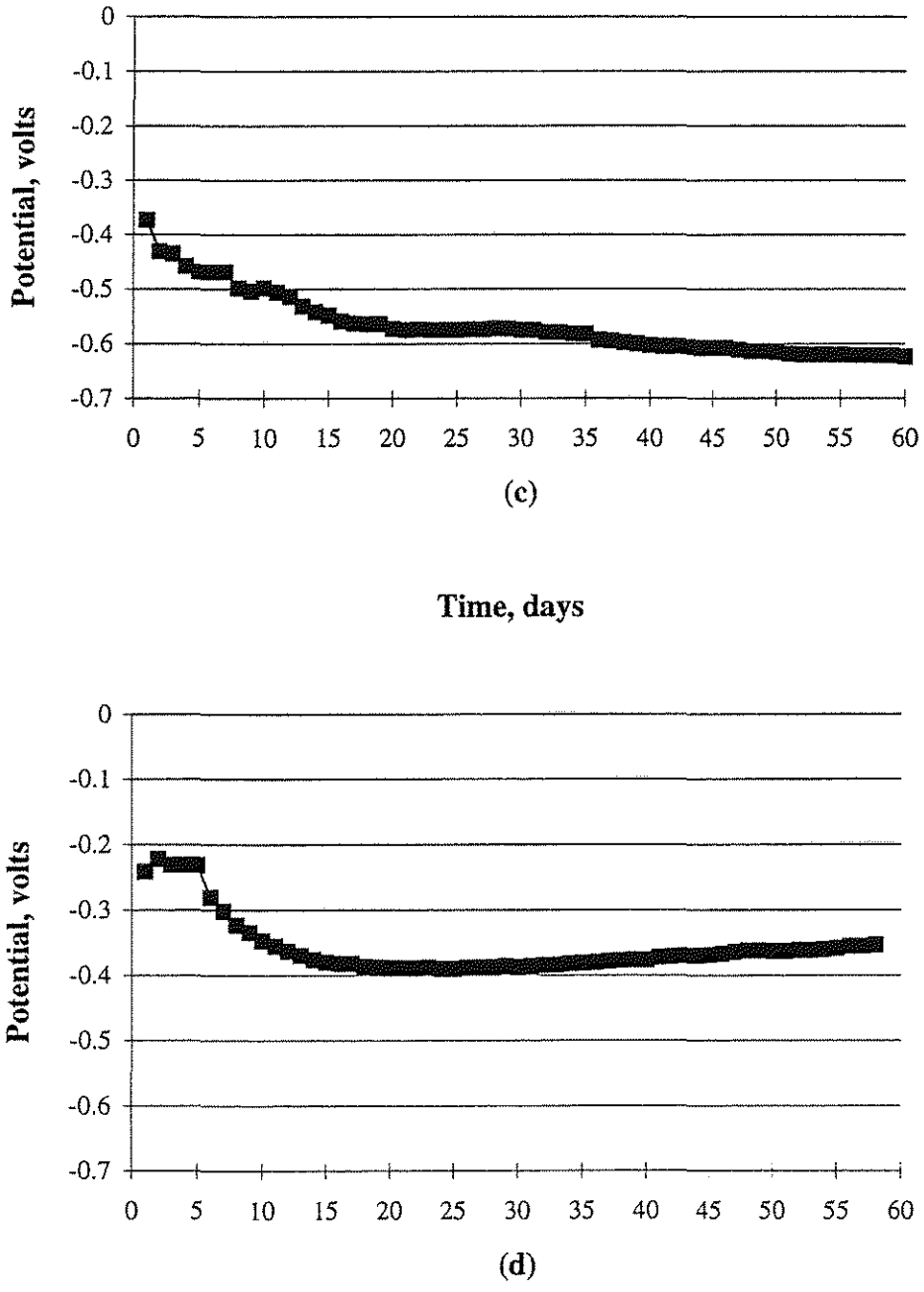

Fig. 14 Corrosion potential versus time for specimens exposed to 6.04 m CMA in simulated pore solution. (a) H steel, (b) T steel, (c) CRSH steel, and (d) CRST steel.

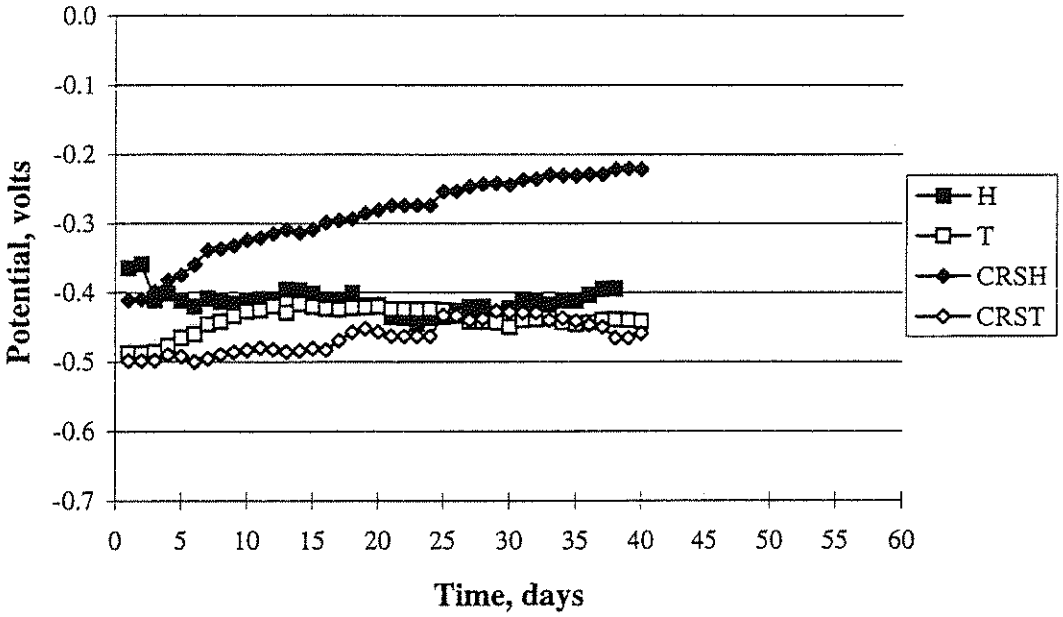

Fig. 15 Corrosion potential versus time for specimens exposed to simulated pore solution.

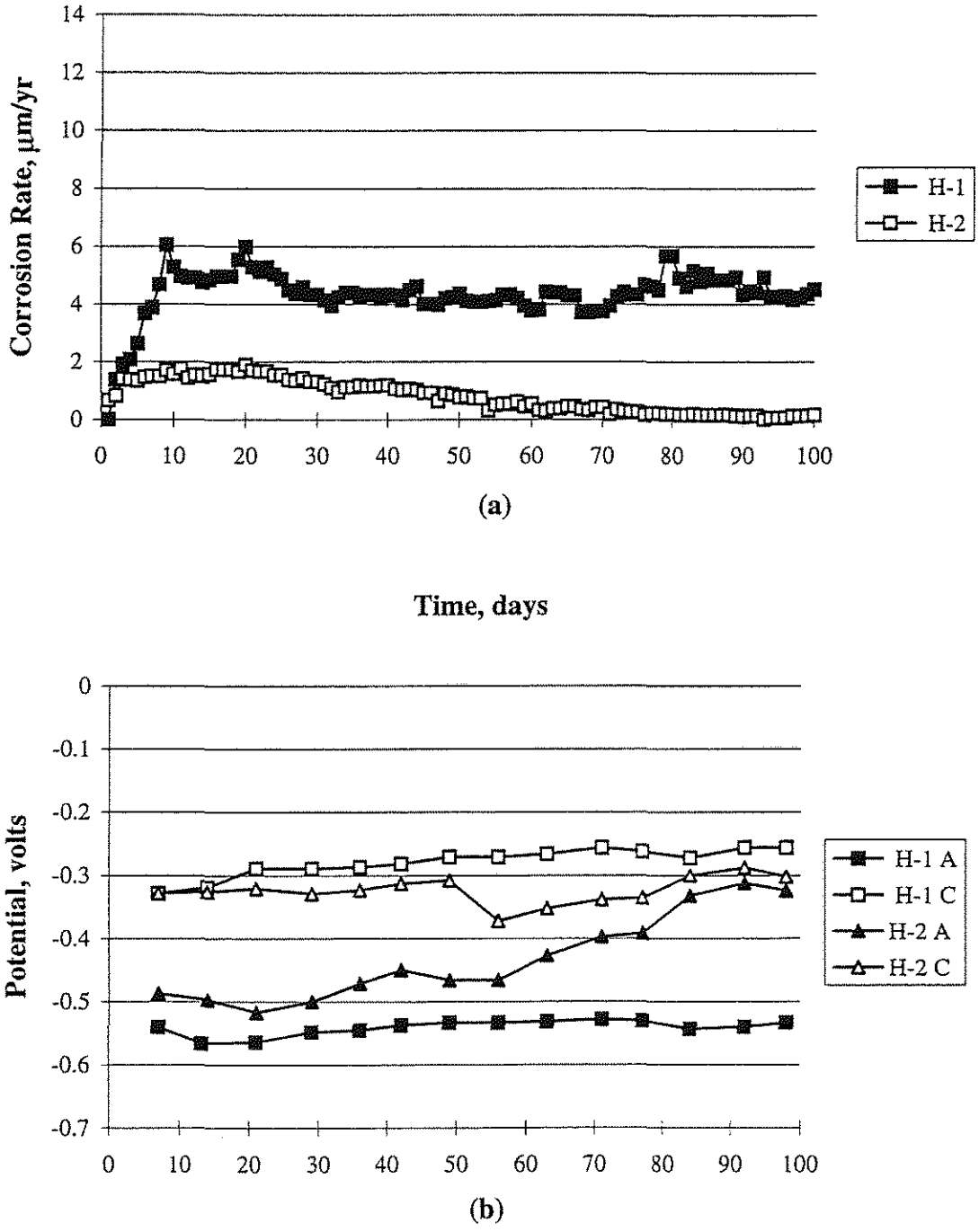

Fig. 16 H steel specimens exposed to 0.4 m $CaCl_2$ in simulated pore solution: (a) Macrocell corrosion rate, (b) Corrosion potential.

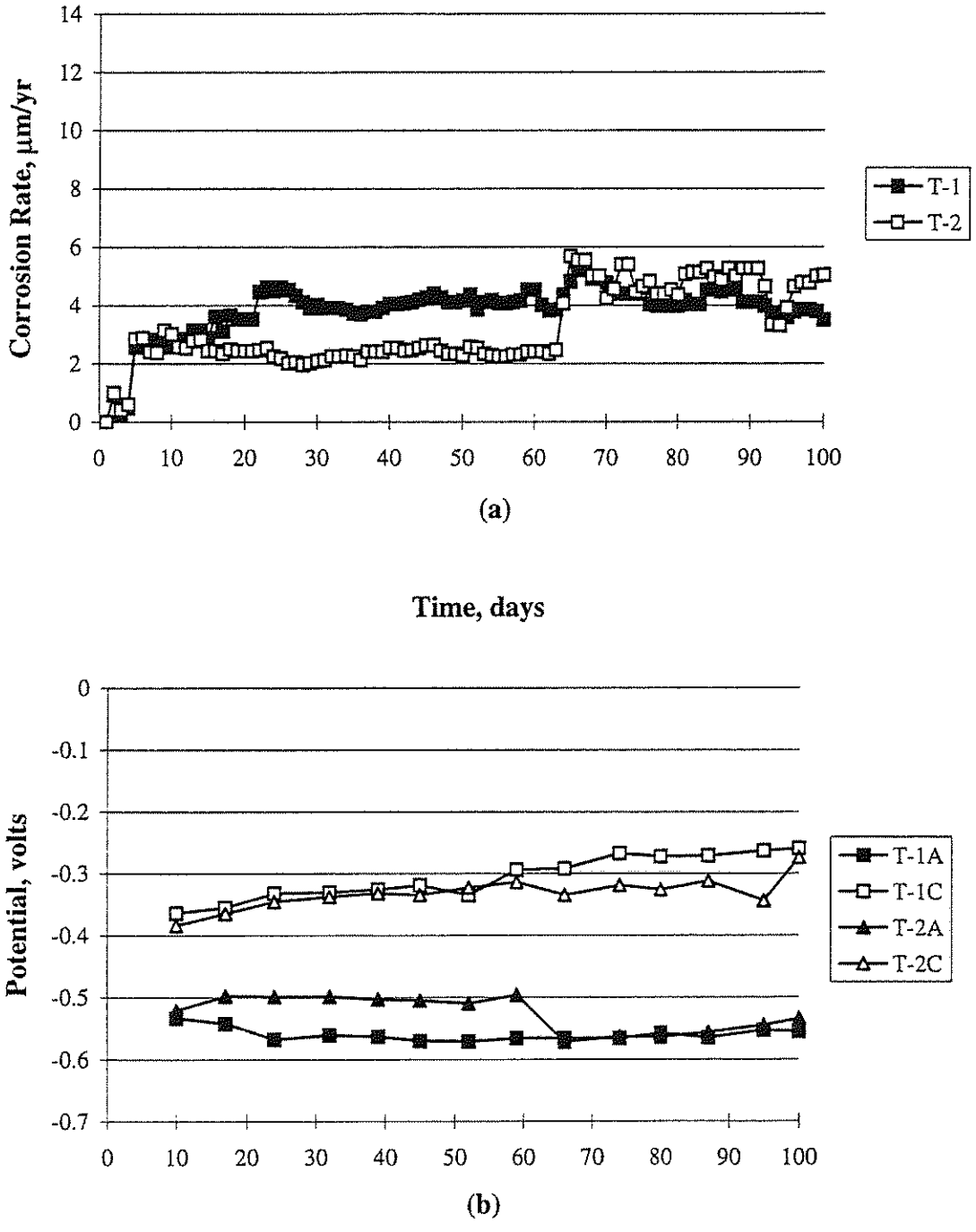

Fig. 17 T steel specimens exposed to 0.4 m $CaCl_2$ in simulated pore solution: (a) Macrocell corrosion rate, (b) Corrosion potential.

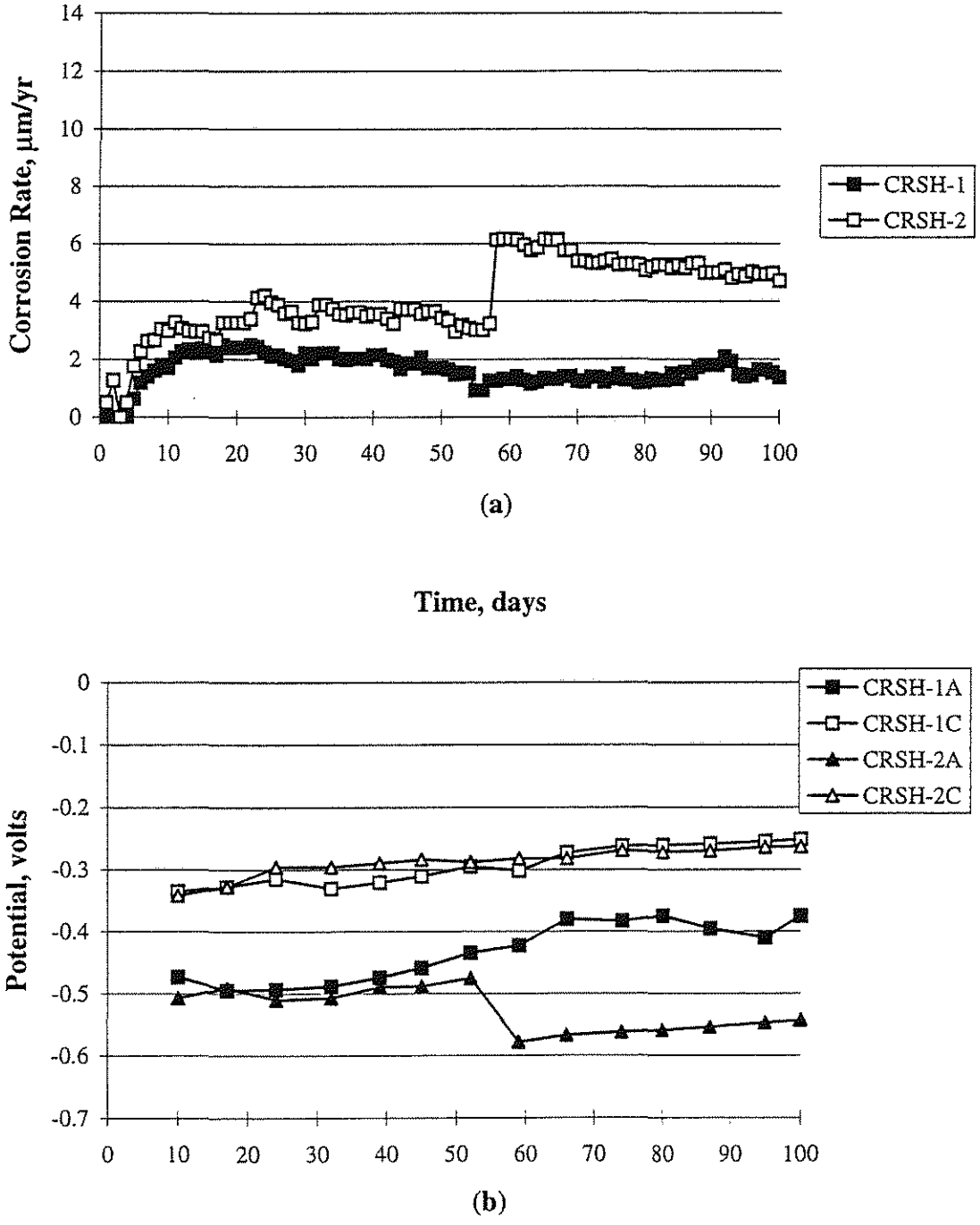

Fig. 18 CRSH steel specimens exposed to 0.4 m $CaCl_2$ in simulated pore solution: (a) Macrocell corrosion rate, (b) Corrosion potential.

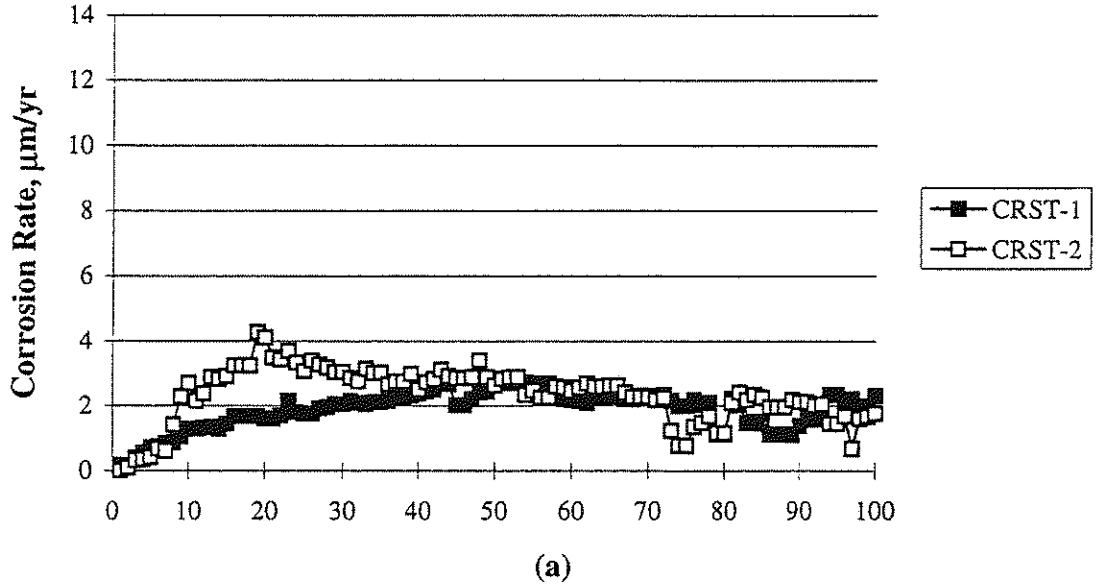

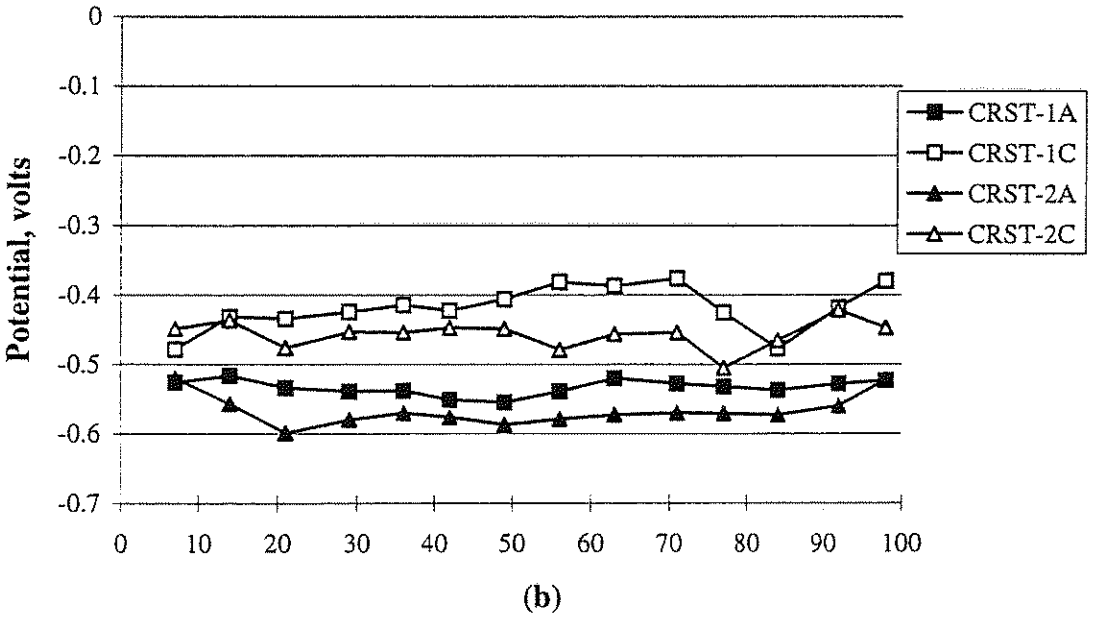

Fig. 19 CRST steel specimens exposed to 0.4 m $CaCl_2$ in simulated pore solution: (a) Macrocell corrosion rate, (b) Corrosion potential.

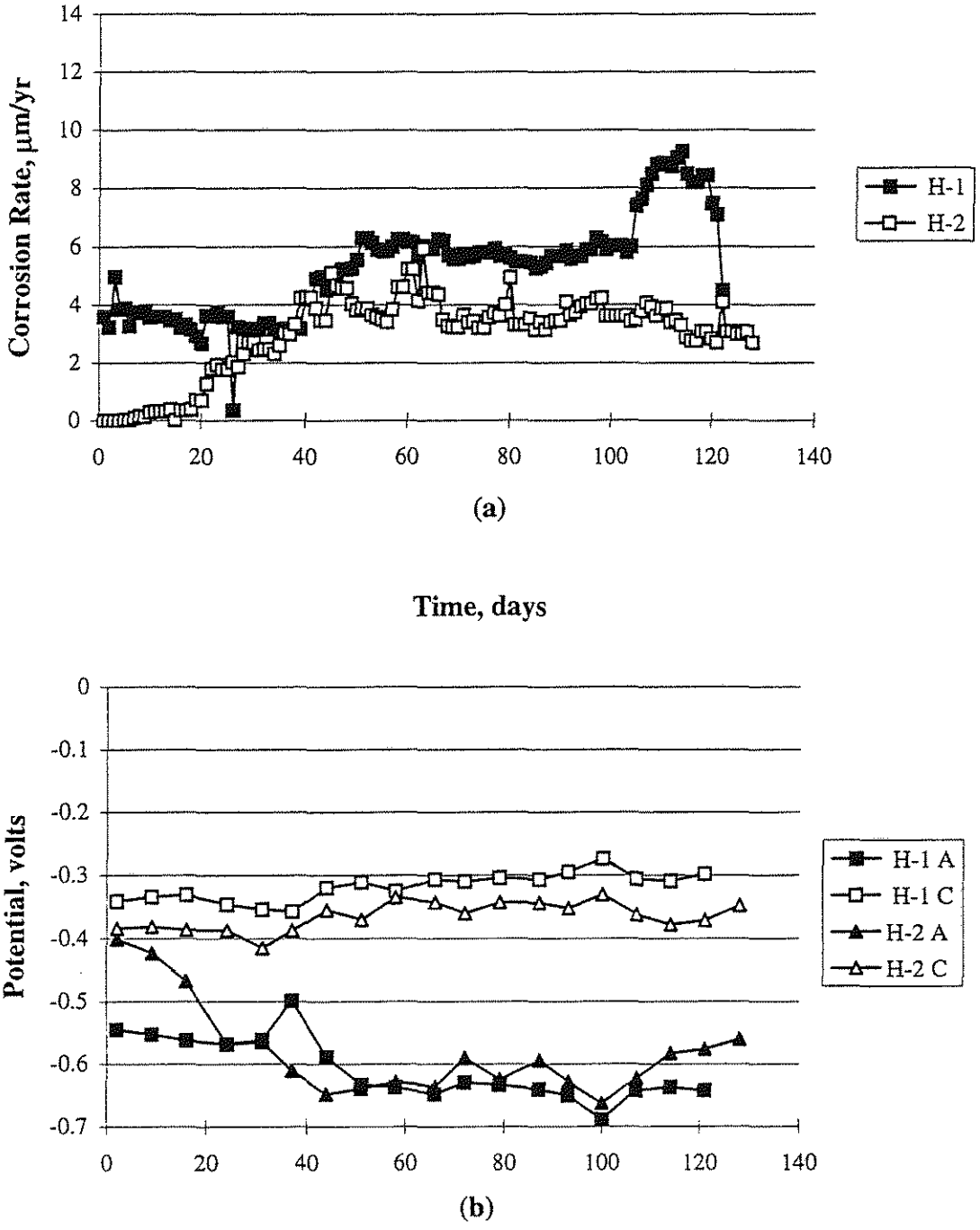

Fig. 20 H steel specimens exposed to 1.6 m $CaCl_2$ in simulated pore solution: (a) Macrocell corrosion rate, (b) Corrosion potential

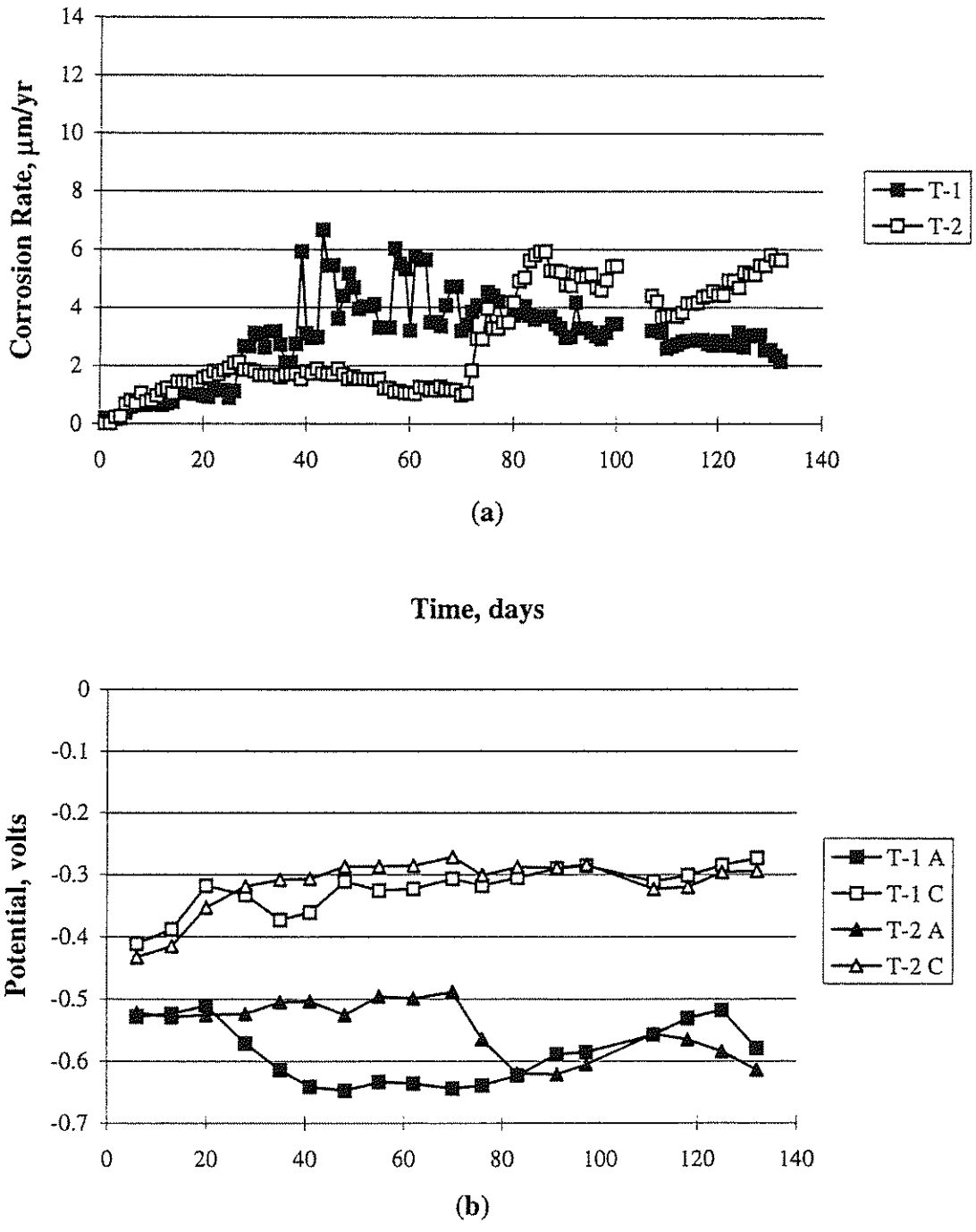

Fig. 21 T steel specimens exposed to 1.6 m $CaCl_2$ in simulated pore solution: (a) Macrocell corrosion rate, (b) Corrosion potential

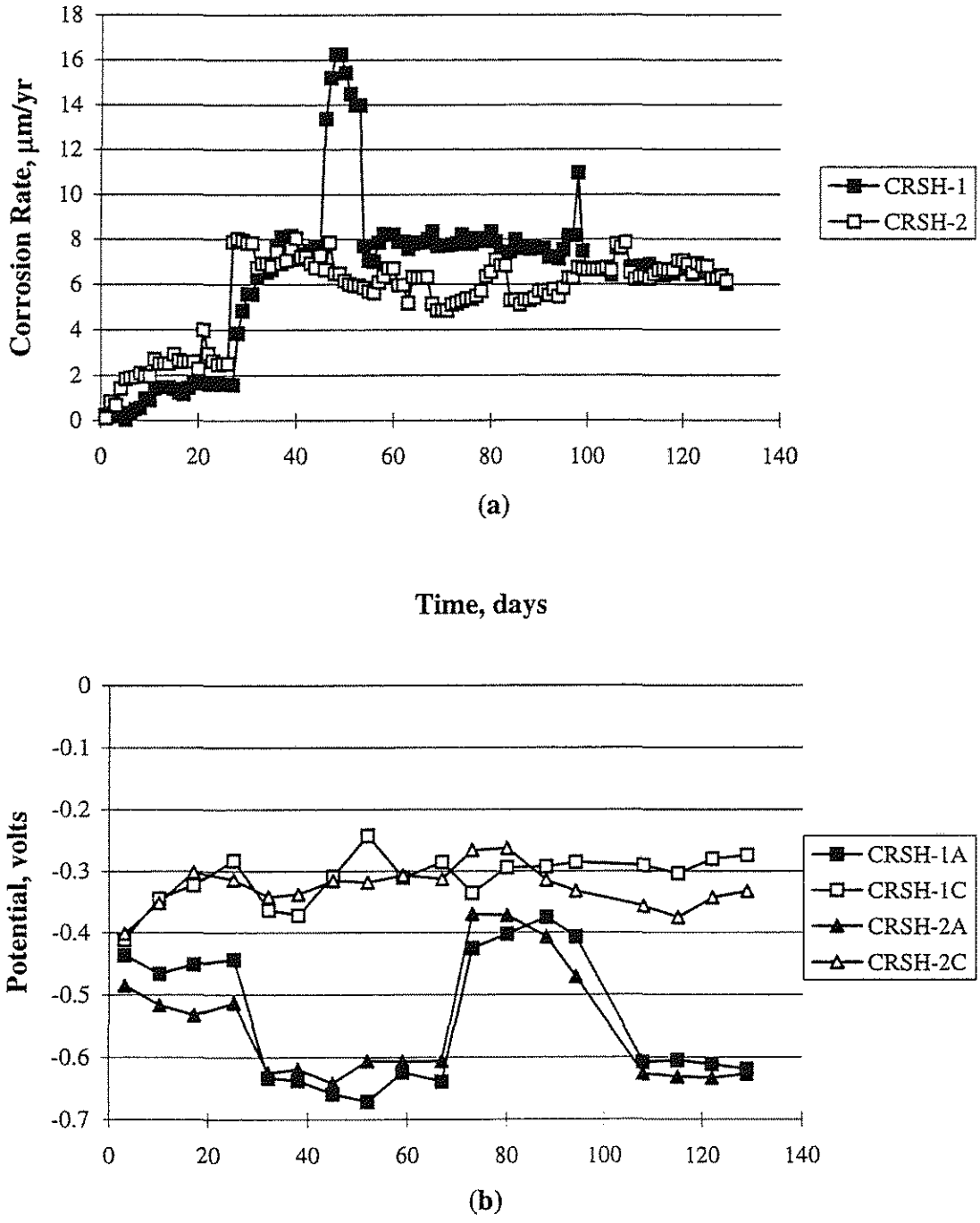

Fig. 22 CRSH steel specimens exposed to 1.6 m $CaCl_2$ in simulated pore solution: (a) Macrocell corrosion rate, (b) Corrosion potential

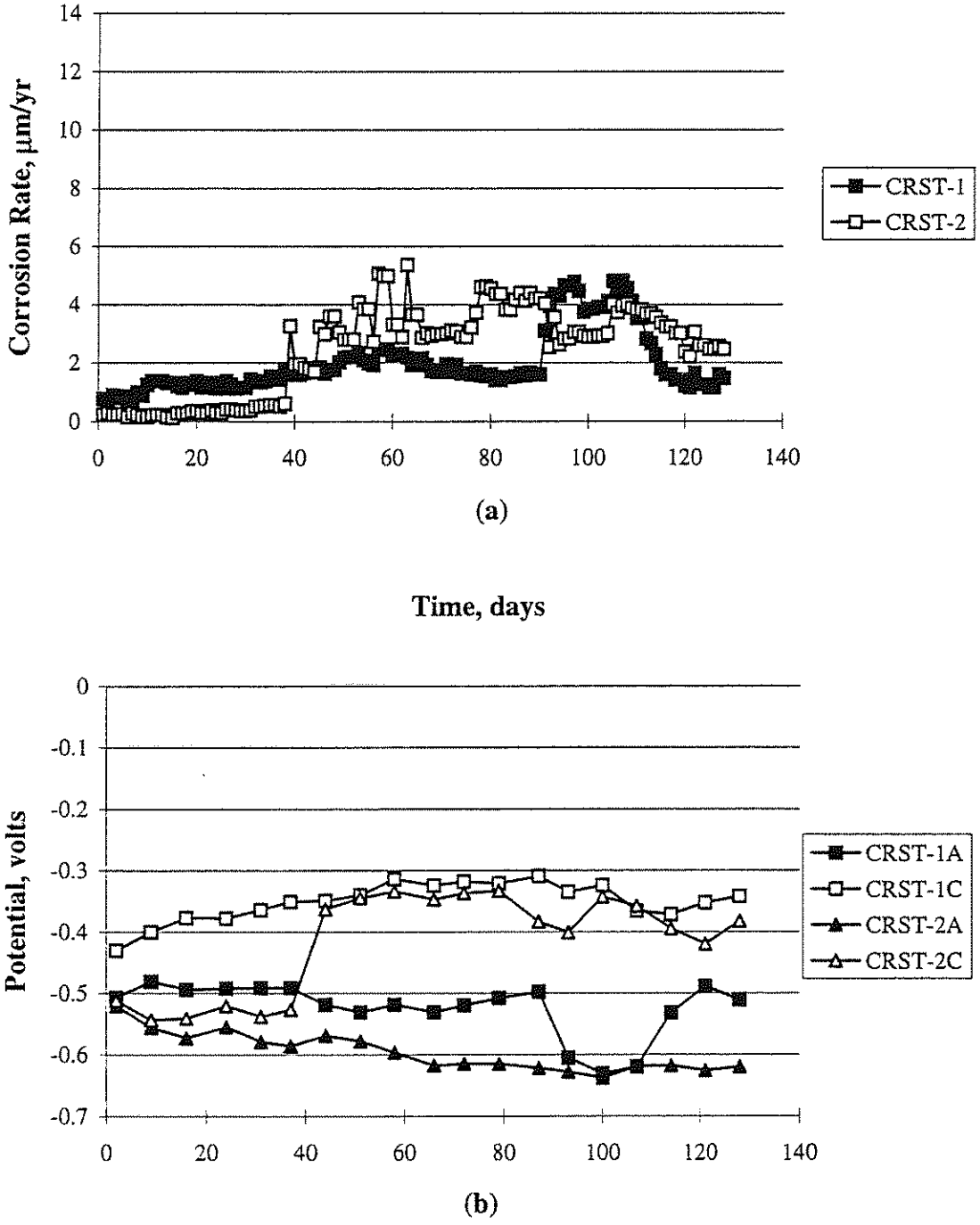

Fig. 23 CRST steel specimens exposed to 1.6 m $CaCl_2$ in simulated pore solution: (a) Macrocell corrosion rate, (b) Corrosion potential

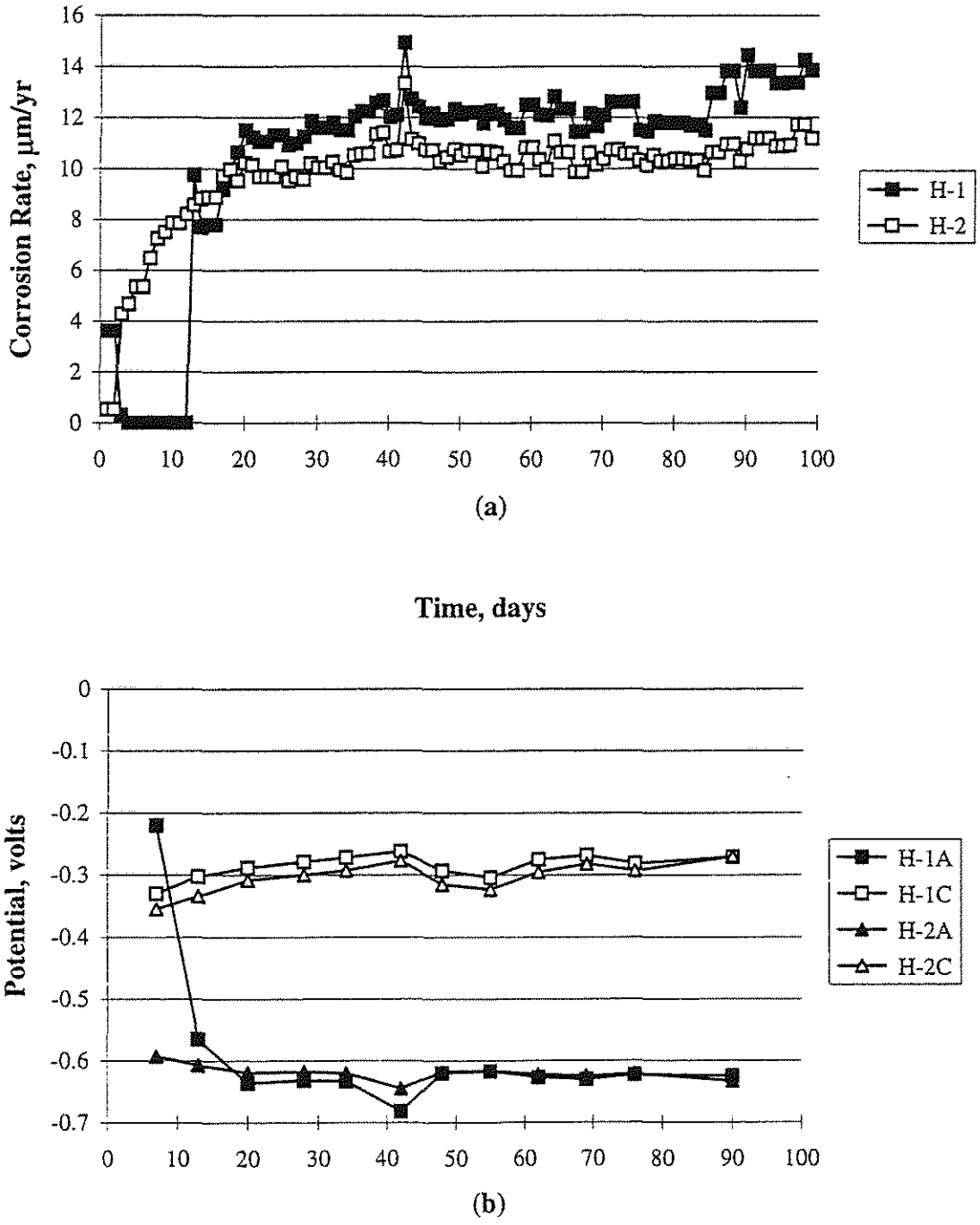

Fig. 24 H steel specimens exposed to 6.04 m $CaCl_2$ in simulated pore solution: (a) Macrocell corrosion rate, (b) Corrosion potential.

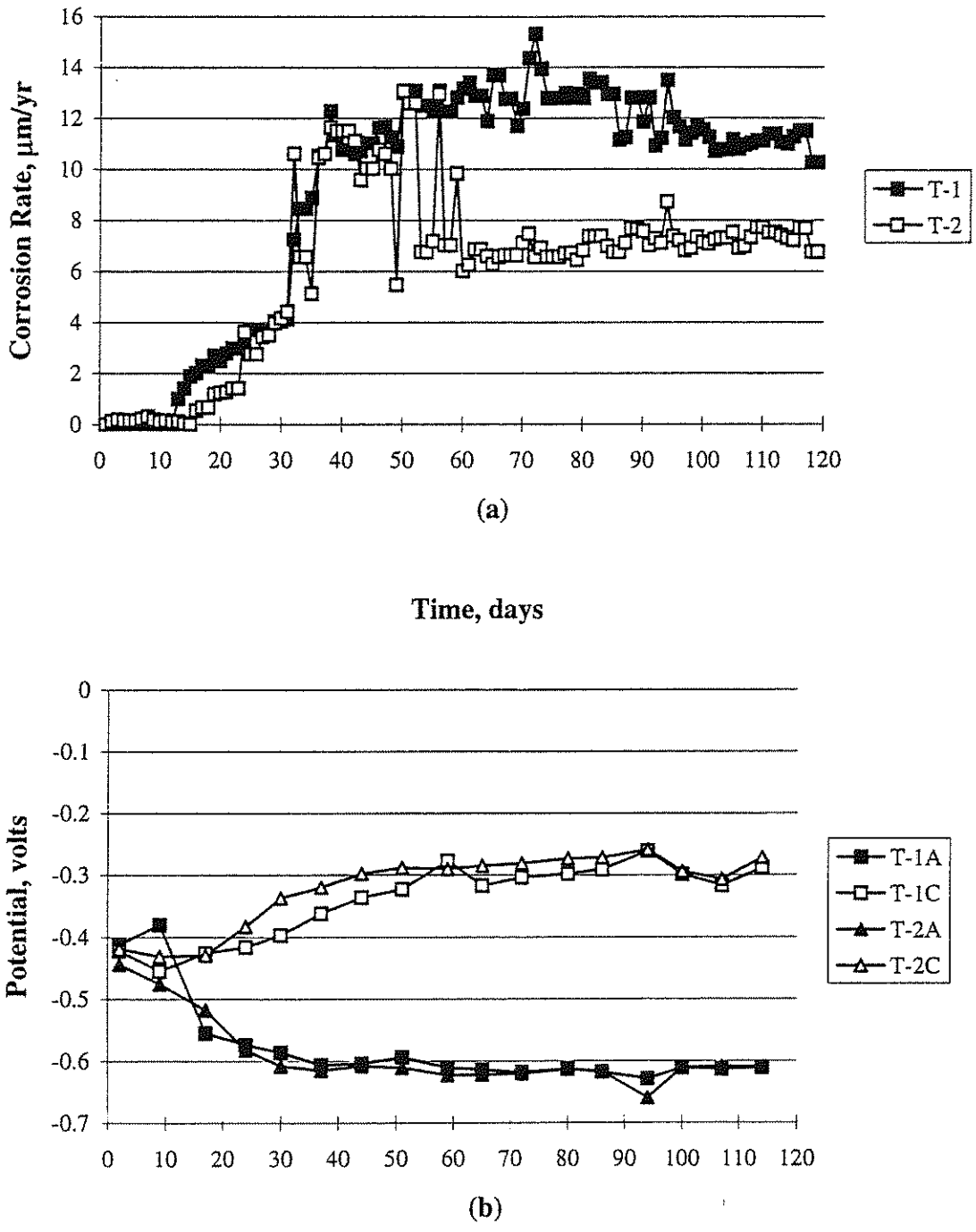

Fig. 25 T steel specimens exposed to 6.04 m $CaCl_2$ in simulated pore solution: (a) Macrocell corrosion rate, (b) Corrosion potential.

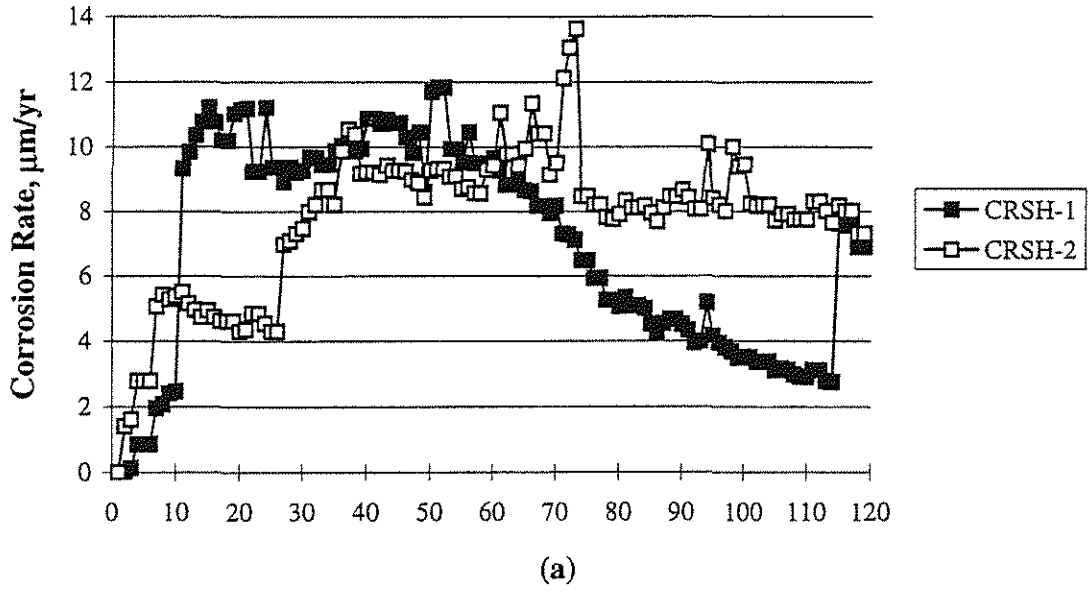

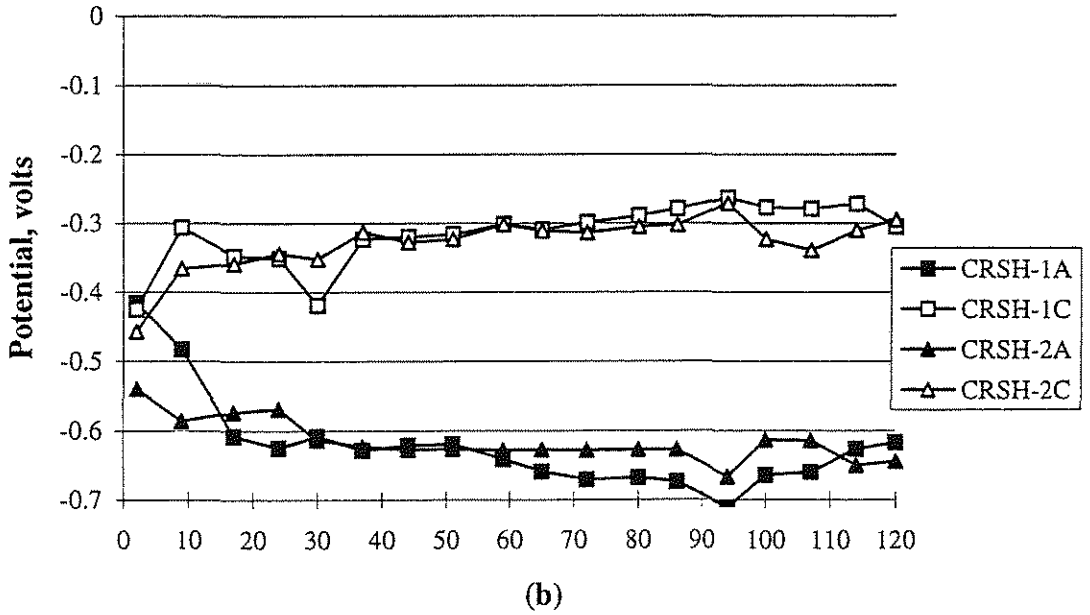

Fig. 26 CRSH steel specimens exposed to 6.04 m $CaCl_2$ in simulated pore solution: (a) Macrocell corrosion rate, (b) Corrosion potential.

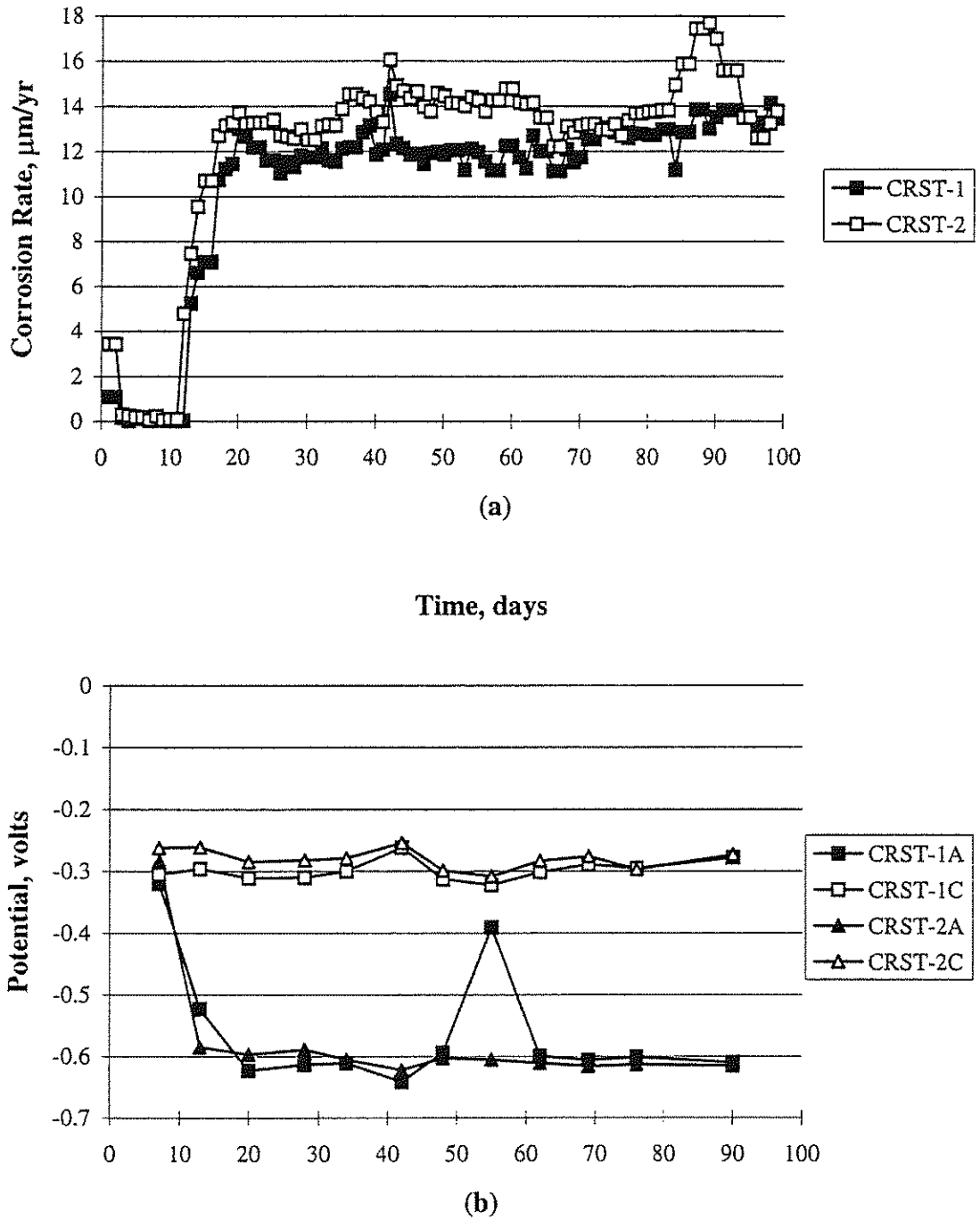

Fig. 27 CRST steel specimens exposed to 6.04 m CaCl2 in simulated pore solution: (a) Macrocell corrosion rate, (b) Corrosion potential.

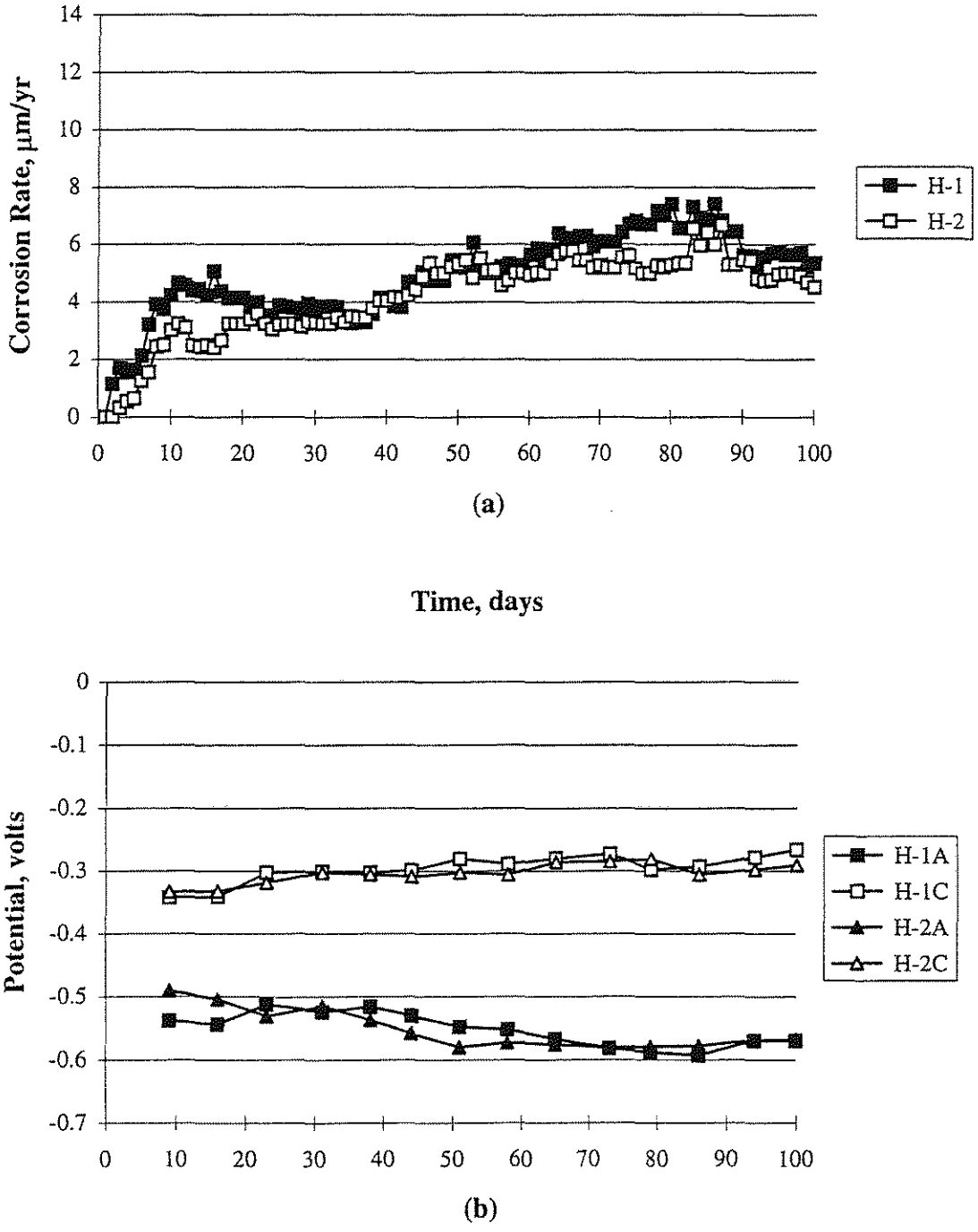

Fig. 28 H steel specimens exposed to 0.4 m CMA in simulated pore solution: (a) Macrocell corrosion rate, (b) Corrosion potential.

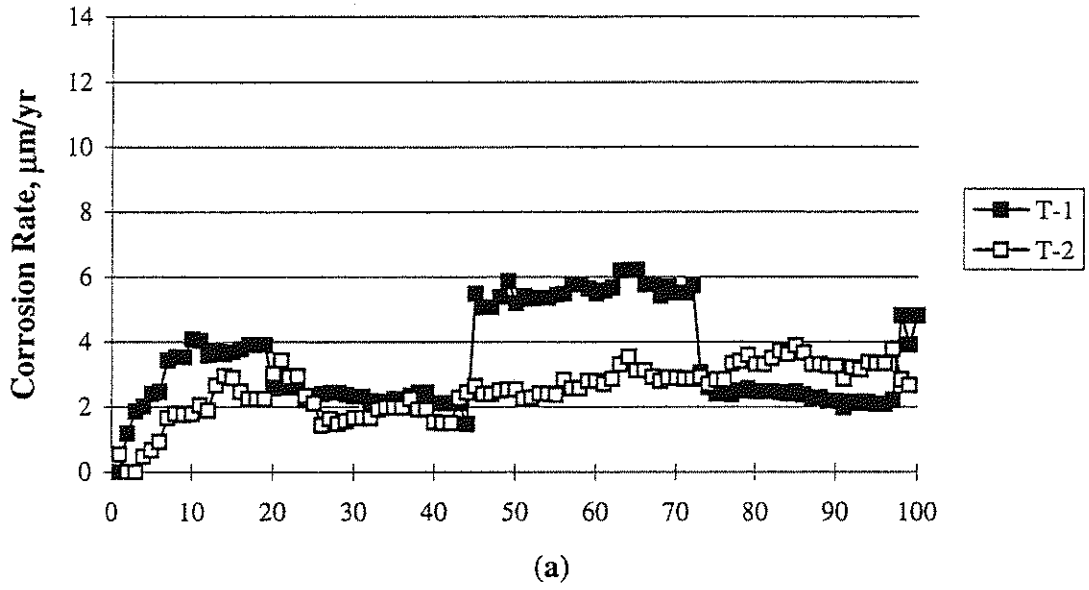

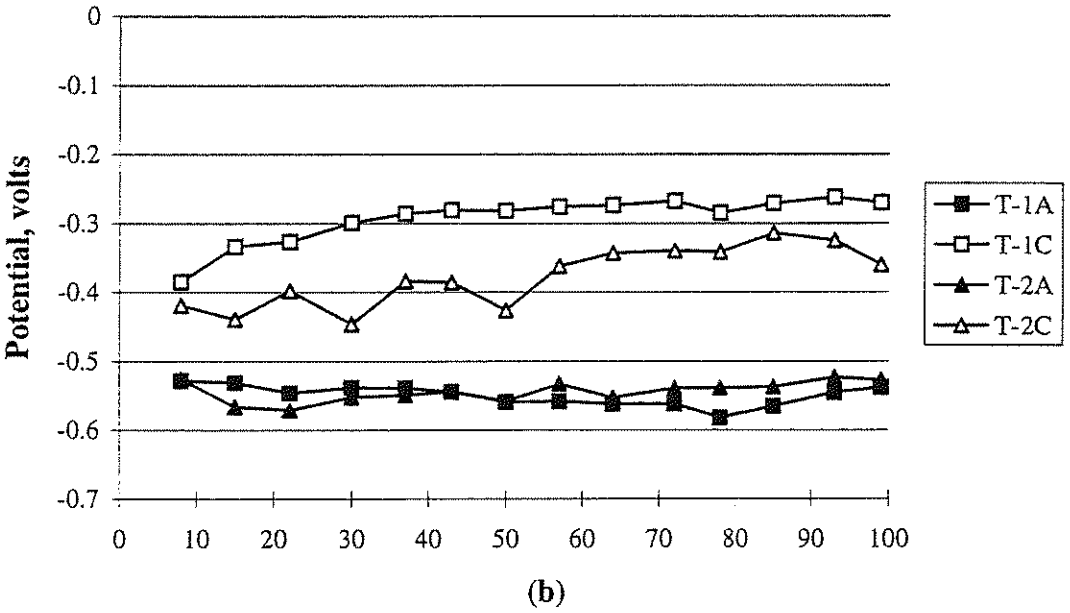

Fig. 29 T steel specimens exposed to 0.4 m CMA in simulated pore solution: (a) Macrocell corrosion rate, (b) Corrosion potential.

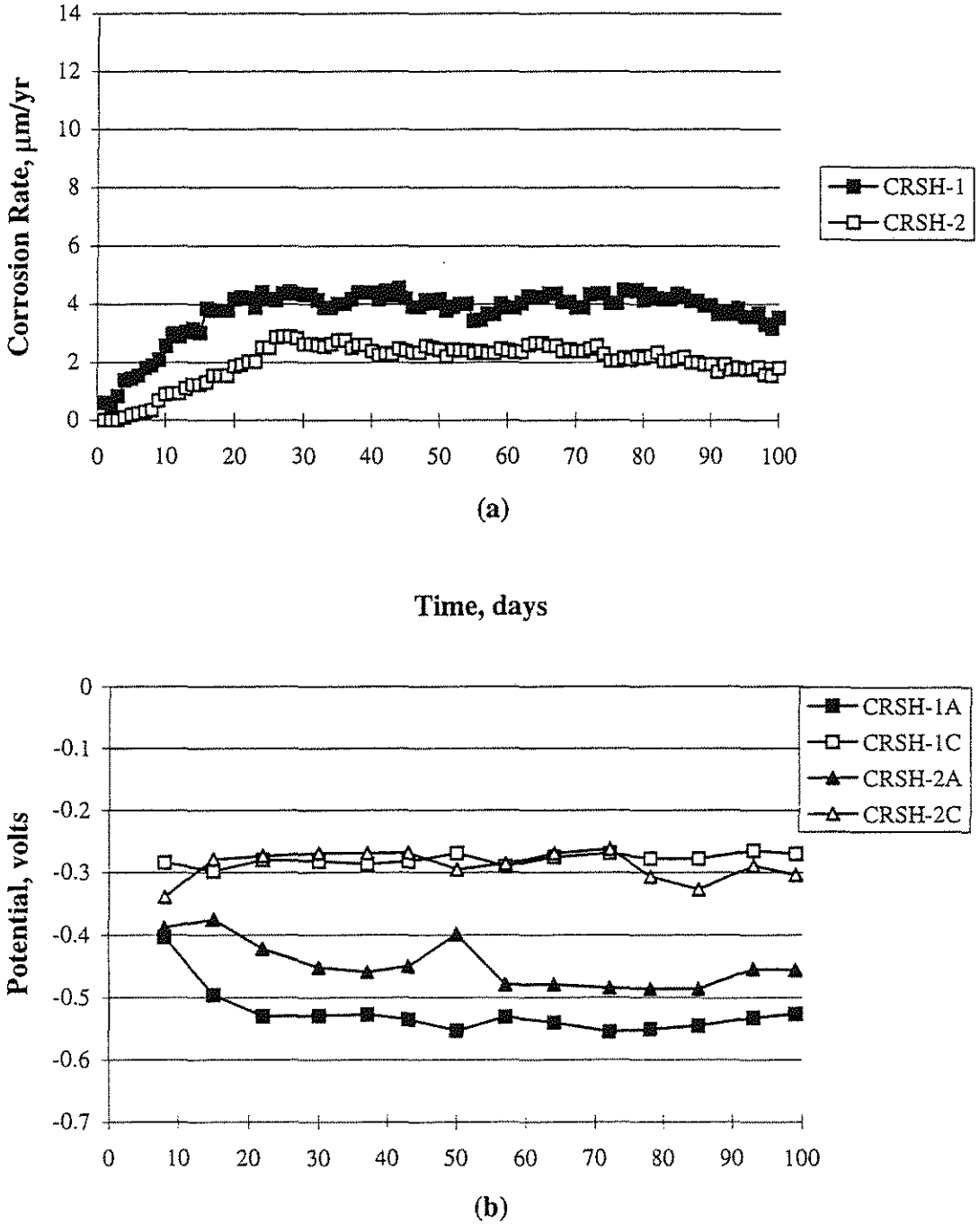

Fig. 30 CRSH steel specimens exposed to 0.4 m CMA in simulated pore solution: (a) Macrocell corrosion rate, (b) Corrosion potential.

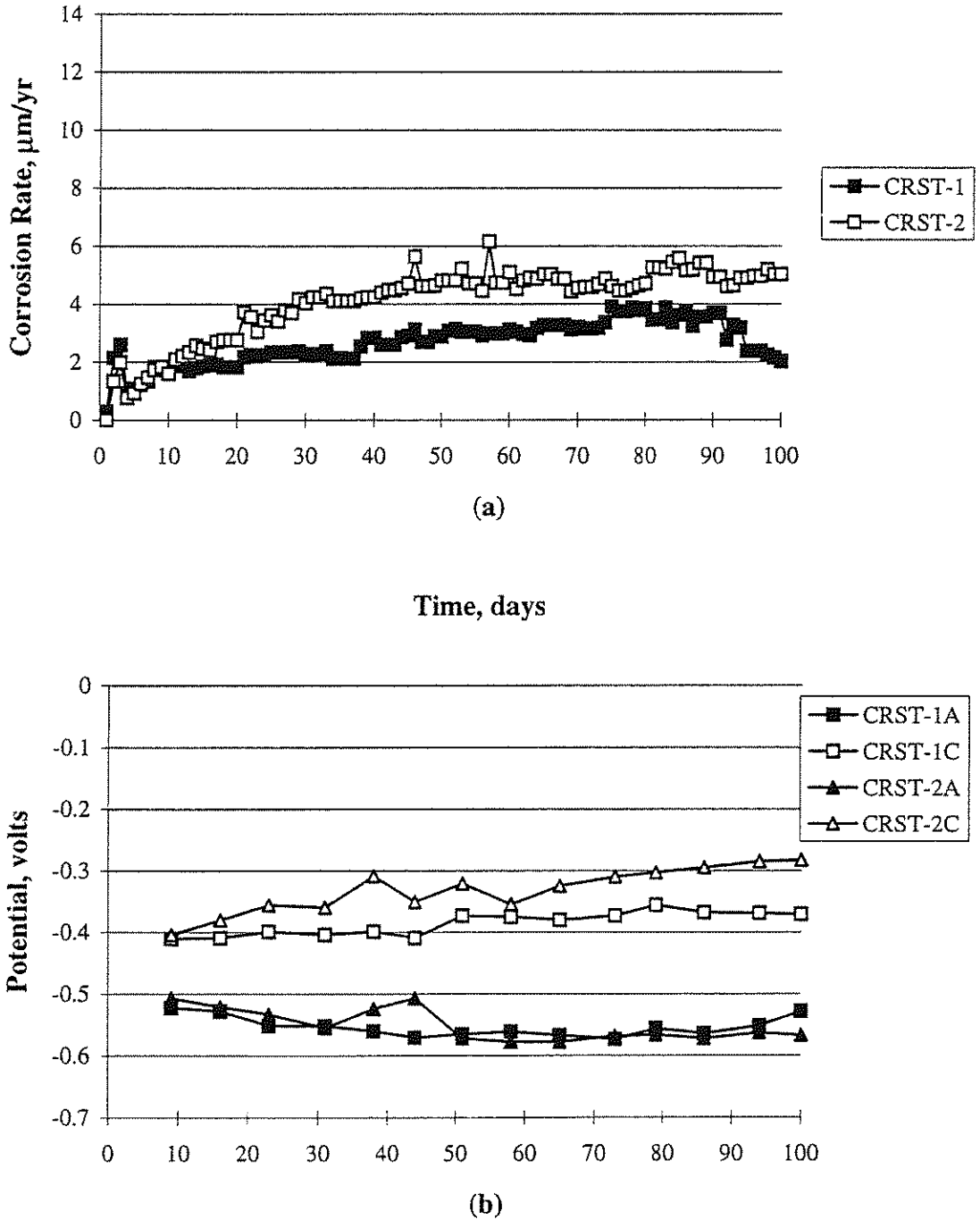

Fig. 31 CRST steel specimens exposed to 0.4 m CMA in simulated pore solution: (a) Macrocell corrosion rate, (b) Corrosion potential.

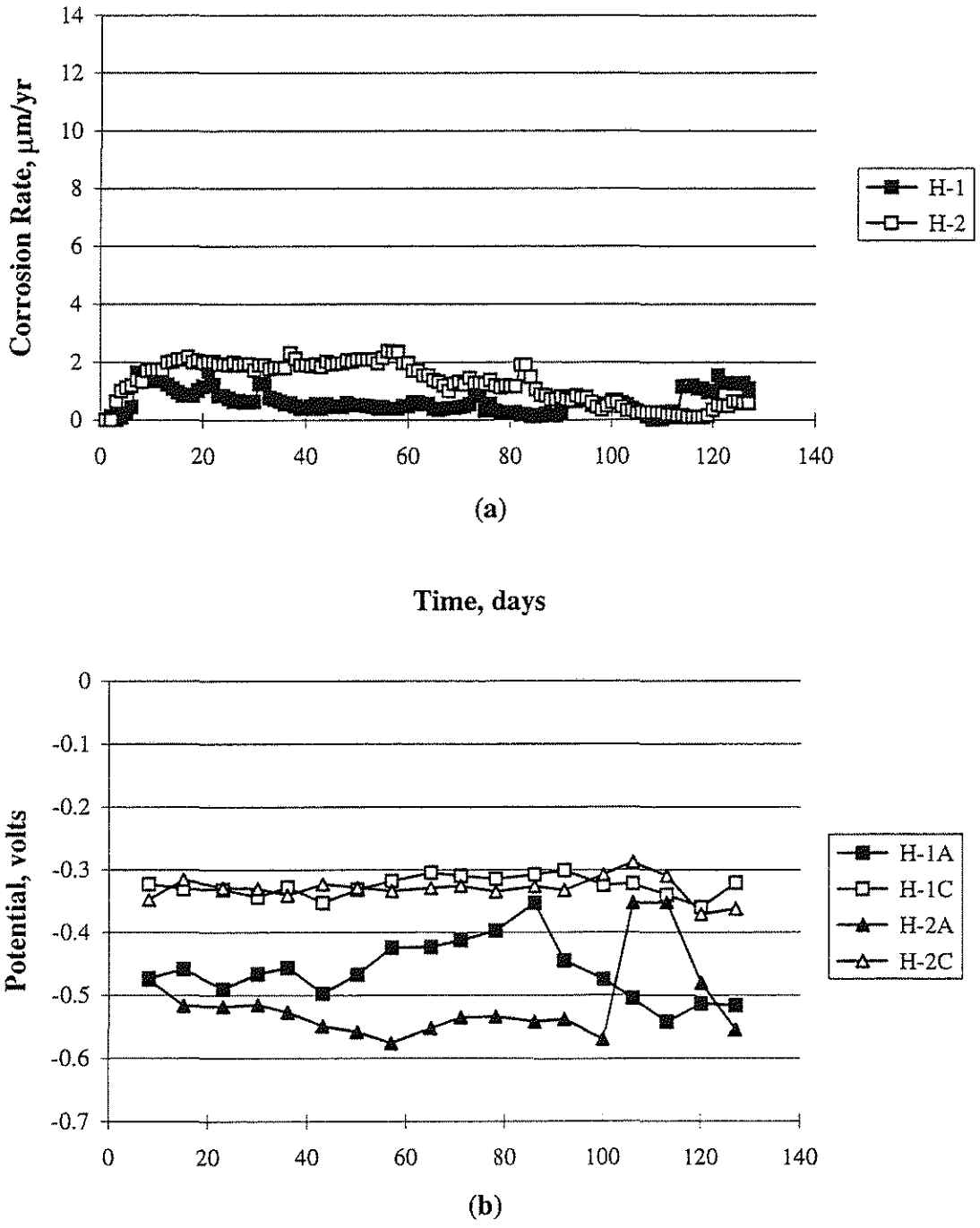

Fig. 32 H steel specimens exposed to 1.6 m CMA in simulated pore solution: (a) Macrocell corrosion rate, (b) Corrosion potential.

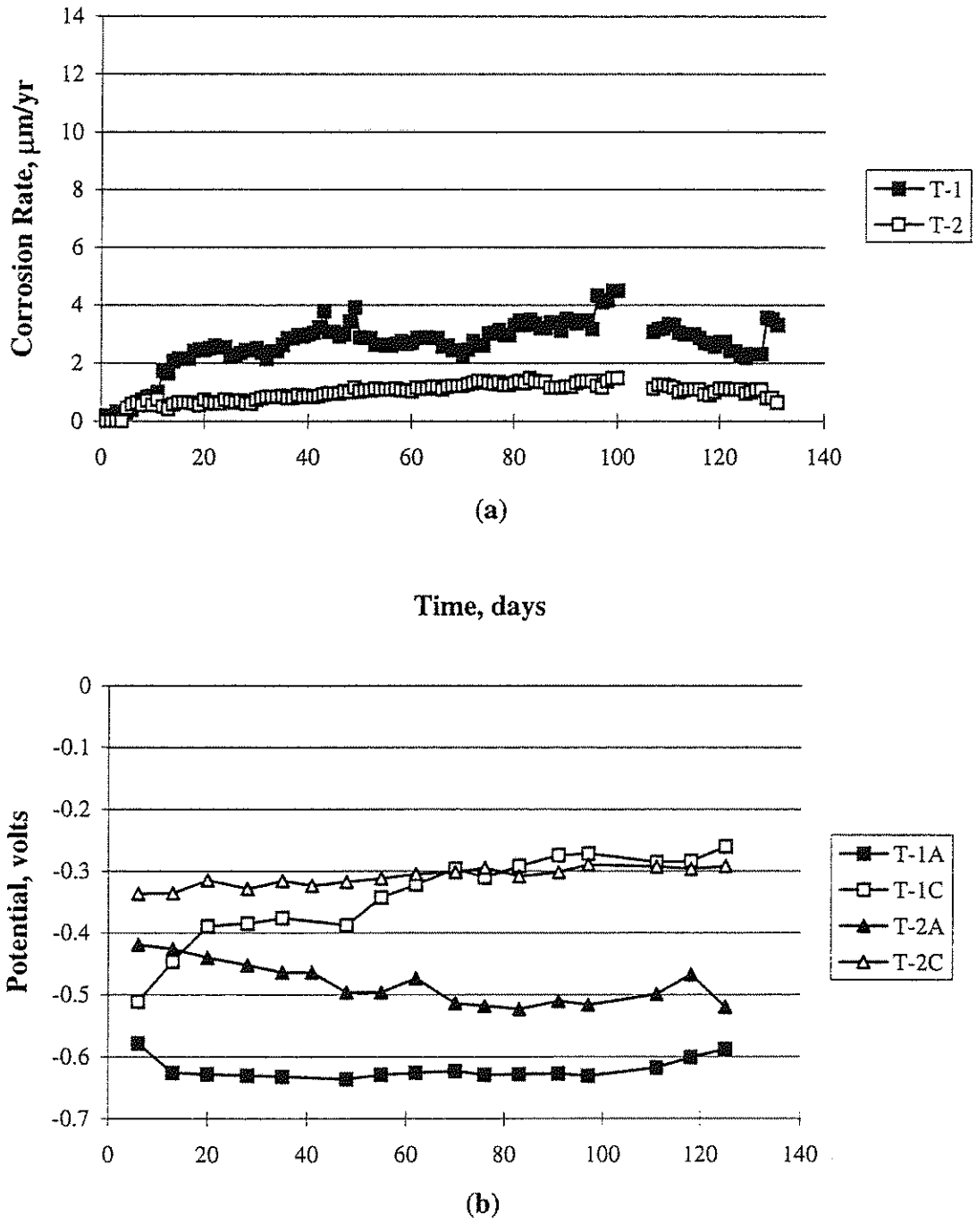

Fig. 33 T steel specimens exposed to 1.6 m CMA in simulated pore solution: (a) Macrocell corrosion rate, (b) Corrosion potential.

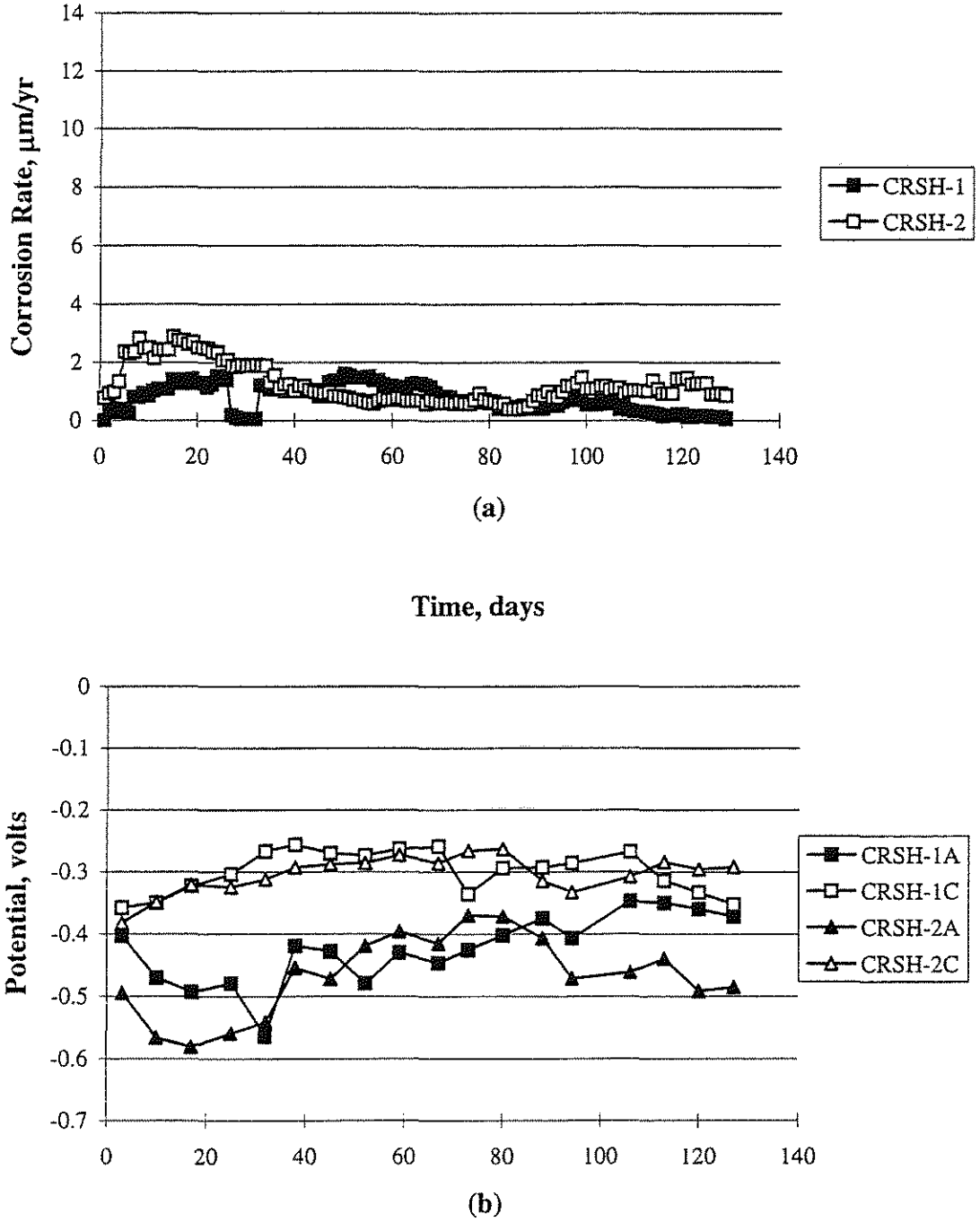

Fig. 34 CRSH steel specimens exposed to 1.6 m CMA in simulated pore solution: (a) Macrocell corrosion rate, (b) Corrosion potential.

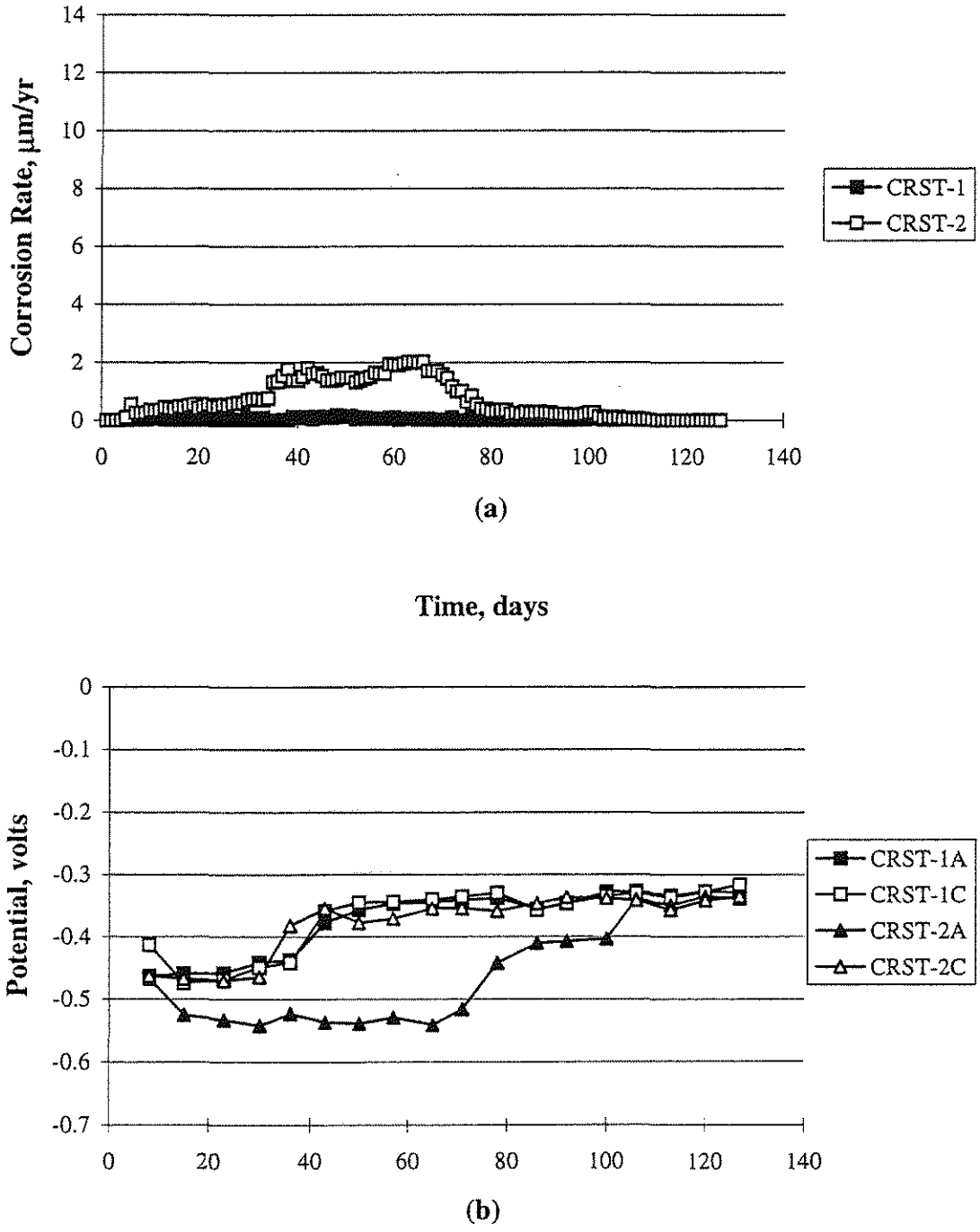

Fig. 35 CRST steel specimens exposed to 1.6 m CMA in simulated pore solution: (a) Macrocell corrosion rate, (b) Corrosion potential.

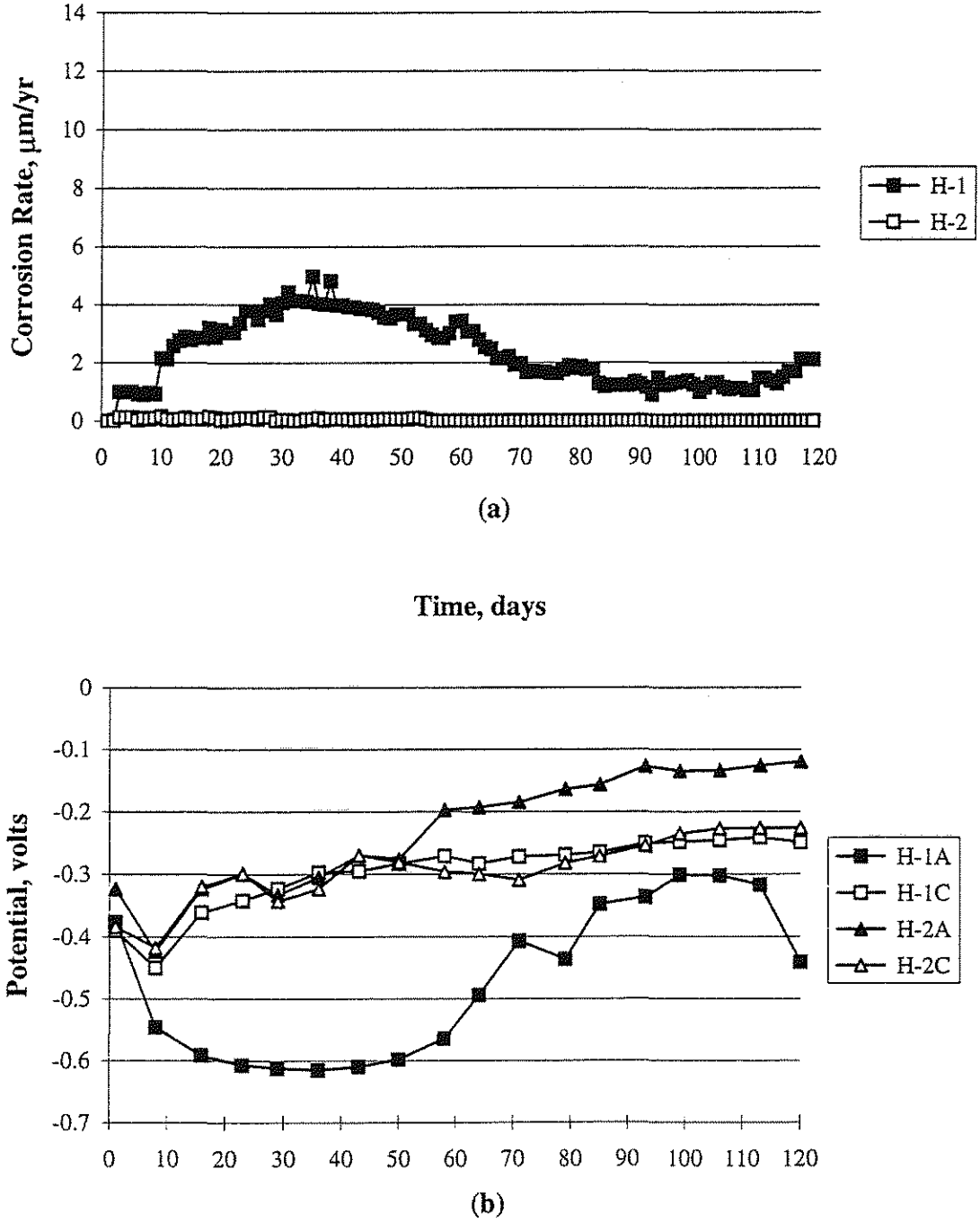

Fig. 36 H steel specimens exposed to 6.04 m CMA in simulated pore solution: (a) Macrocell corrosion rate, (b) Corrosion potential.

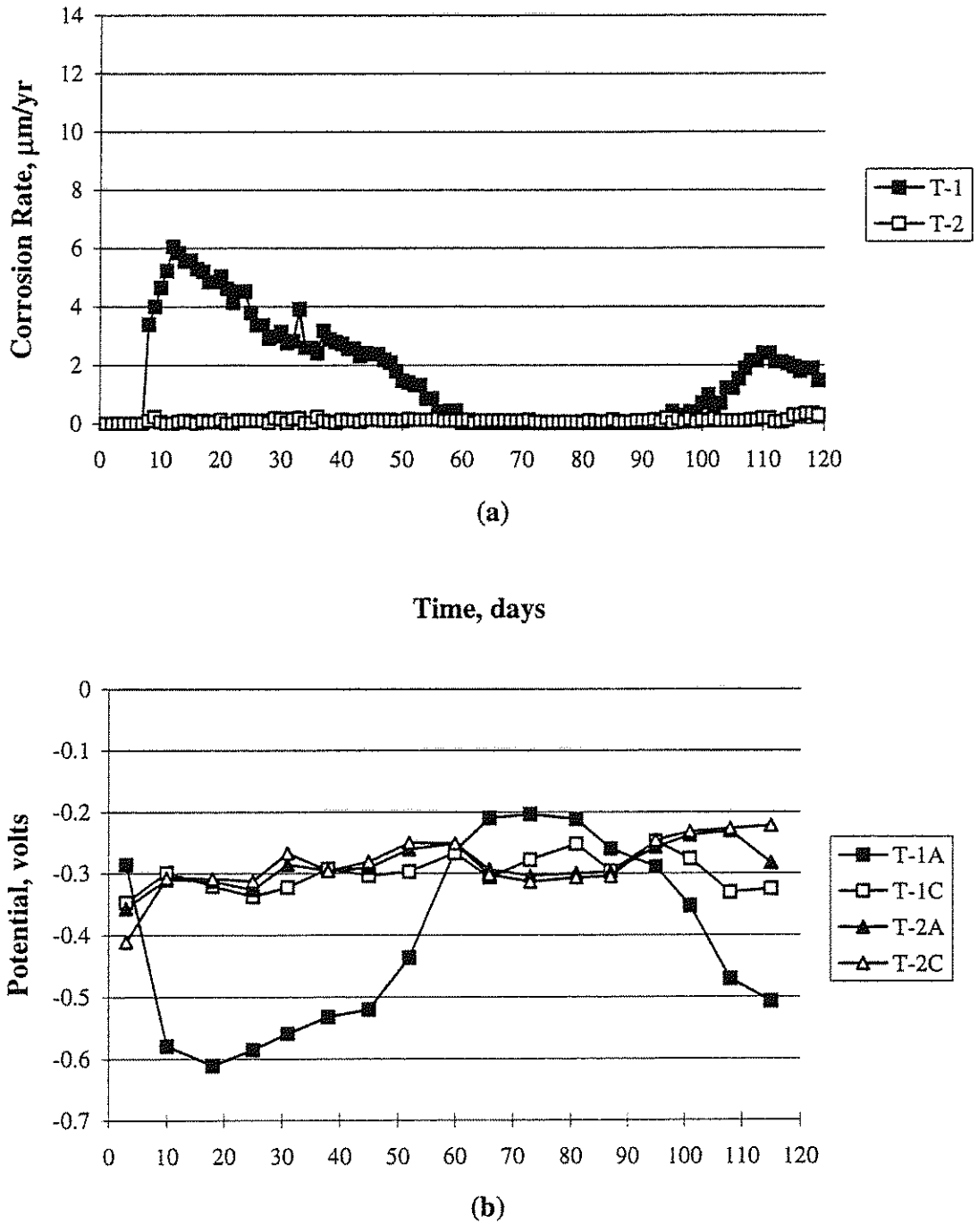

Fig. 37 T steel specimens exposed to 6.04 m CMA in simulated pore solution: (a) Macrocell corrosion rate, (b) Corrosion potential.

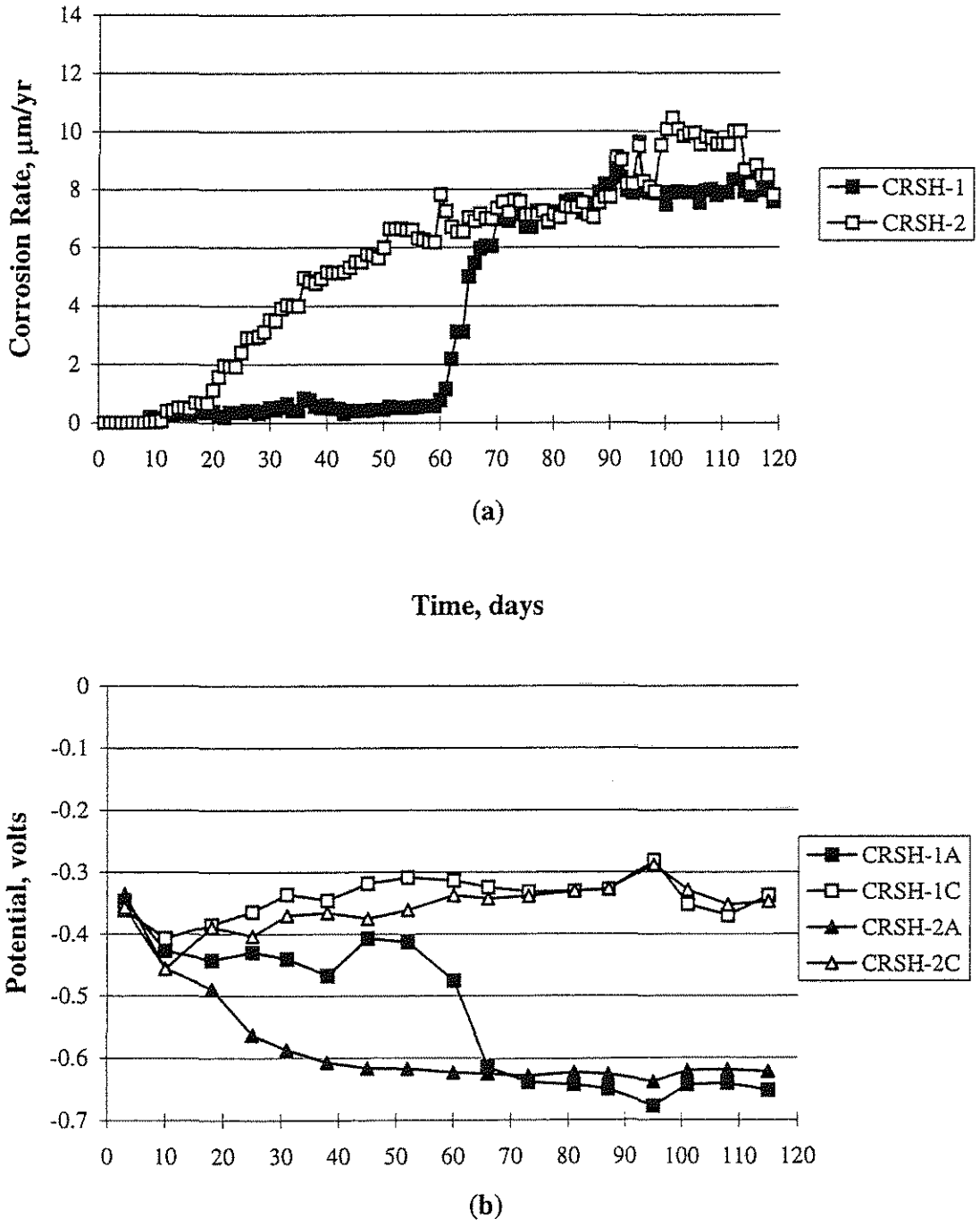

Fig. 38 CRSH steel specimens exposed to 6.04 m CMA in simulated pore solution: (a) Macrocell corrosion rate, (b) Corrosion potential.

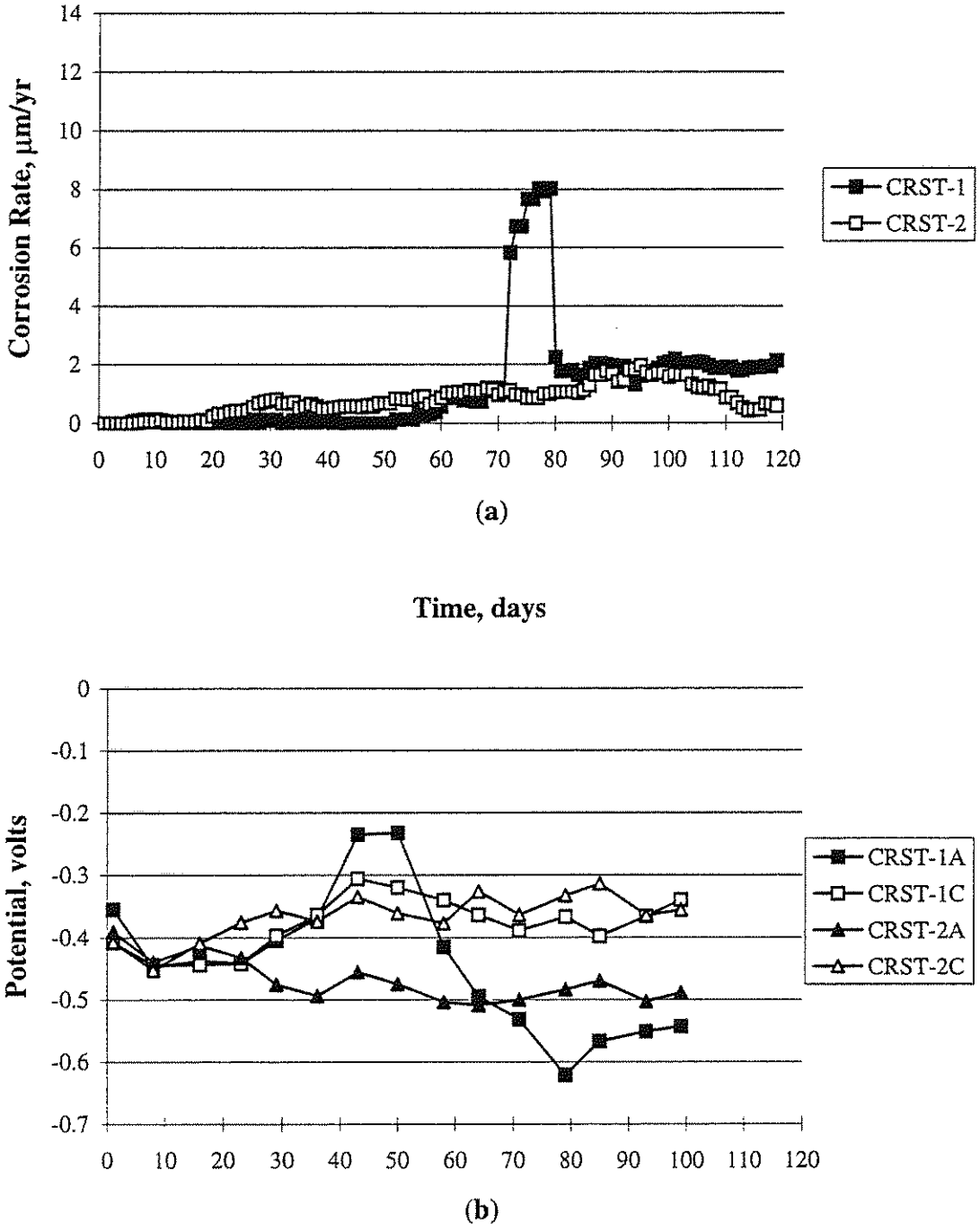

Fig. 39 CRST steel specimens exposed to 6.04 m CMA in simulated pore solution: (a) Macrocell corrosion rate, (b) Corrosion potential.

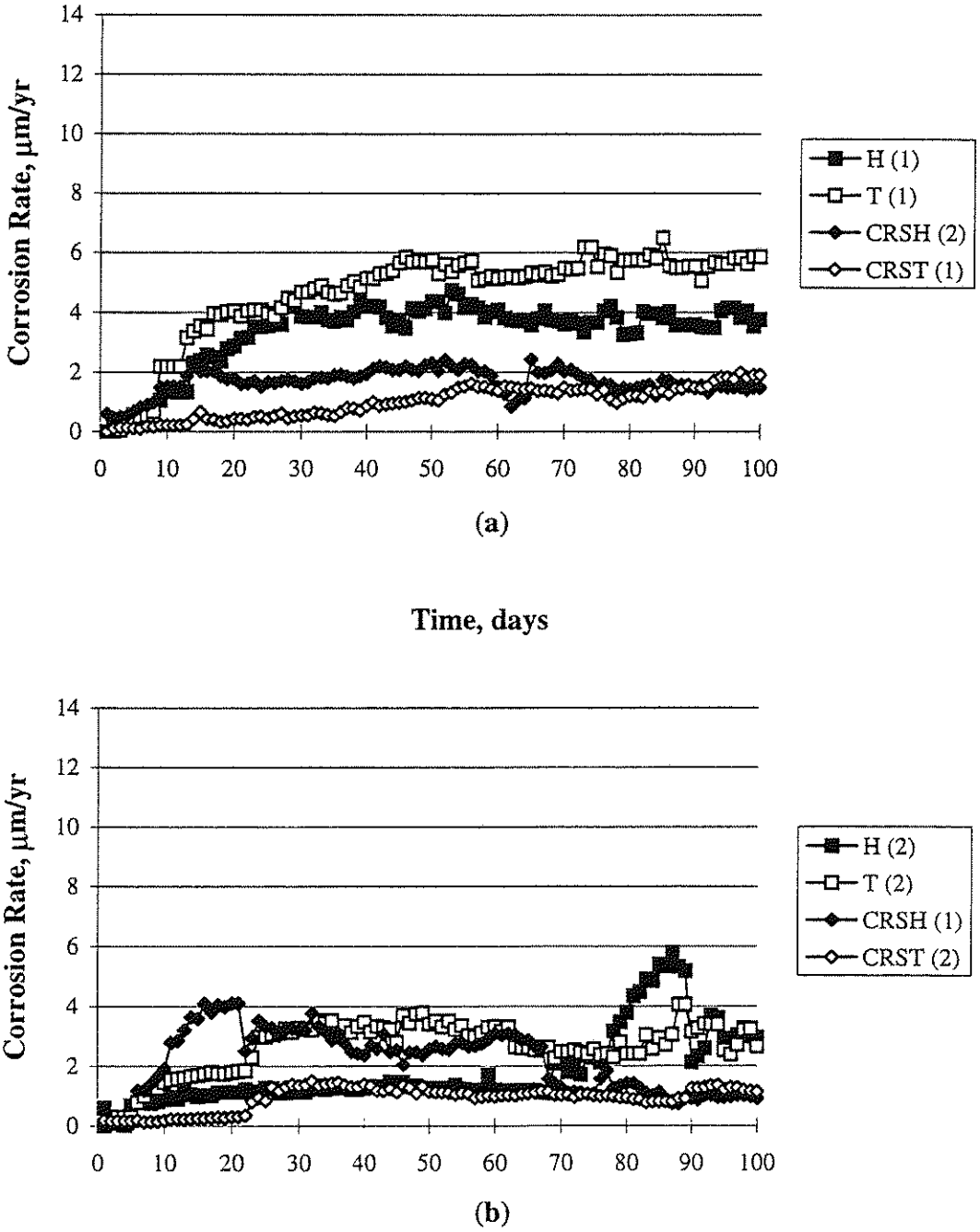

Fig. 40 Average macrocell corrosion rates versus time for specimens exposed to sodium chloride in simulated pore solution: (a) 0.4 m, (b) 1.0 m, (c) 1.6 m, and (d) 6.04 m

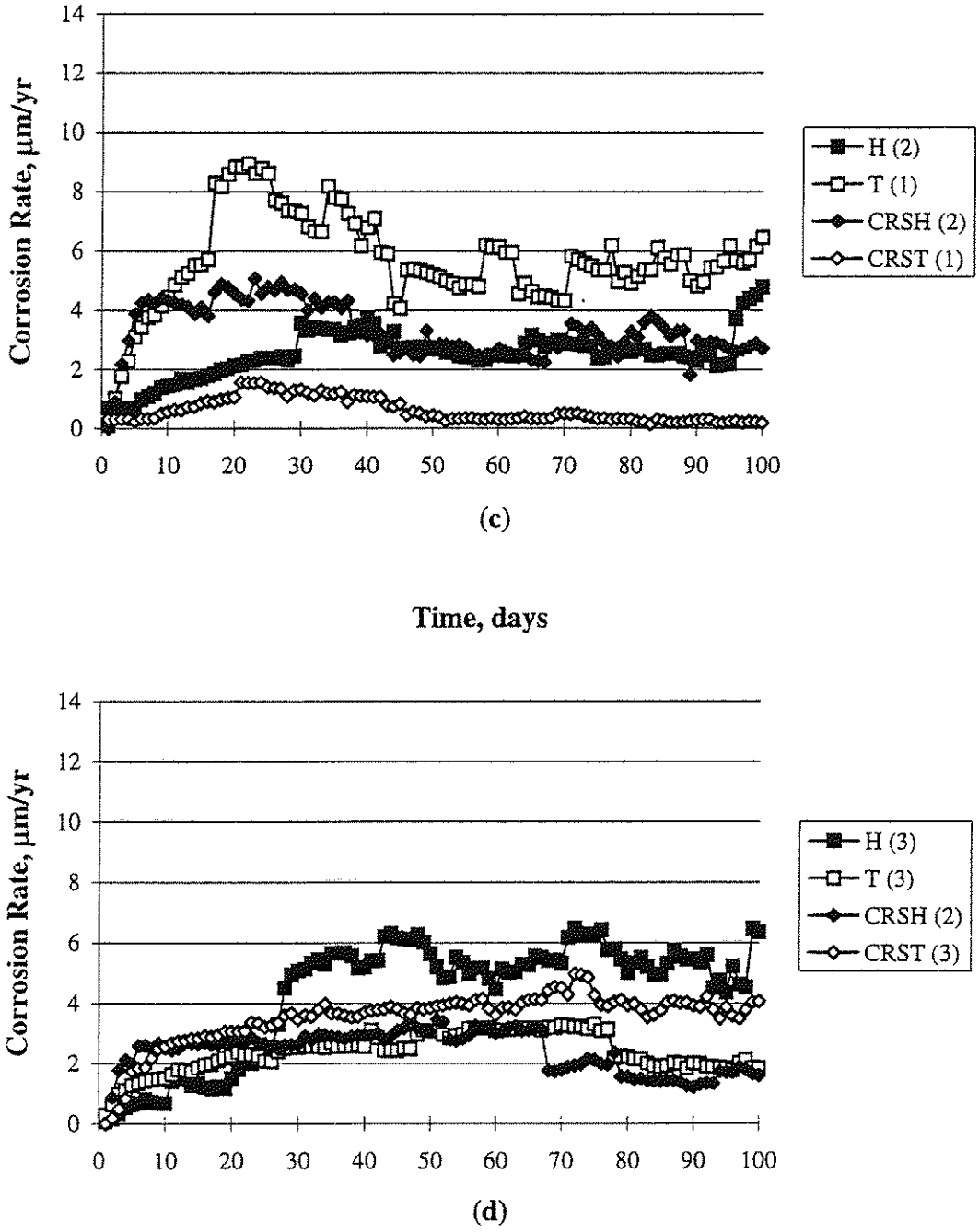

Fig. 40 Average macrocell corrosion rates versus time for specimens exposed to sodium chloride in simulated pore solution: (a) 0.4 m, (b) 1.0 m, (c) 1.6 m, and (d) 6.04 m

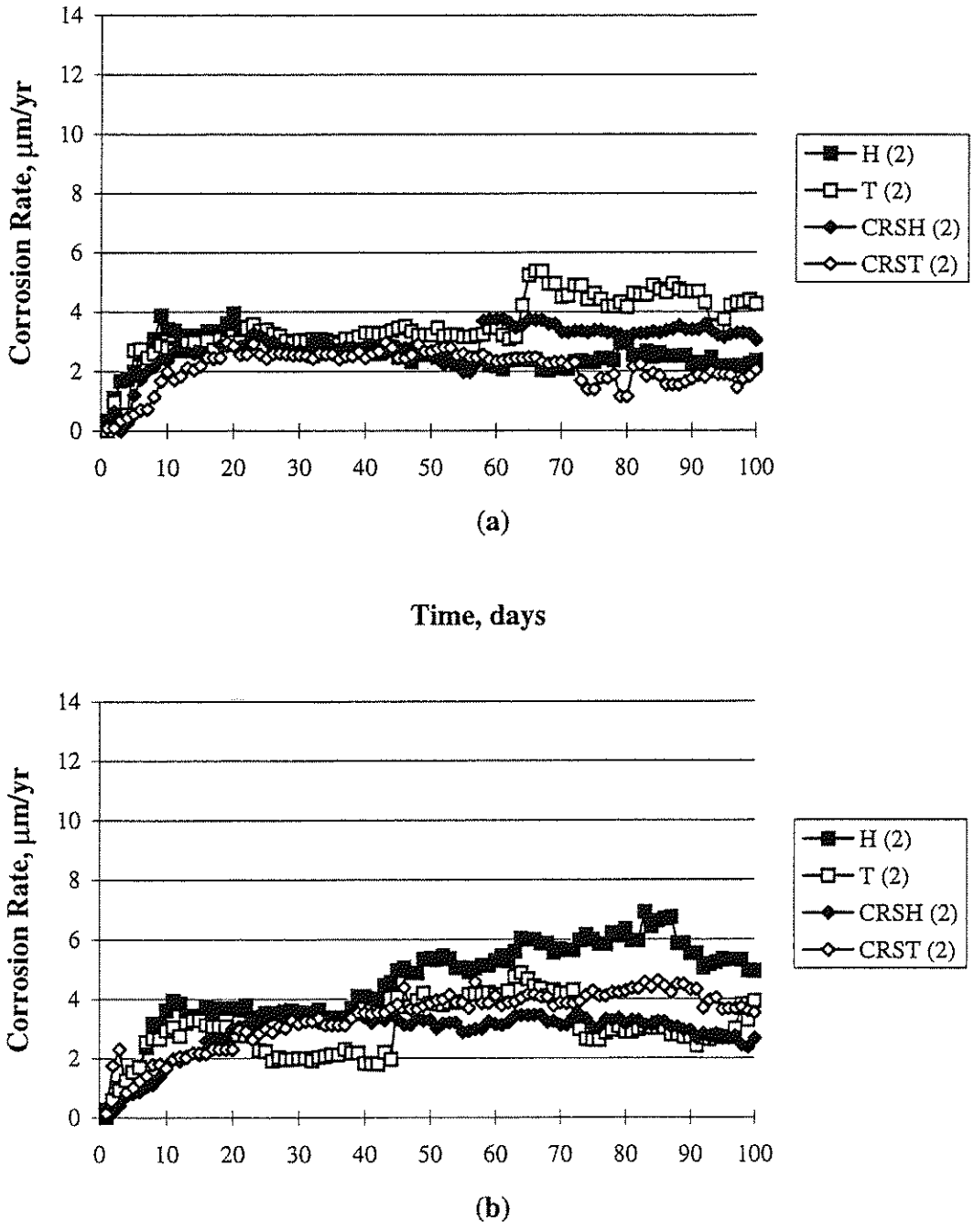

Fig. 41 Average macrocell corrosion rates versus time for specimens exposed to calcium chloride and calcium magnesium acetate in simulated pore solution: (a) 0.4 m $CaCl_2$, (b) 0.4 m CMA.

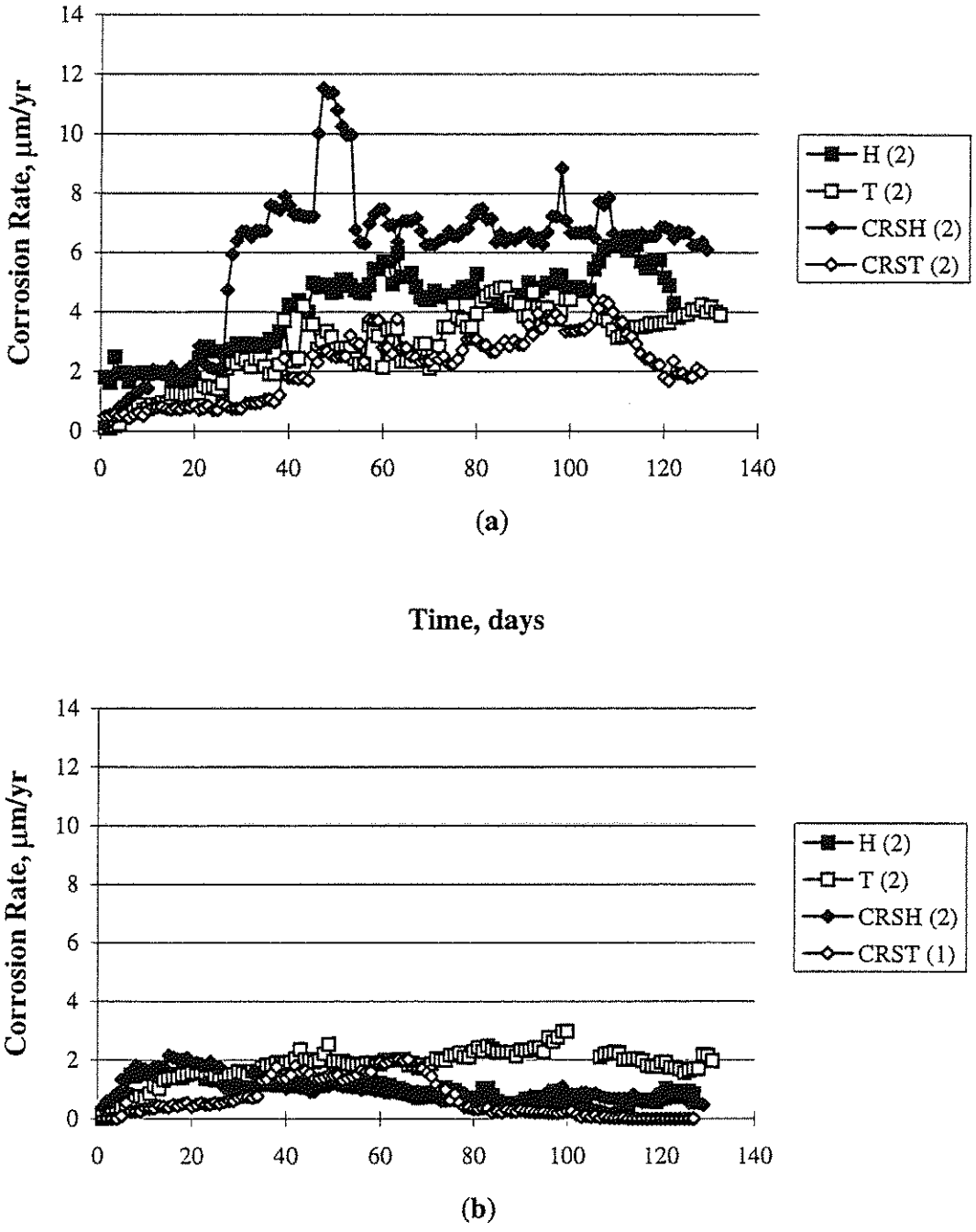

Fig. 42 Average macrocell corrosion rates versus time for specimens exposed to calcium chloride and calcium magnesium acetate in simulated pore solution: (a) 1.6 m $CaCl_2$, (b) 1.6 m CMA.

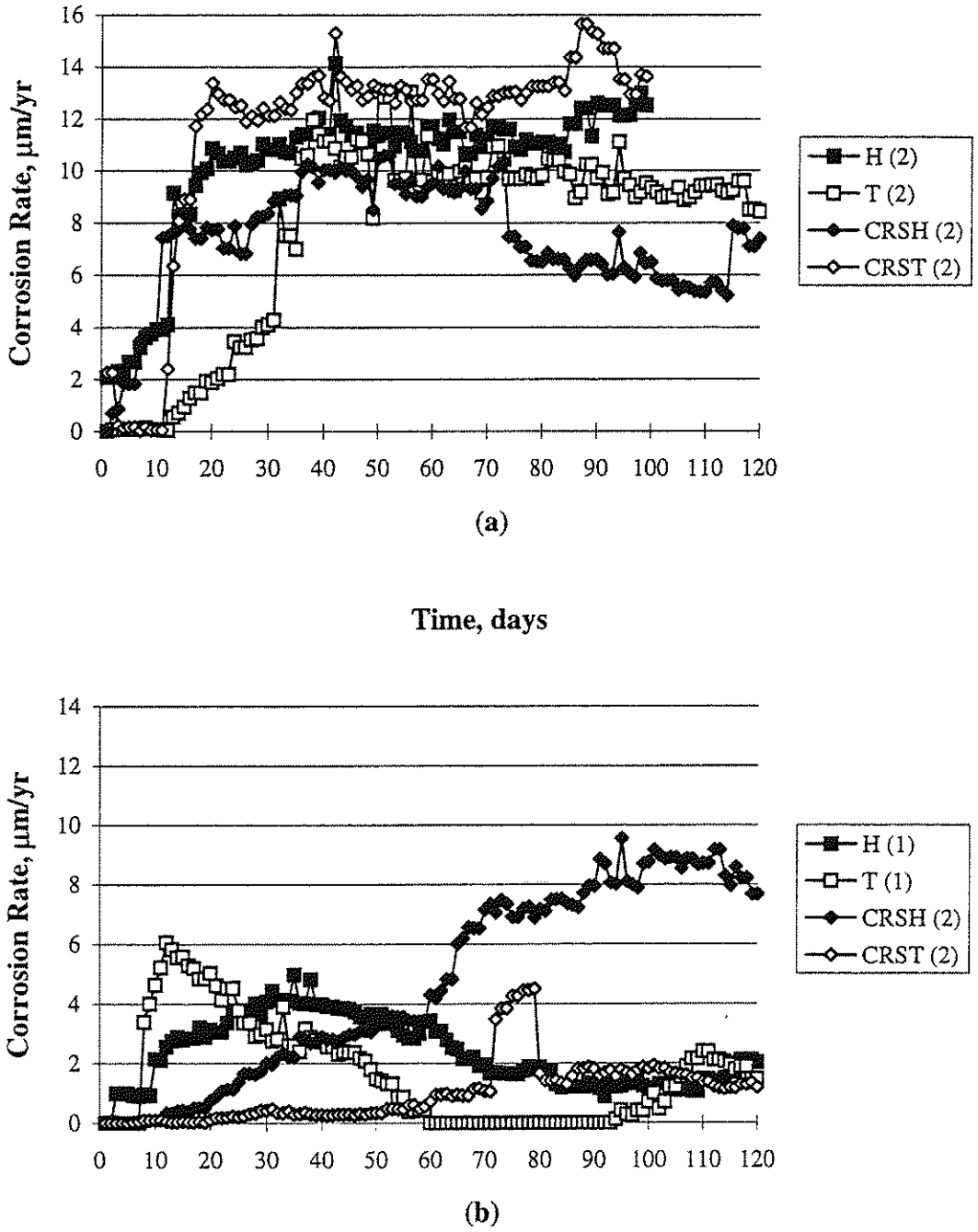

Fig. 43 Average macrocell corrosion rates versus time for specimens exposed to calcium chloride and calcium magnesium acetate in simulated pore solution: (a) 6.04 m $CaCl_2$, (b) 6.04 m CMA.

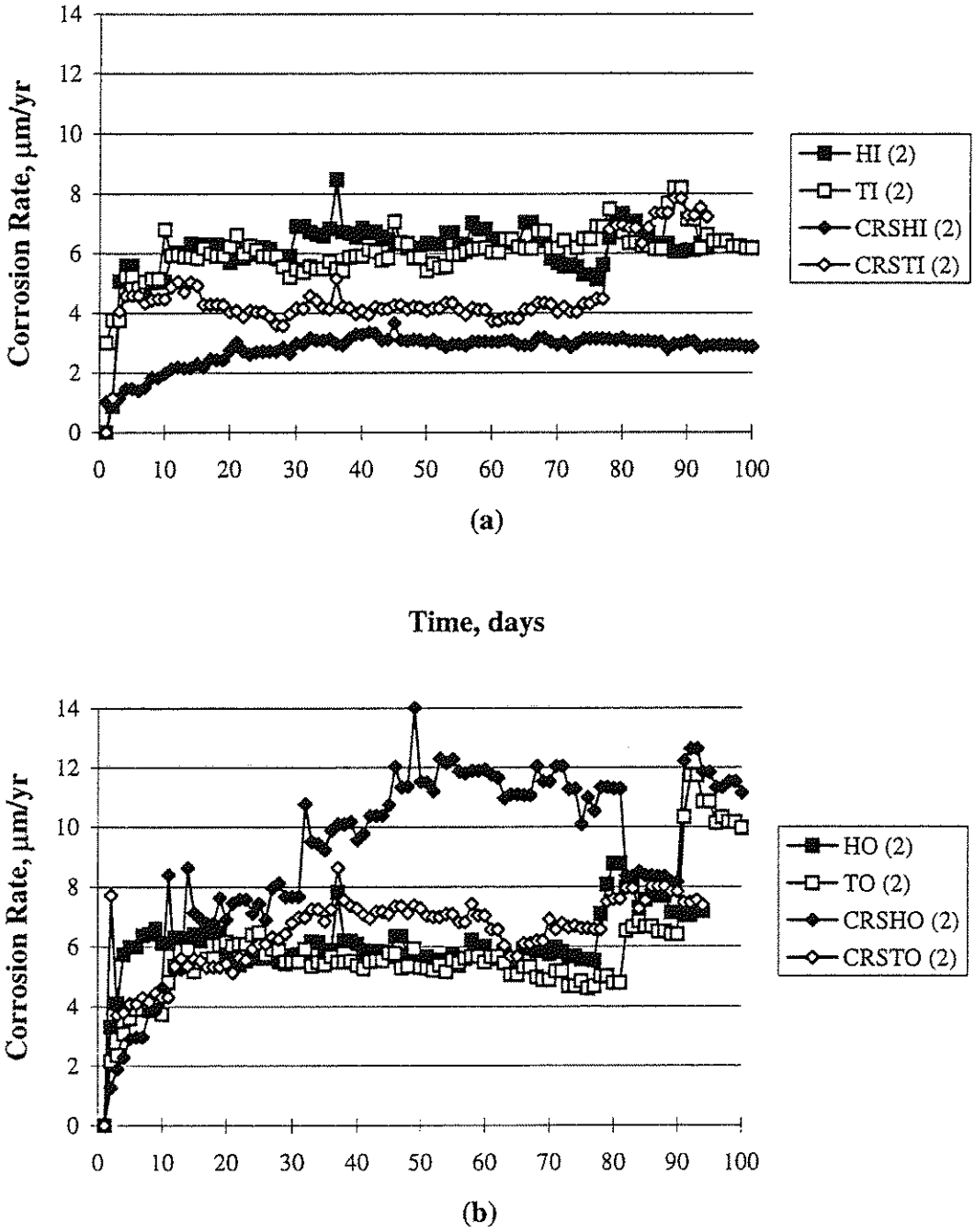

Fig. 44 Average macrocell corrosion rates for specimens evaluating corrosion inhibitors and exposed to 1.6 m sodium chloride in simulated pore solution: (a) Inorganic inhibitor, (b) Organic inhibitor.

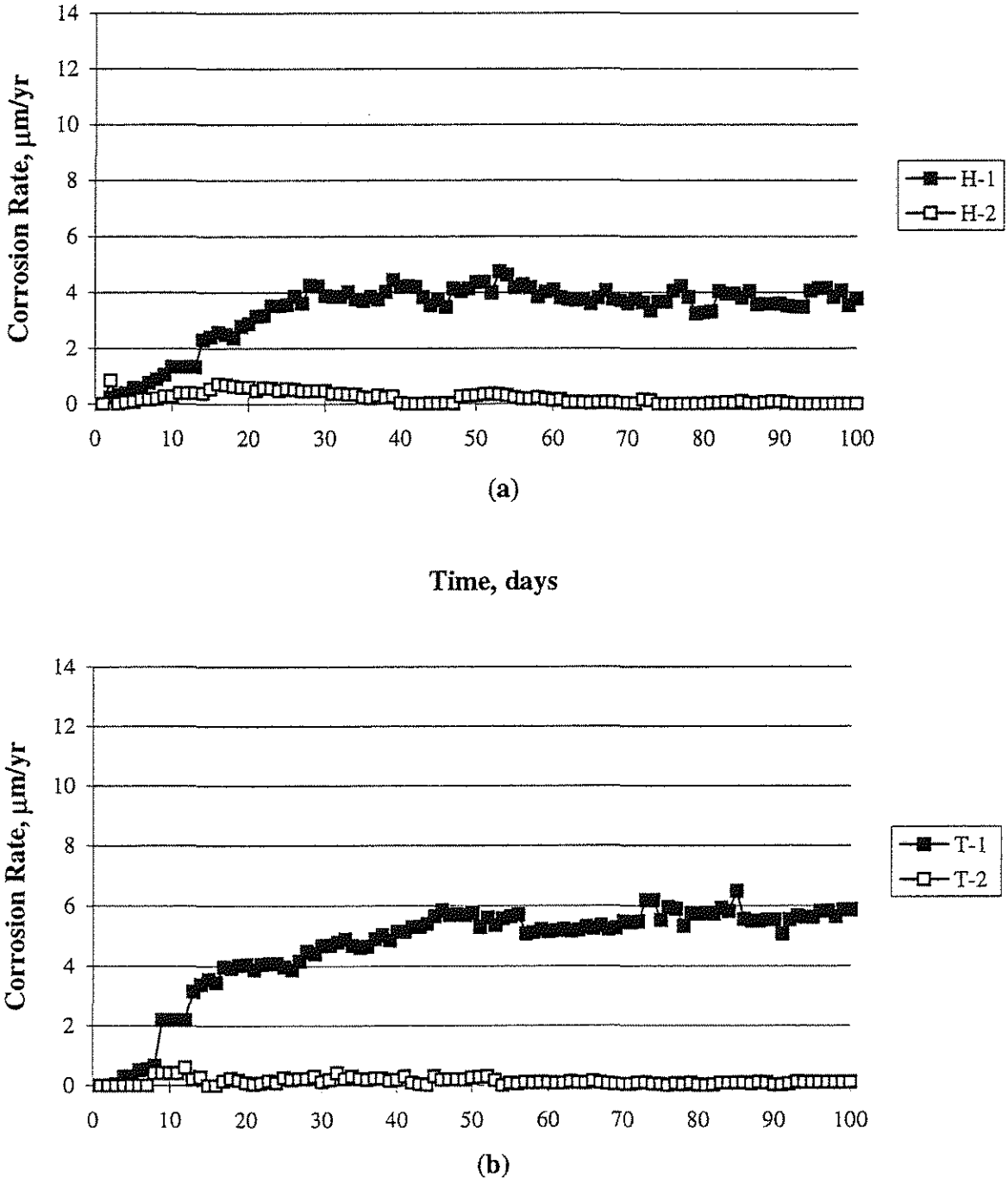

Fig. 45 Macrocell corrosion rate versus time for specimens exposed to 0.4 m NaCl in simulated pore solution: (a) H steel, (b) T steel, (c) CRSH steel, and (d) CRST steel.

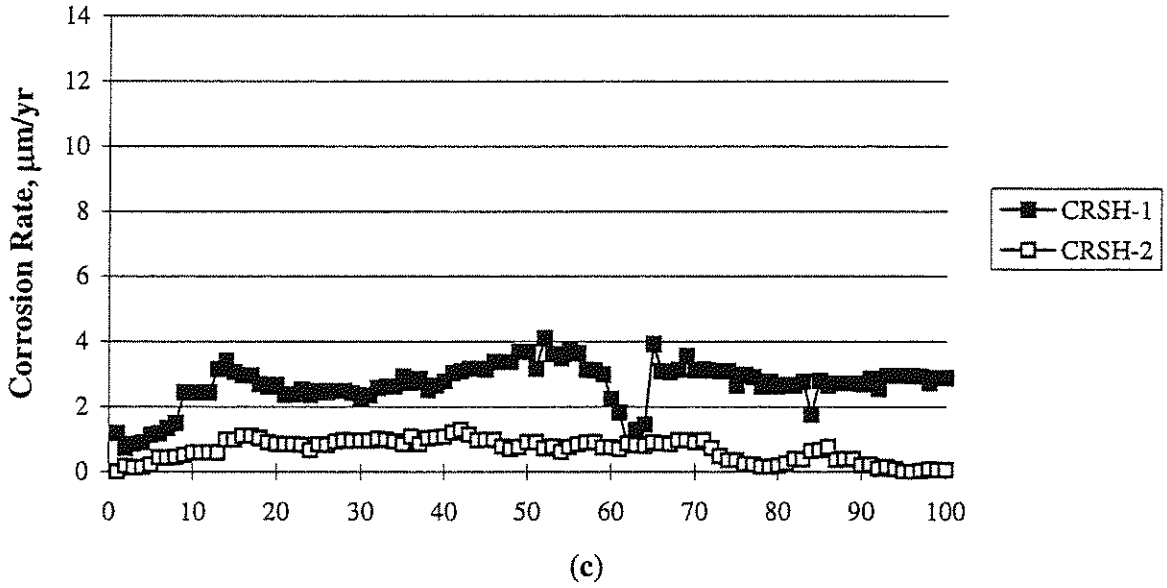

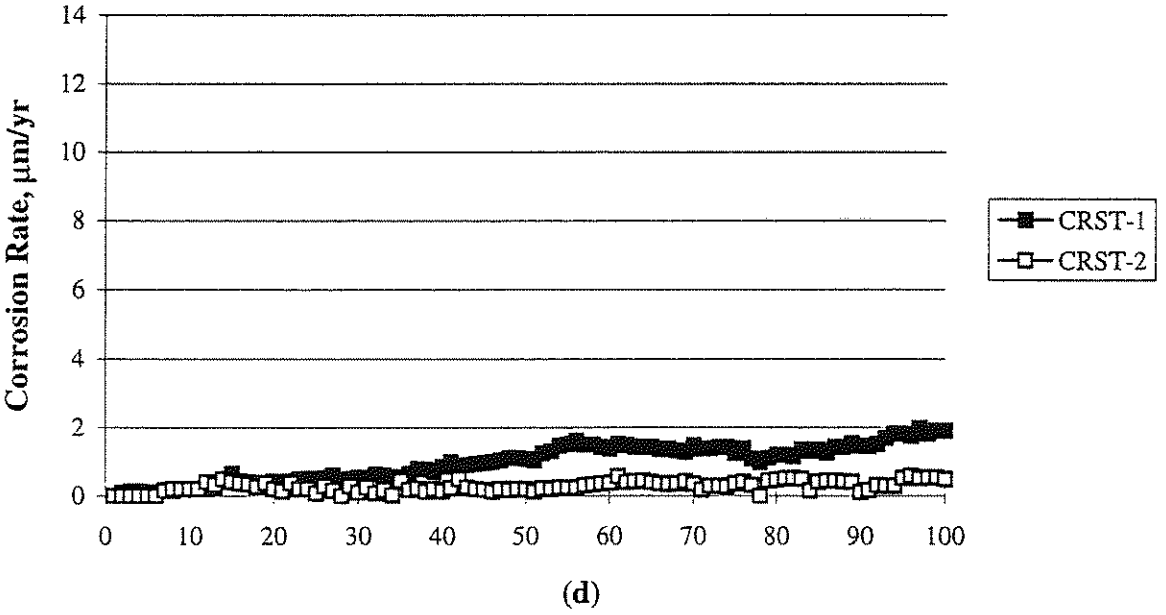

Fig. 45 Macrocell corrosion rate versus time for specimens exposed to 0.4 m NaCl in simulated pore solution: (a) H steel, (b) T steel, (c) CRSH steel, and (d) CRST steel.

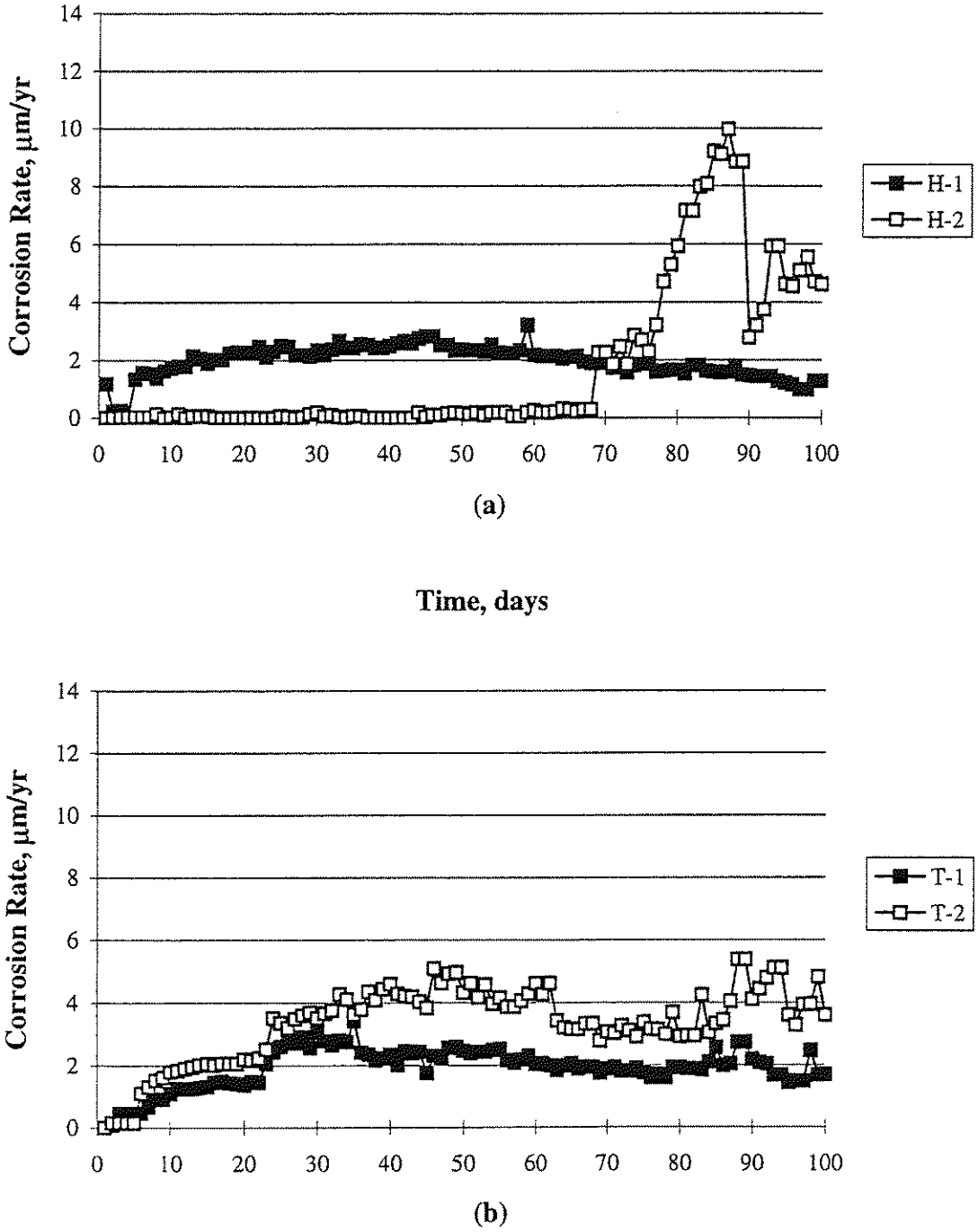

Fig. 46 Macrocell corrosion rate versus time for specimens exposed to 1.0 m NaCl in simulated pore solution: (a) H steel, (b) T steel, (c) CRSH steel, and (d) CRST steel.

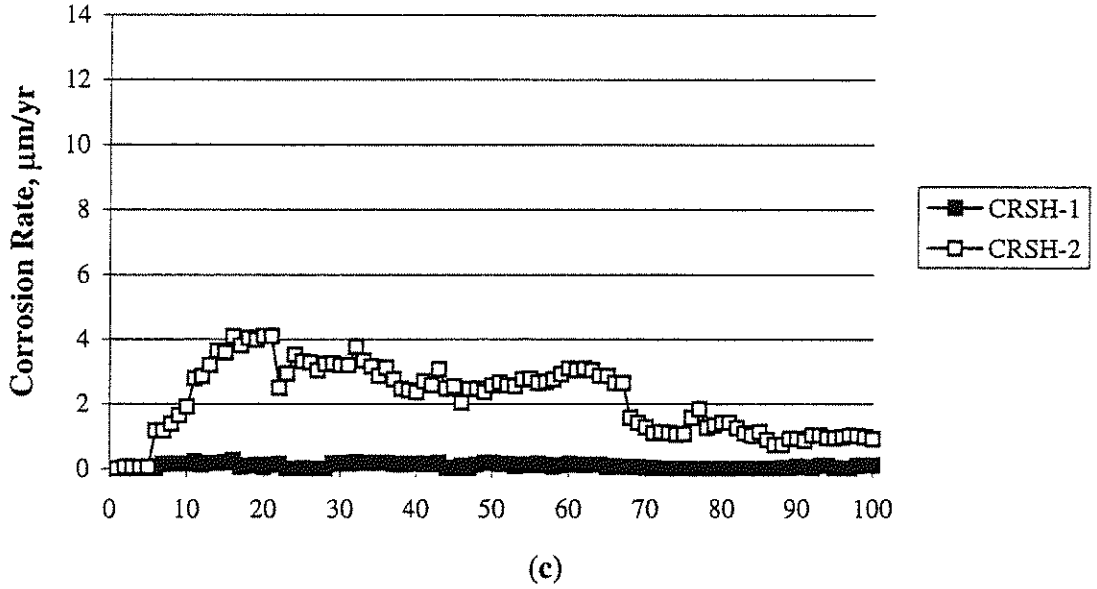

(c)

Time, days

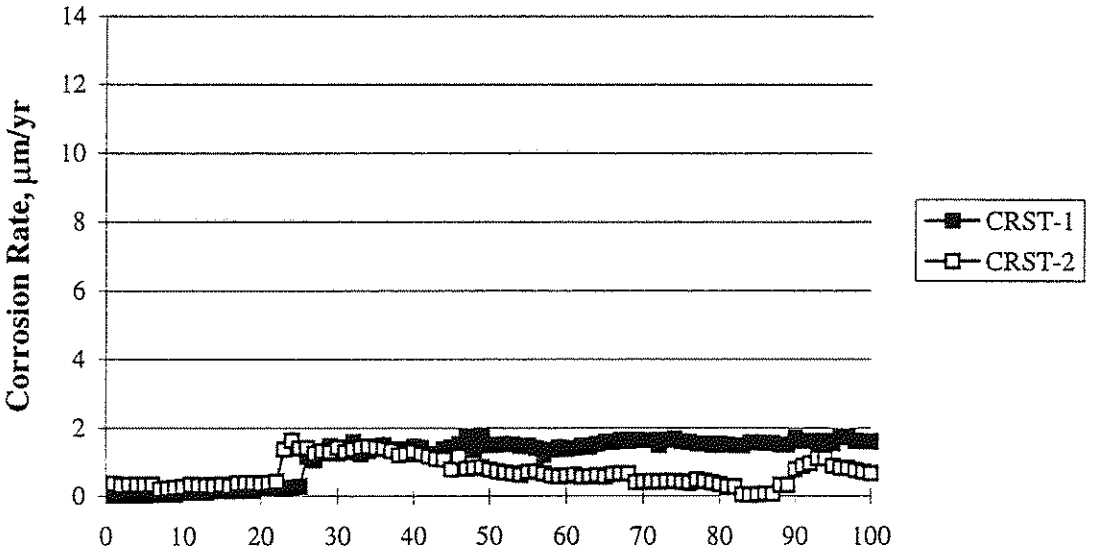

(d)

Fig. 46 Macrocell corrosion rate versus time for specimens exposed to 1.0 m NaCl in simulated pore solution: (a) H steel, (b) T steel, (c) CRSH steel, and (d) CRST steel.

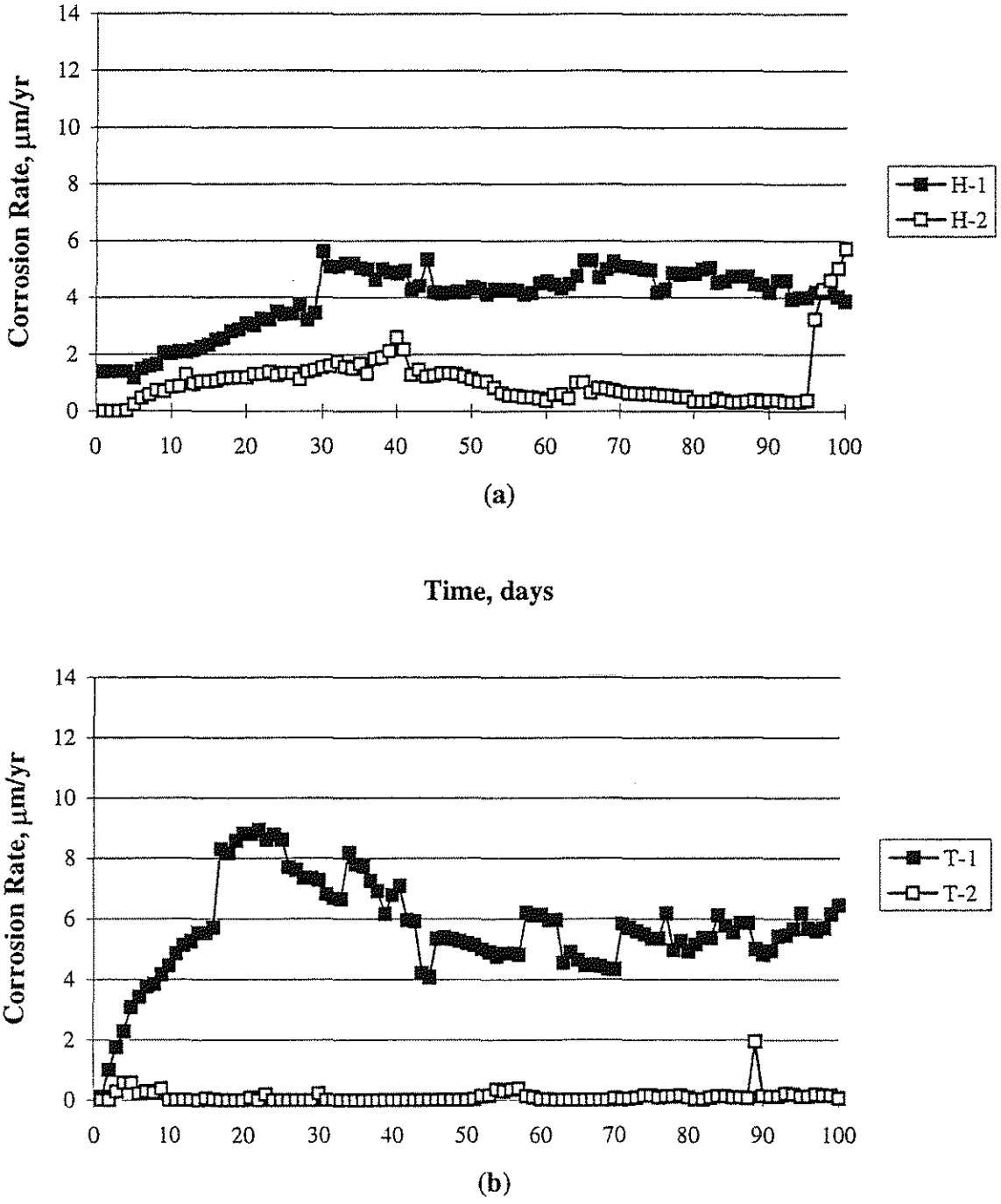

Fig. 47 Macrocell corrosion rate versus time for specimens exposed to 1.6 m NaCl in simulated pore solution: (a) H steel, (b) T steel, (c) CRSH steel, and (d) CRST steel.

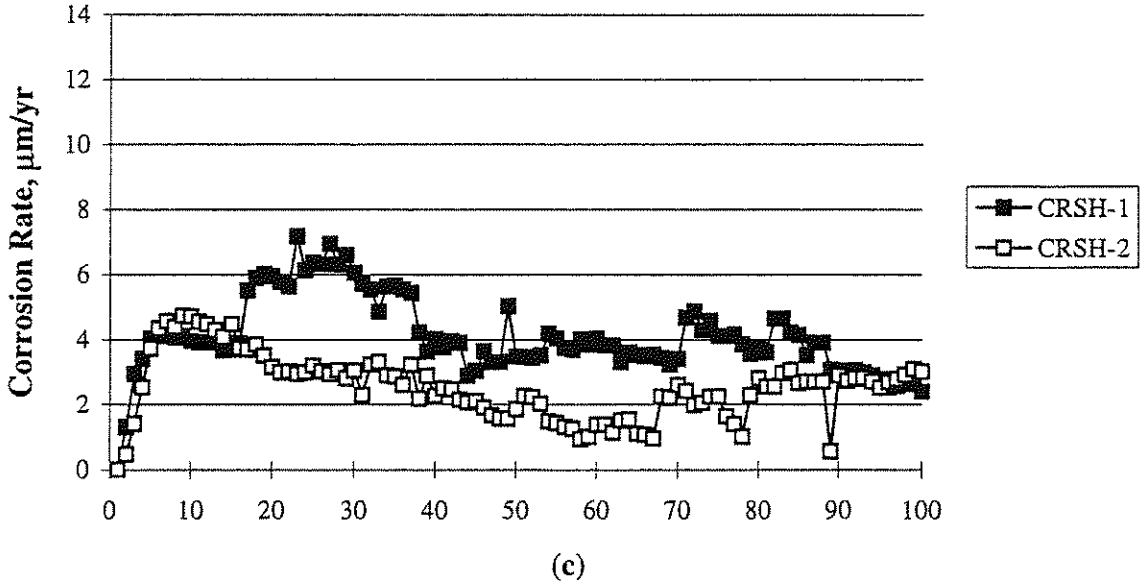

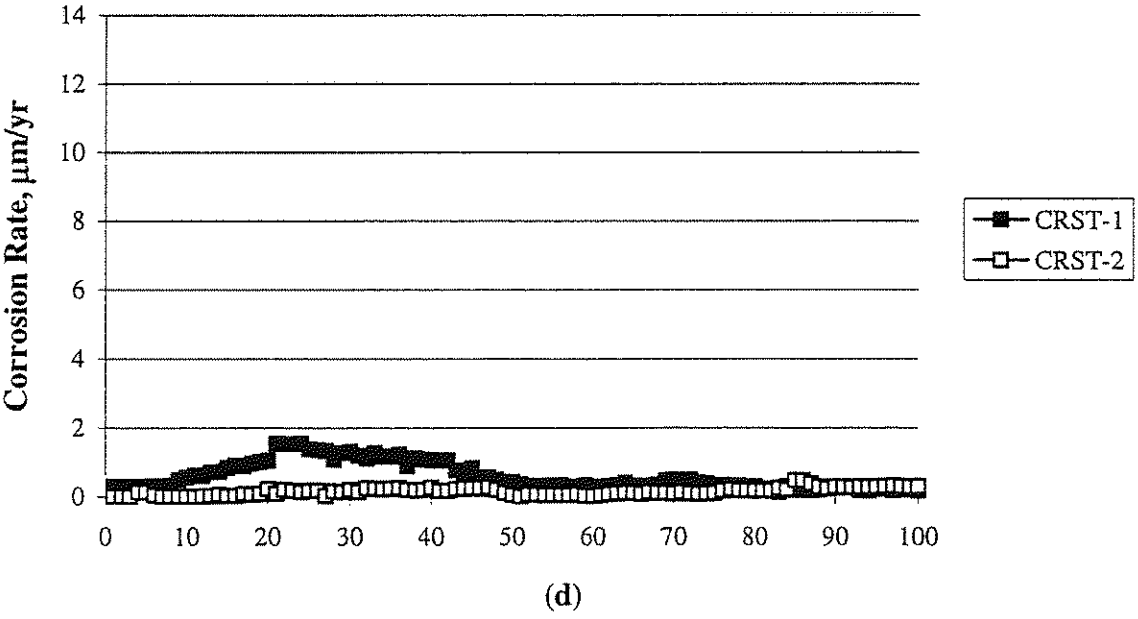

Fig. 47 Macrocell corrosion rate versus time for specimens exposed to 1.6 m NaCl in simulated pore solution: (a) H steel, (b) T steel, (c) CRSH steel, and (d) CRST steel.

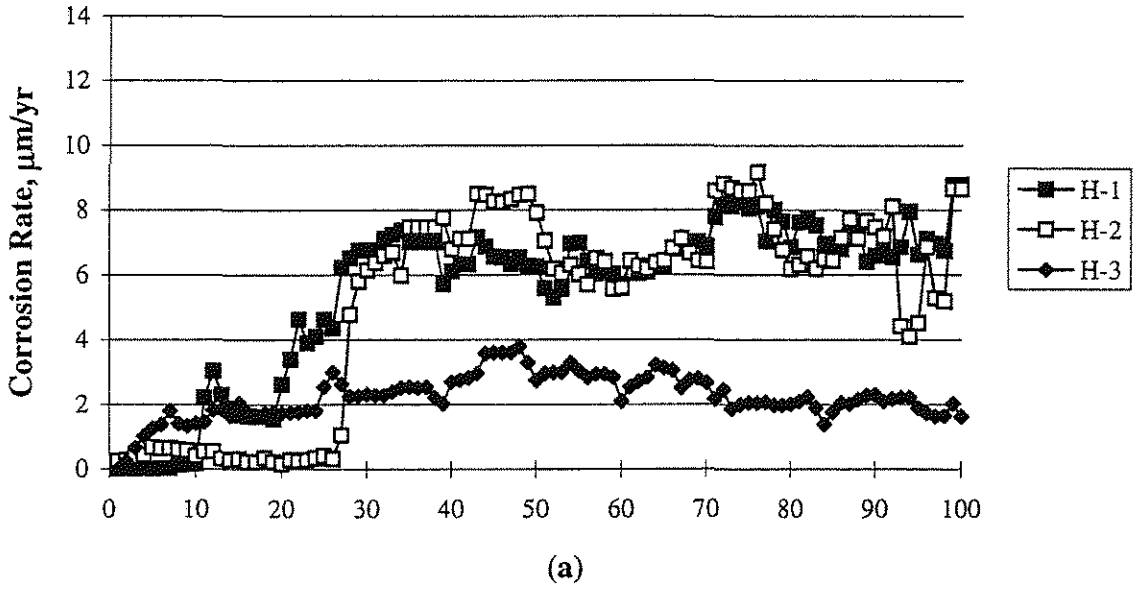

(a)

Time, days

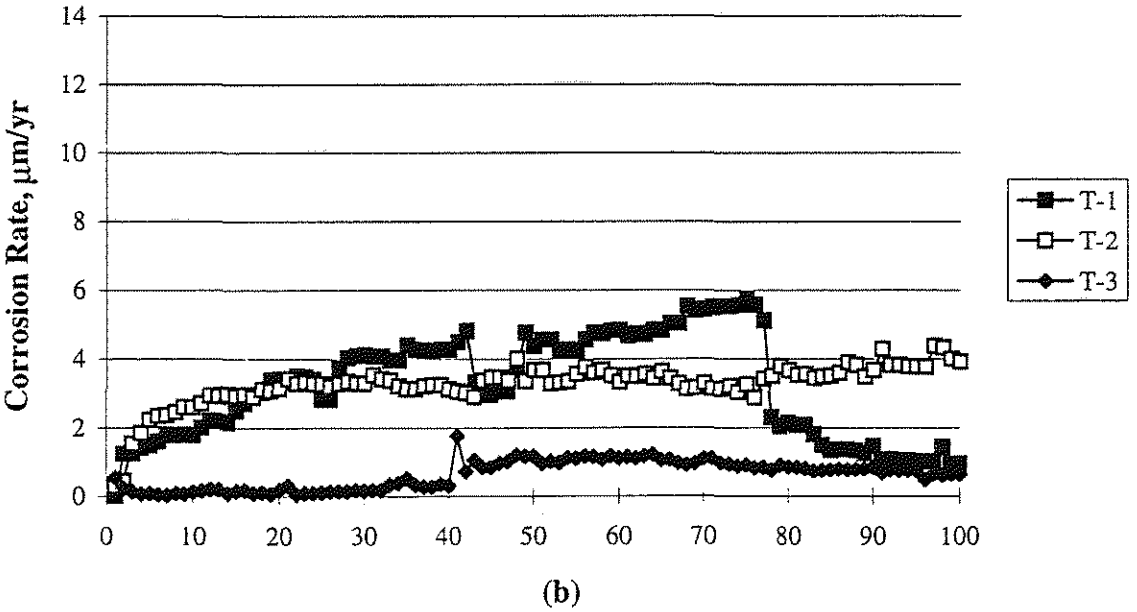

(b)

Fig. 48 Macrocell corrosion rate versus time for specimens exposed to 6.04 m NaCl in simulated pore solution: (a) H steel, (b) T steel, (c) CRSH steel, and (d) CRST steel.

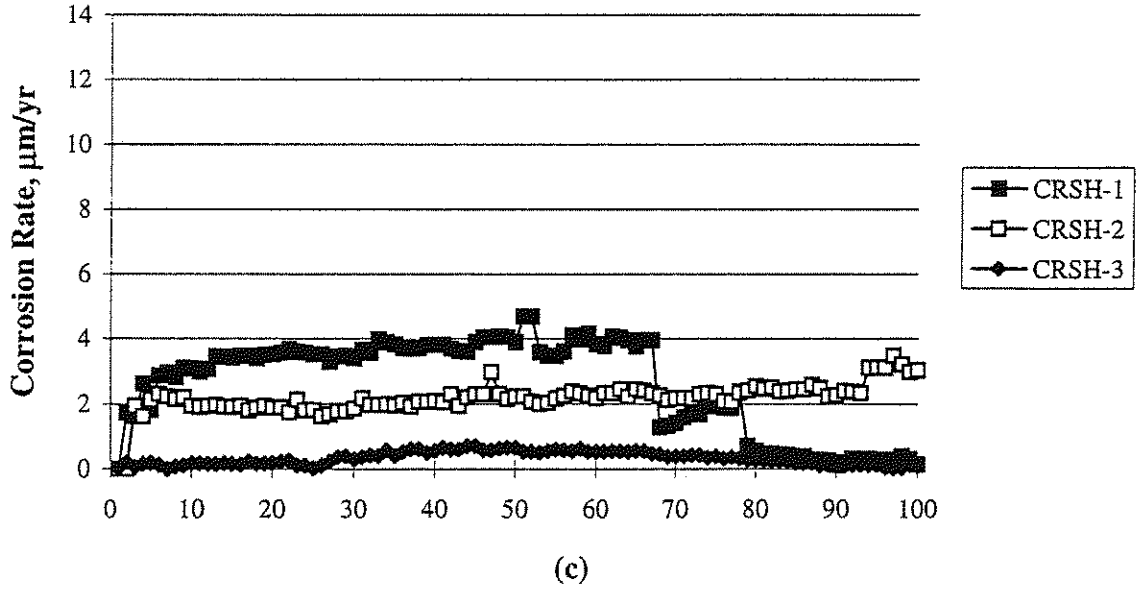

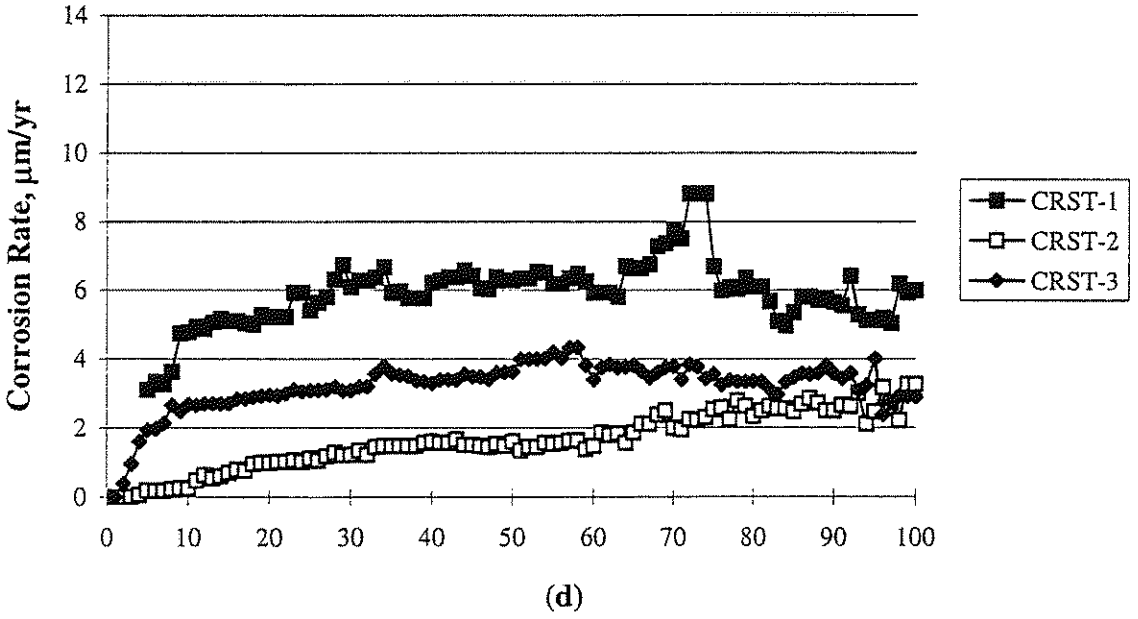

Fig. 48 Macrocell corrosion rate versus time for specimens exposed to 6.04 m NaCl in simulated pore solution: (a) H steel, (b) T steel, (c) CRSH steel, and (d) CRST steel.

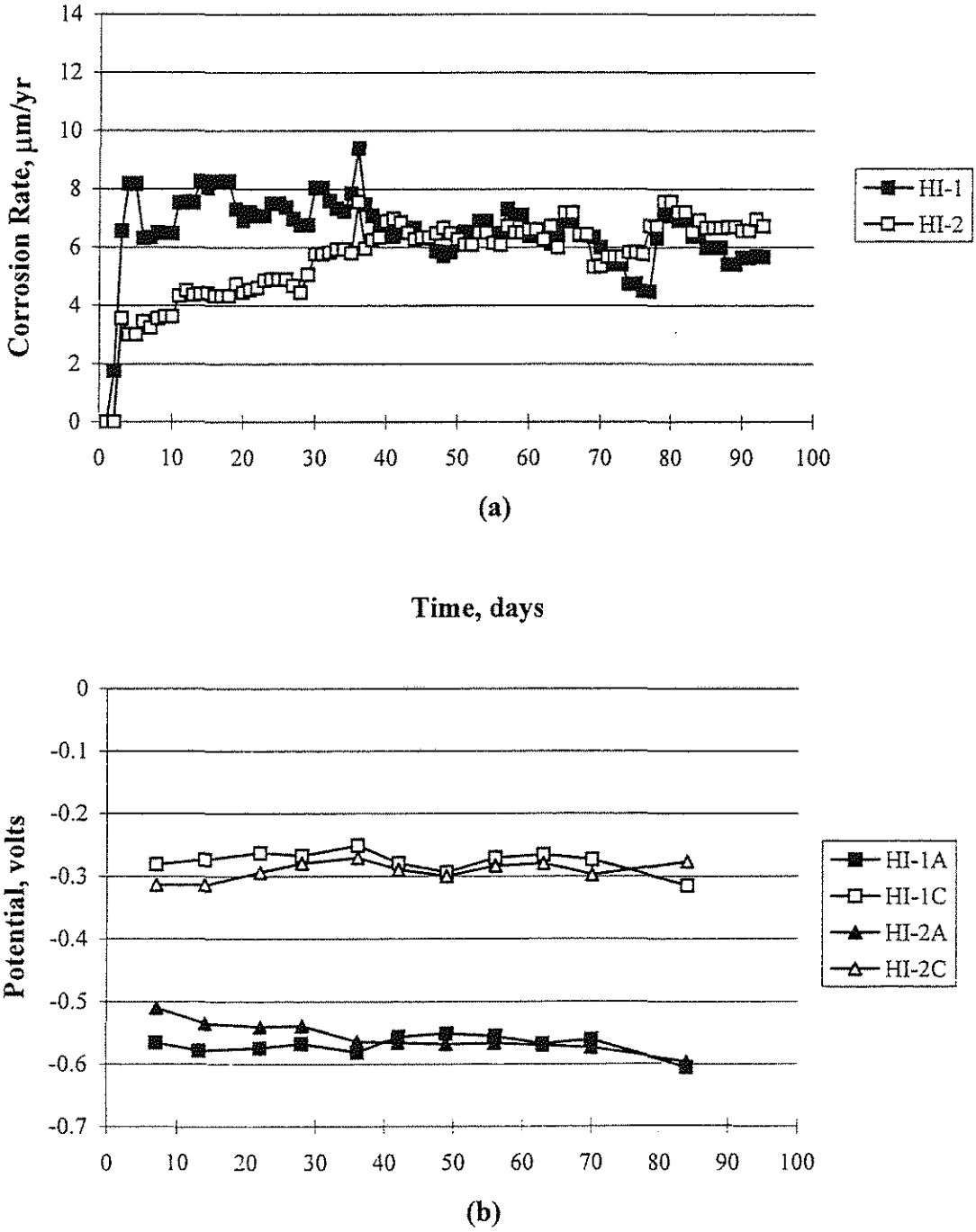

Fig. 49 H steel specimens cast in mortar with inorganic corrosion inhibitor, exposed to 1.6 m NaCl in simulated pore solution: (a) Macrocell corrosion rate, (b) Corrosion potential.

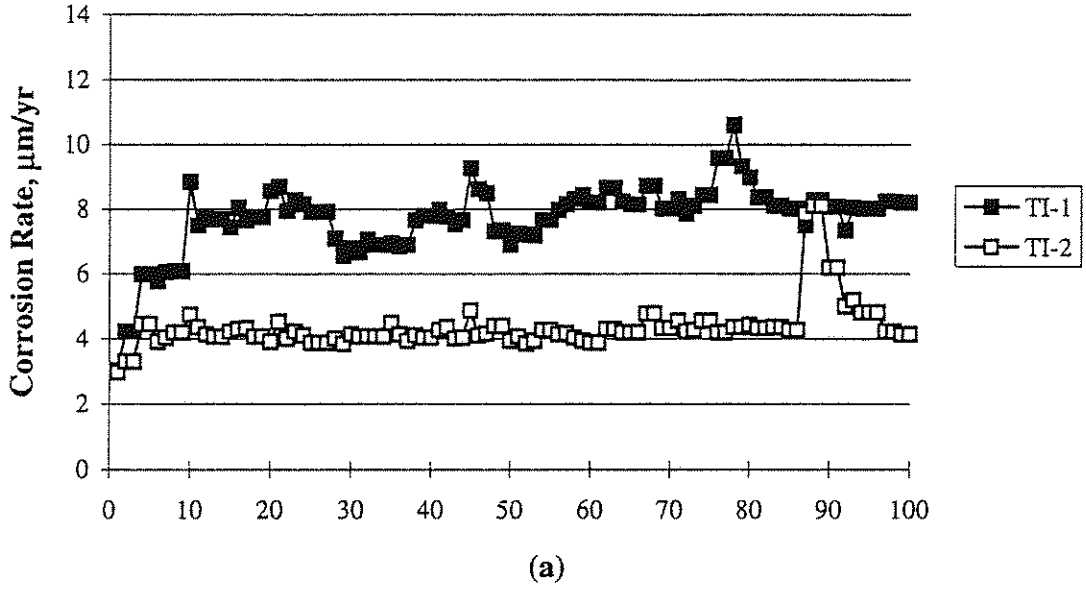

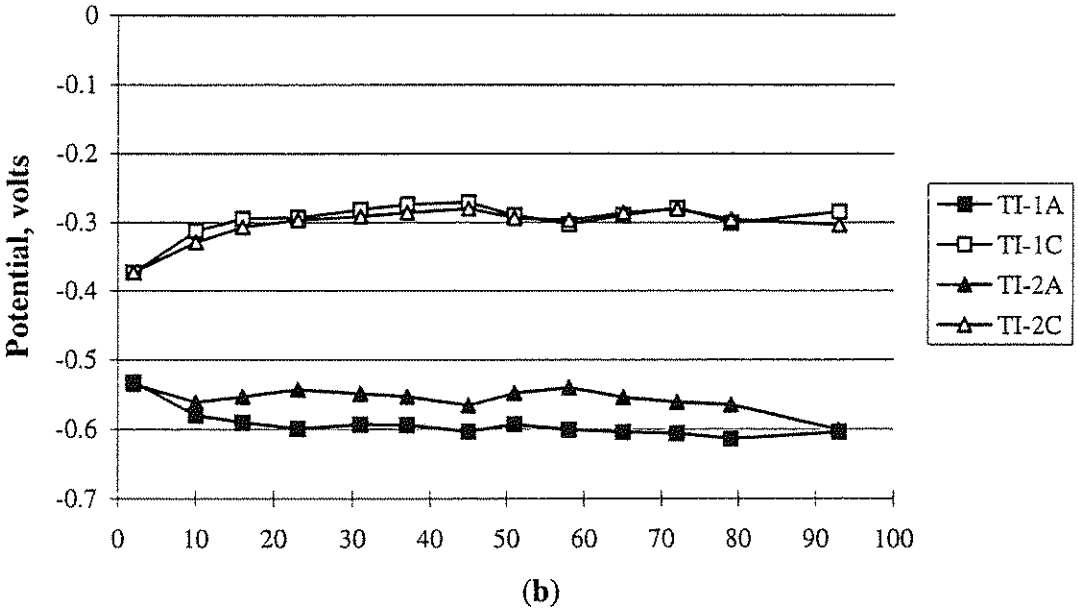

Fig. 50 T steel specimens cast in mortar with inorganic corrosion inhibitor, exposed to 1.6 m NaCl in simulated pore solution: (a) Macrocell corrosion rate, (b) Corrosion potential.

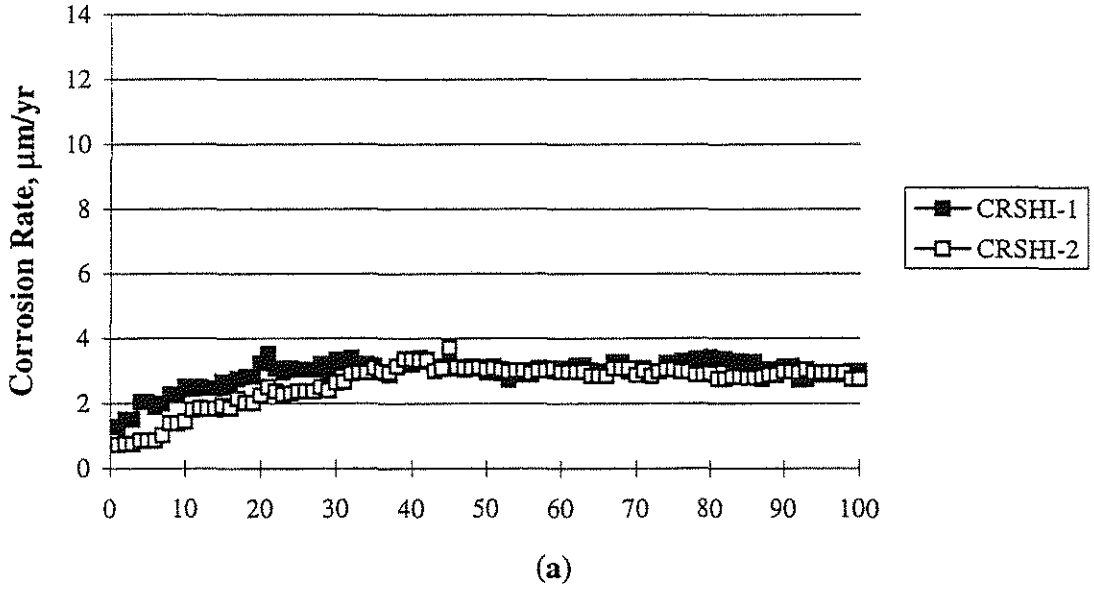

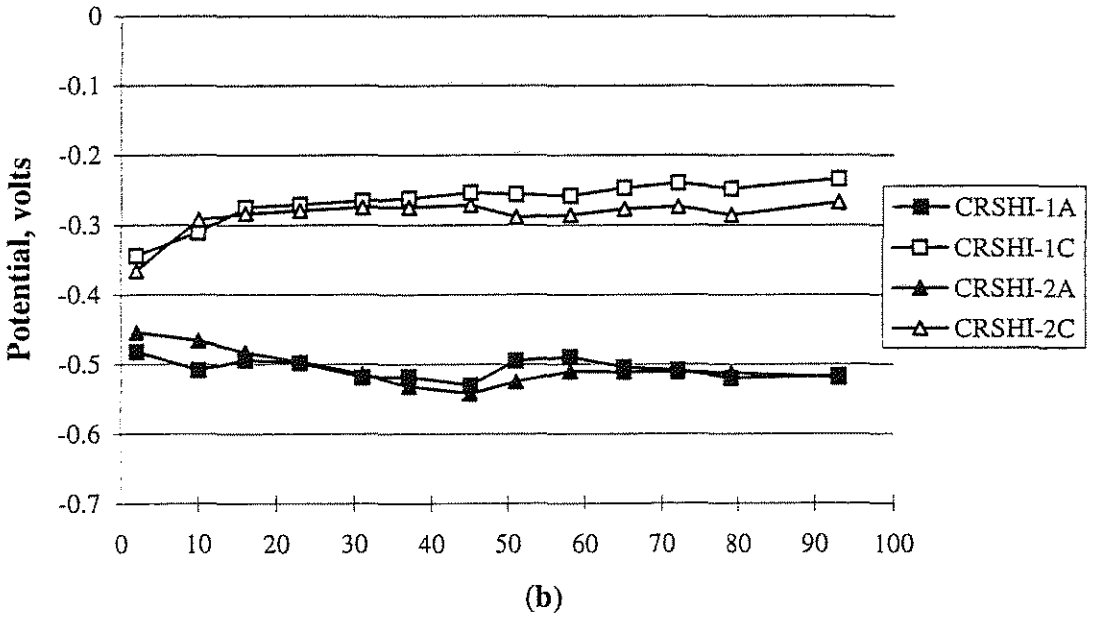

Fig. 51 CRSH steel specimens cast in mortar with inorganic corrosion inhibitor, exposed to 1.6 m NaCl in simulated pore solution: (a) Macrocell corrosion rate, (b) Corrosion potential.

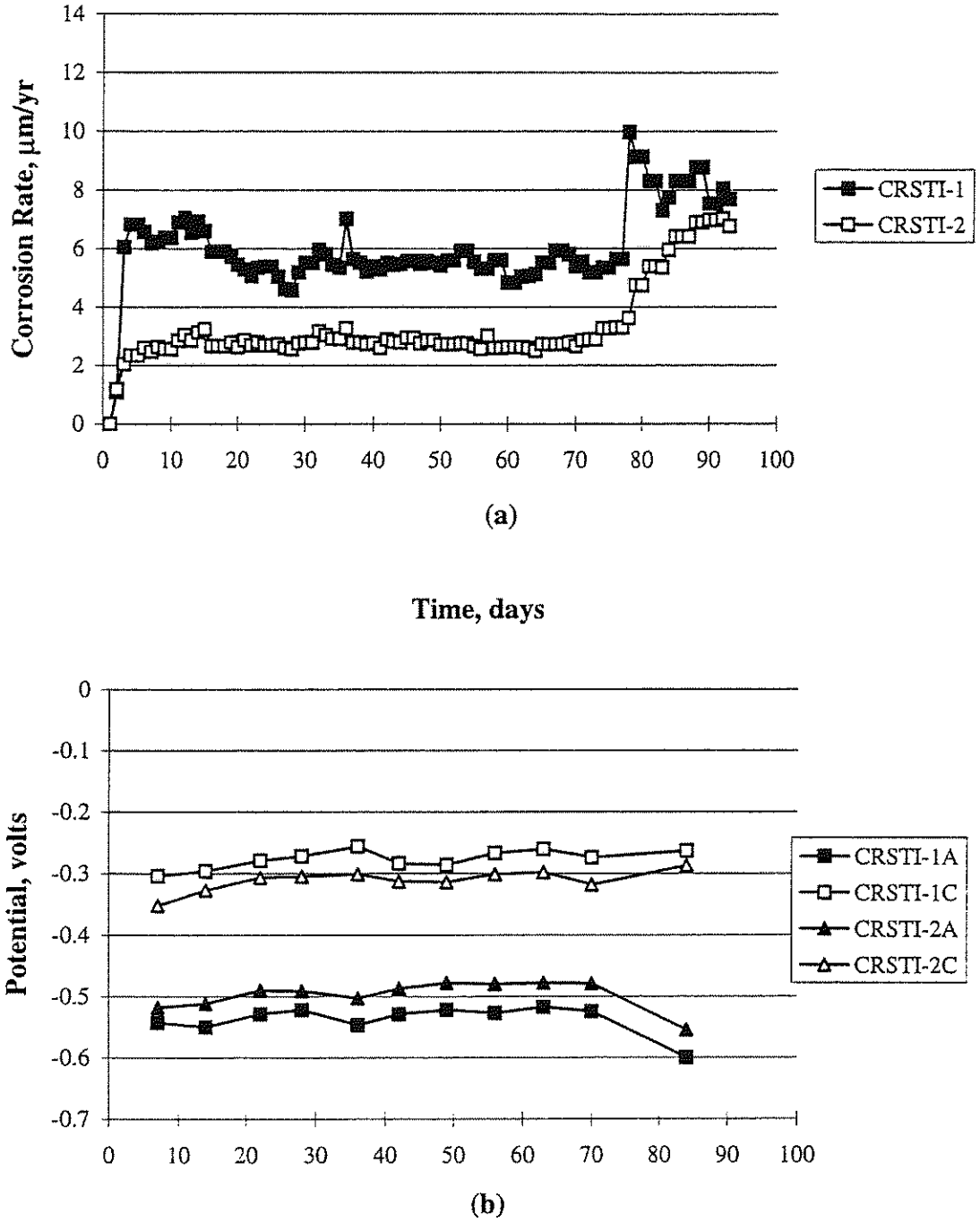

Fig. 52 CRST steel specimens cast in mortar with inorganic corrosion inhibitor, exposed to 1.6 m NaCl in simulated pore solution: (a) Macrocell corrosion rate, (b) Corrosion potential.

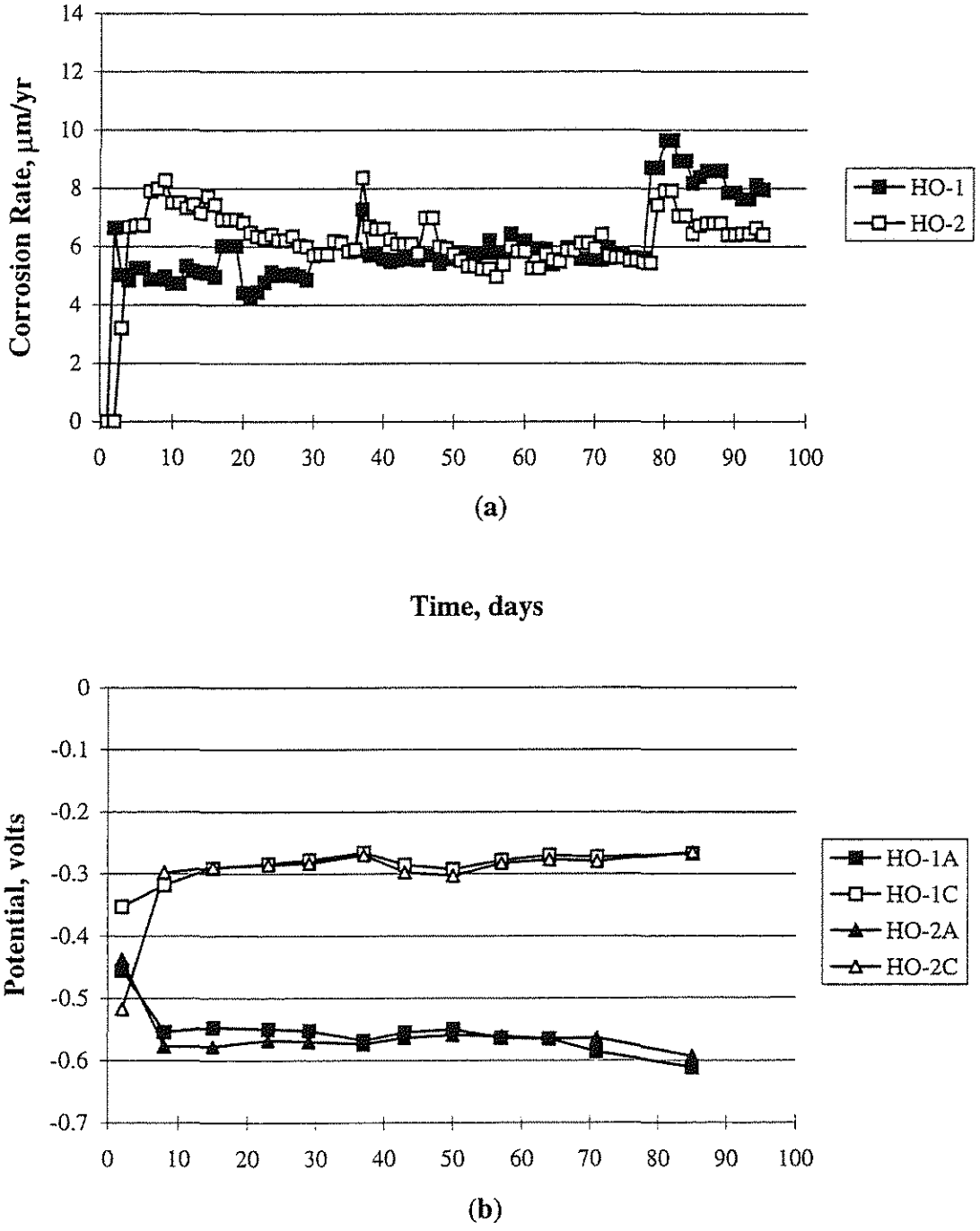

Fig. 53 H steel specimens cast in mortar with organic corrosion inhibitor, exposed to 1.6 m NaCl in simulated pore solution: (a) Macrocell corrosion rate, (b) Corrosion potential.

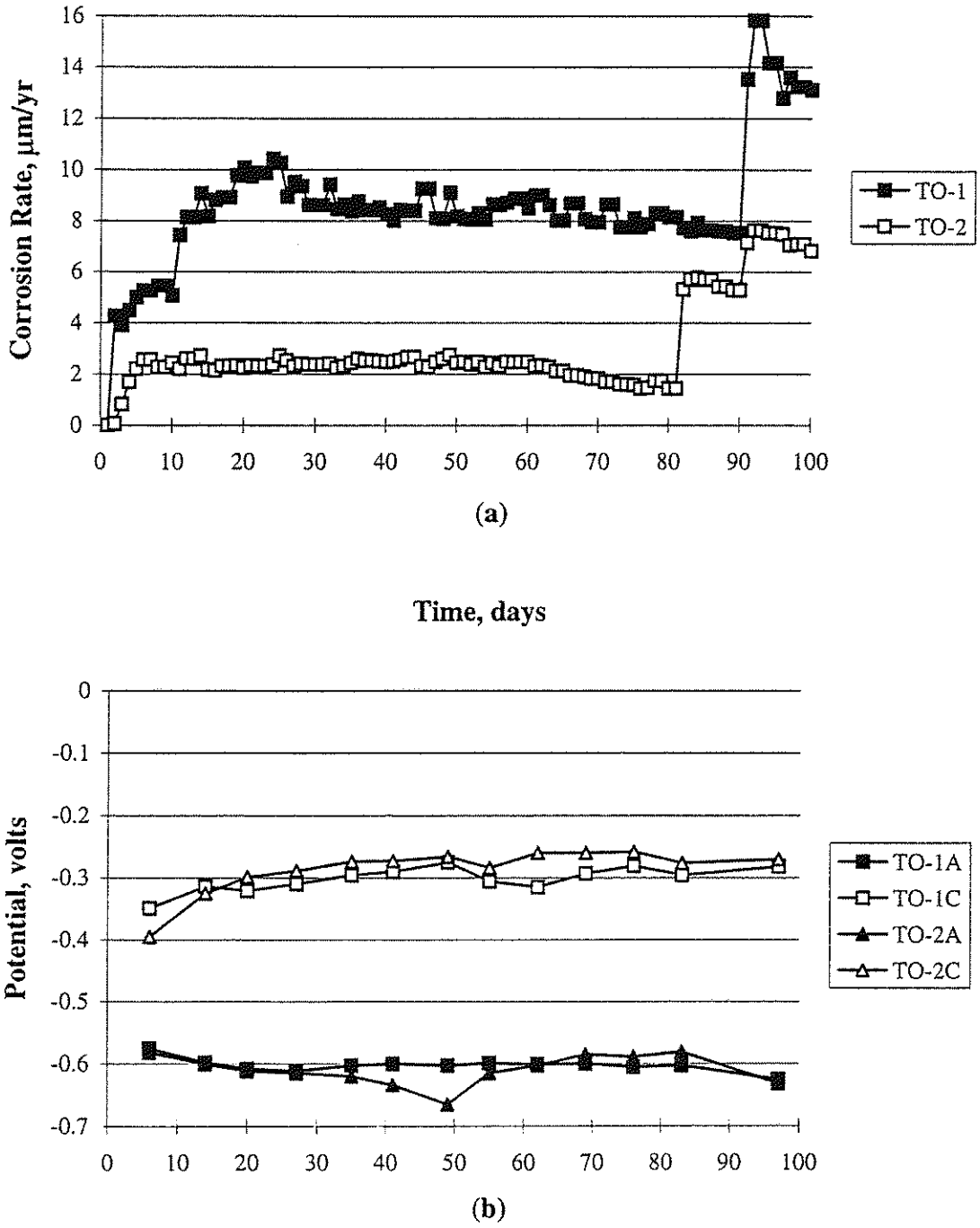

Fig. 54 T steel specimens cast in mortar with organic corrosion inhibitor, exposed to 1.6 m NaCl in simulated pore solution: (a) Macrocell corrosion rate, (b) Corrosion potential.

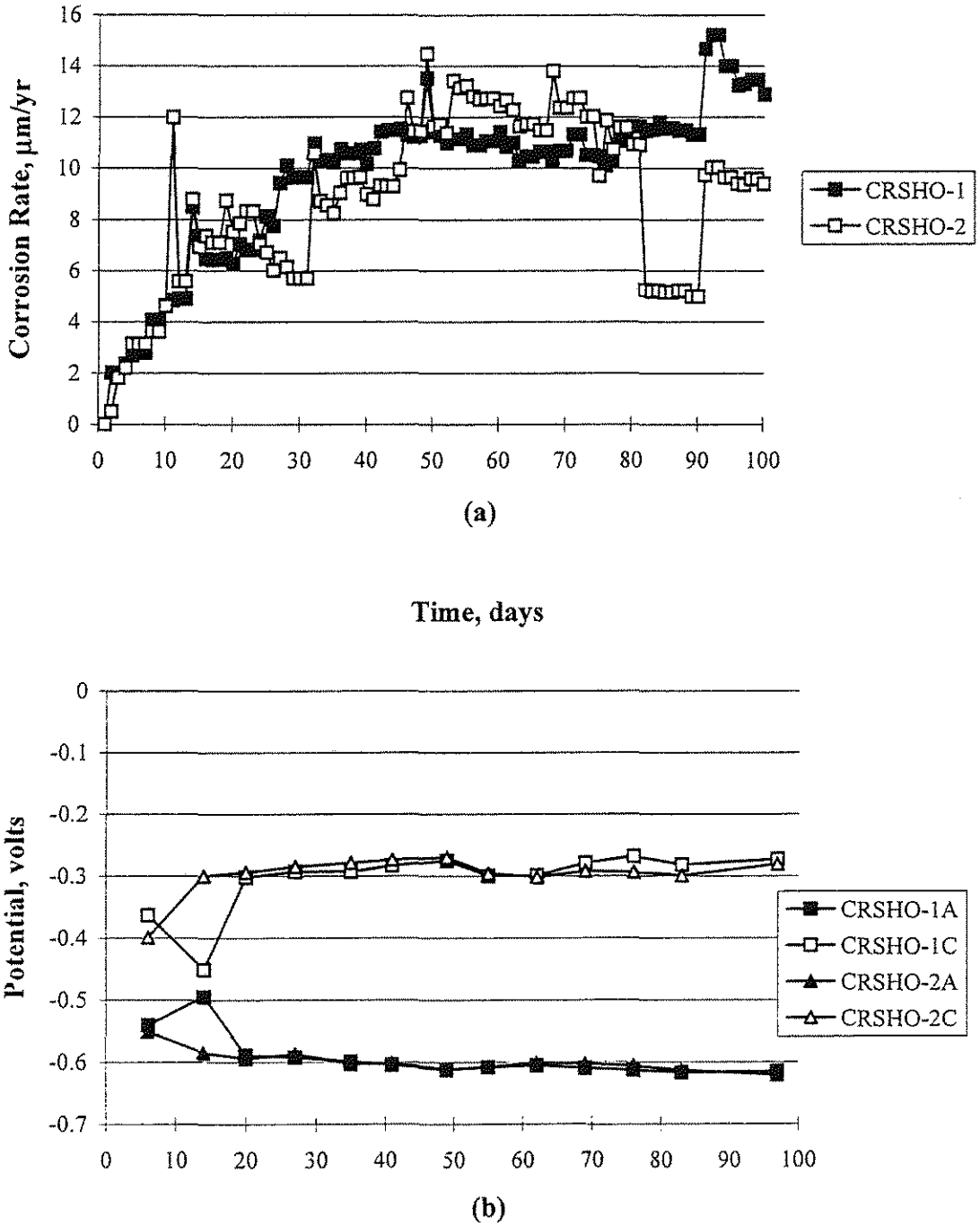

Fig. 55 CRSH steel specimens cast in mortar with organic corrosion inhibitor, exposed to 1.6 m NaCl in simulated pore solution: (a) Macrocell corrosion rate, (b) Corrosion potential.

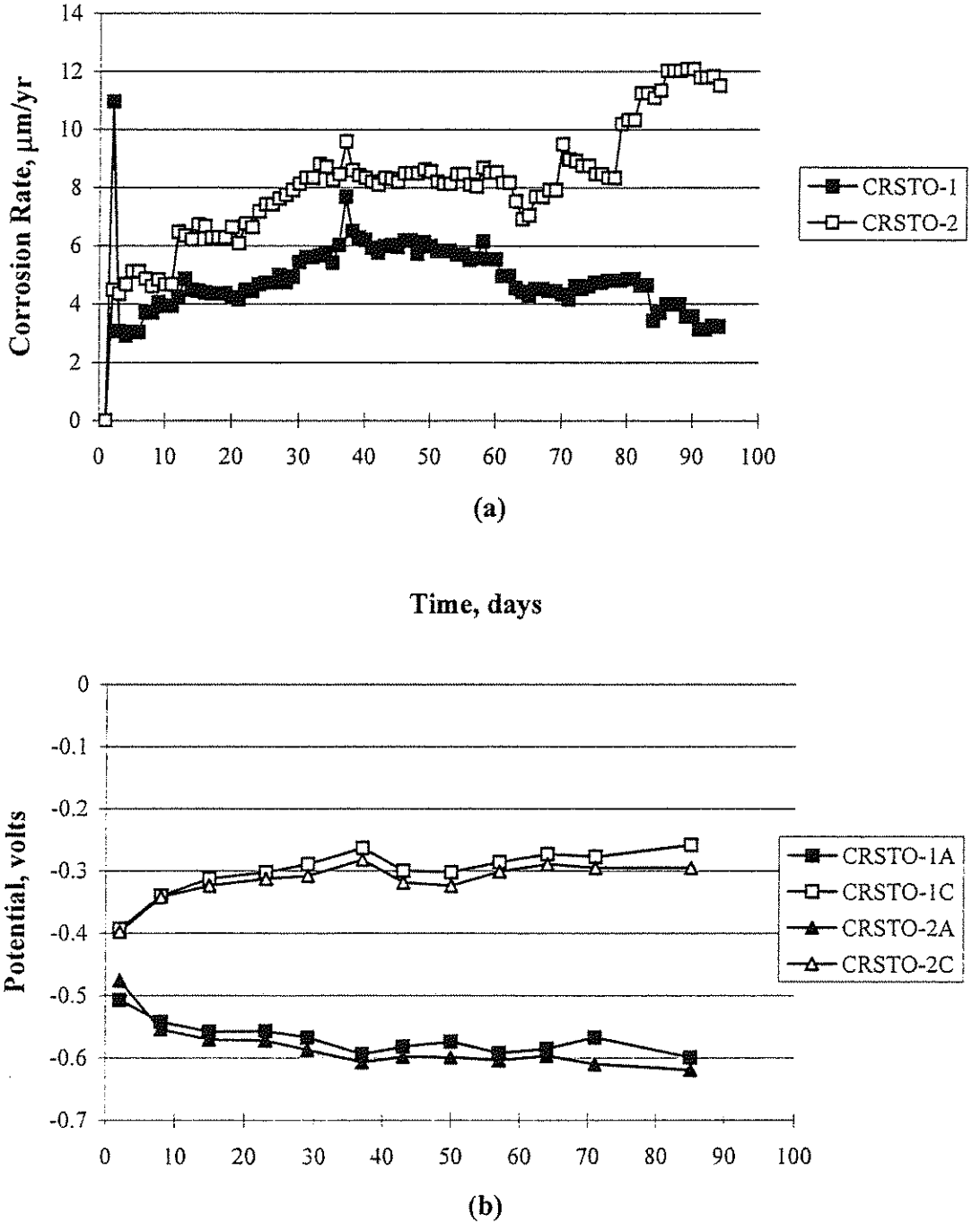

Fig. 56 CRST steel specimens cast in mortar with organic corrosion inhibitor, exposed to 1.6 m NaCl in simulated pore solution: (a) Macrocell corrosion rate, (b) Corrosion potential.

Appendix A

Corrosion Rate Sample Calculations

Corrosion rates are expressed in terms of the thickness of the metal lost over a length of time. The corrosion rate, r, of a macrocell is calculated using Faraday's Law.

$$r = \frac{ia}{nF}$$

in which i = Current density (amperes/cm^2 or coulombs/cm^2 sec)

a = Atomic weight (the weight of a gram-mole). In this case, Fe = 55.84 g

n = Number of equivalents exchanged (the number of electrons transferred). In this case, $Fe^{++} = 2$

F = Faraday's Constant = 96500 coulombs/equivalent

Example

The potential drop of a macrocell is: $V = 0.1 \times 10^{-3}$ volts

The corrosion current density is then: $i = \frac{V}{RA} = \frac{0.1 \times 10^{-3} \text{ volts}}{(10 \text{ ohms})(49.5 \text{ cm})} = 2.02 \times 10^{-7} \text{ coulomb} / \text{cm}^2 \cdot \text{sec}$

in which V = Potential drop (volts)

R = Resistance of resistor over which potential drop is measured (ohms)

A = Surface area of steel exposed to deicing solution (49.5 cm^2)

The corrosion rate, r, can now be calculated. The density of steel (7.87 g/cm^3) is used to obtain a thickness from a known mass and area. Time conversions are also included.

$$r = \frac{(2.02 \times 10^{-7} \text{ coulombs} / \text{cm}^2 \cdot \text{sec})(55.84 \text{ g})(31536000 \text{ sec} / \text{yr})}{(2 \text{ equivalents})(96500 \text{ coulombs} / \text{equivalent})(7.87 \text{ g} / \text{cm}^3)(0.0001 \text{ cm} / \mu\text{m})} = 2.34 \text{ micrometers / year}$$